Spatial Analysis and Modeling of Visual Interest:

A New Methodology for Visual Resource Assessment

Using Geospatial Information Tools

Koun Sugimoto

Ph.D

2013

TOKYO METROPOLITAN UNIVERSITY

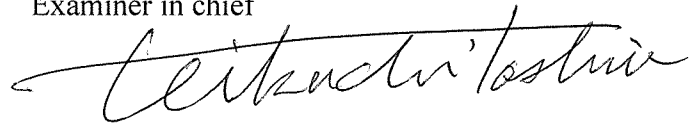DISSERTATION FOR A DEGREE OF DOCTOR OF TOURISM SCIENCE

TITLE:

Spatial Analysis and Modeling of Visual Interest:

A New Methodology for Visual Resource Management Using Geospatial
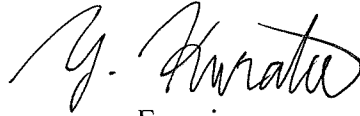Information Tools

AUTHOR

Koun SUGIMOTO

EXAMINED BY

Examiner in chief

Examiner

Examiner

QUALIFIED BY

THE GRADUATE SCHOOL OF URBAN ENVIRONMENTAL SCIENCES

Dean

Date

首都大学東京

博士（観光科学）　学位論文（課程博士）

論文名

関心生起の空間分析とモデリング
―地理空間情報技術を応用した景観資源評価の新たな方法論

著者

杉本　興運

審査担当
主査

菊地　俊夫

副査

倉田　陽平

副査

沼内直也

上記の論文を合格と判定する
平成　　年　　月　　日

首都大学東京大学院 都市環境科学研究科 教授会

研究科長

Abstract

This thesis provides new methods for visual resource assessment and modeling, an important research theme in micro-scale level tourist/recreational site planning and management. By acquiring and manipulating a combination of digital camera images and geospatial information tools such as geographic information systems, the proposed assessment method draws results from the analysis and modeling of visitors' visual interest during their on-site experiences of geographic space.

To acquire spatial data on visitors' visual interest, two surveys are conducted. First, participants are requested to photograph positive scenes while walking using digital cameras embedded with GPS and electronic compass. Next, the participants complete questionnaires that help them to evaluate their visual experiences and categorize visual objects. Second, the height or width of the visual objects projected in the photographs taken by the participants is measured using a laser distance meter. Based on the data acquired from these surveys, spatial point and line data of visitors' visual interest, named points of visual interest (PVI) and lines of visual interest (LVI), are extracted.

Four types of applications for the analysis and modeling of visual interest are presented. Two applications attempt to analyze visual interest from location point data that visitors' interest generate. The first application conducts an exploratory analysis of spot characteristics; several spatial clusters are extracted based on similarities in preference levels. The characteristics of the representative spots are statistically described using multiple indicators including the above clusters. The second

application involves modeling and visualizing the sightseeing potential of locations. Embedded into the algorithm of density computation are mechanisms for removing bias and weighting preference level scores.

The subsequent two applications focus mainly on spatial line data of visitors' interest visual lines. The third application creates a visualization of the spatial intensity of visual lines. Three map representation techniques are presented: density estimation for line data, grid-based aggregation, and flow data representation. In addition, the advantages and disadvantages of each technique are described. The final application described is the construction of a prediction model for visual interest flows. Spatial interaction models are used to predict the level of total flow between locations through explanatory variables related to origin and destination potentials, landscape elements, and distance between locations.

These models allow one to assess the entire target area, rather than being limited strictly to the scenes that visitors perceive. They also overcome the notable limitations of typical photographic surveys, and they clearly show new and useful techniques in visual resource management and modeling for specific sites. The spatial intensity of PVI, LVI, and geovisualization provide location-specific potential and attractiveness of scores for scenes and spaces.

Acknowledgements

Table of Contents

ix

List of Figures

List of Tables

Chapter 1

Introduction

1.1. Visual Resource and Tourism/Recreation Management

Landscapes existing around us often influence our behavior in various situations; people perceive a great deal of information, and a variety of emotions may be evoked through observation, gleaning cultural and natural backgrounds, or recognition of invisible meanings. As a consequence of these acts, people can integrate their own values and views into landscape. Such human-landscape interaction particularly occurs in tourism and recreation settings; beautiful scenes of natural or man-made landscapes have great power that attract us through their visual qualities and values in several contexts including the natural, the cultural and the social. This power, in many cases, catalyzes the desire to go traveling and see those beautiful scenes.

One essential aspect of the modern tourism system consists of above interactive relationship between the human observer (tourist) and environment (landscape). Marketers provide tourism information with various expressive styles to potential tourists as promotional material for a given destination. Visual information, such as a photograph, is one most important and effective representation media, being able to provide direct images about tourist sites (Chiou et al., 2008). For example, in tourist guidebooks, the typology of photographic representation generally includes the types of both space and subject; the former is characterized by landscapes, situations and

products, and the latter is defined from tourists, hosts and non-human subjects (Hunter, 2008). Such visual images inspire travel to distant places (Jenkins, 2003). People actually visit desired locations and observe the visual scenes they expect. However, in the on-site situation, those visitors encounter not only particular scenes they imagined but also other various scenes, and they evaluate both the expected and the unexpected visual experiences. After all trips and activities have ended, visitors modify their initial destination images in the mental processes (Li, 2000; Dorwart et al., 2009). If they are satisfied with the overall experience, they may return in the future to the destination or the attractions already visited, and may also recommend the destination to relatives and friends. Therefore, the attractiveness of the visual resource at a certain site constitutes a competitive advantage in contrast to other destinations (Schirpke et al., 2013).

From the perspective of the host region, if aiming to offer the appropriate service and experience to visitors, an assessment of visual resource is required as one component of planning and management of a given tourist or recreational site. The quality assessment of the visual resources may be conducted from either an objective or subjective view, or both; objective methods assess the physical components of landscape, subjective methods analyze persons' environmental perceptions (Schirpke et al., 2013). These efforts contribute to the maintenance of visual quality of the landscape, the effective promotion of attractive scenes, and the planning touring routes.

Methods of visual quality assessment have varied in recent times. For management purposes, applicable to tourism and recreation sites, studies have mainly focused on visitors' evaluations to destination landscapes in settings before, after, or during their on-site experiences. To record and collect visitors' responses in such multiple situations,

the "photograph" has been traditionally a commonly used tool and various methodologies using photographs have been developed even recently. However, a robust technical definition is still developing. In spite of the recent remarkable evolution of photographic instruments such as digital cameras, their full potential has not been utilized effectively in visual resource assessment research. Moreover, as various information technologies continue to develop, digital data from photographs can be used for not only image analysis but also other unique purposes by integrating other types of information. This has great potential to assist research innovation. For example, combination with geo-spatial information technologies such as geographic information system (GIS) and global positioning system (GPS) information could enable us to extract various kinds of data and analyze them.

This thesis aims to provide new and innovative approaches regarding the analysis of visitors' perceptions and assessment of tourist/ recreational spaces, especially focusing on visitor-oriented photographs and computer-aided techniques.

1.2. Spatial Scale of Study

In the analysis and assessment of geographical features including human behavior, a scale is one important factor to consider when selecting a suitable method (Andrienko et al., 2010). For example, a set of tourist behaviors taking in multiple phases has been researched by a distinctive methodology in a different scale. An international, or internal, tourist flow which shows number of tourists visiting from a particular country or region to another, is the largest geographical scale for analysis. This type focuses on the interaction of the tourist trade between two countries or regions, which is

represented as supply and demand relation. In contrast, visitor movement in a specific tourist site is perceived in a smallest geographical scale, focusing on the interaction between visitor and site specific environment.

Similarly, the assessment of tourist/recreational space also needs to consider the scale of the targeted area. Most of visual resource assessments have been mainly targeted to model the visual quality of landscapes in large-scale areas. However, to reflect visitors' direct evaluations to real scenes during on-site experiences in the assessment, a study in a small area only should be managed. However, the small area assessment based on visitor's on-site scenic preferences is a hard task because of the difficulty in acquiring precise location data that associated with points of interest. The use of geospatial information tools can assist to overcome such limitations.

1.3. Research Approach

Visual resource assessment research has been conducted through various approaches by different researchers in different situations (although the research trend and purpose tends to be characterized in academic disciplines). To argue research novelty, I describe the major characteristics of the research approach adopted in this thesis in advance; a more detailed explanation follows in the next chapter. Figure 1-1 highlights three significant aspects of this thesis.

First, this thesis can be regarded as an environment perception study specifically targeting visitors' on-site scenic perception in tourism/recreational settings. This type of research is both fundamental and applied. The knowledge obtained is important to

understand people's environmental preference to ensure the appropriate design, planning, and management of tourist/recreational sites.

Second, this thesis is conducted based on computer-aided techniques. Recent visual resource assessment has developed significantly because of geospatial information tools such as GIS. Various kinds of spatial data such as behavioral, social, artificial, and natural are combined and processed in a common digital geographical space, and the landscape potential is modeled mathematically and visualized through digital mapping. In a new approach, clearly distinct from previous studies, I analyze spatial data representing visitors' on-site visual interest in visual objects to spatially clarify their environmental preference.

Third, this thesis employs micro-scale assessment methodologies—methodologies to conduct an assessment in human-scale—because the data to be used are high-resolution micro spatial data acquired from people's behavioral histories.
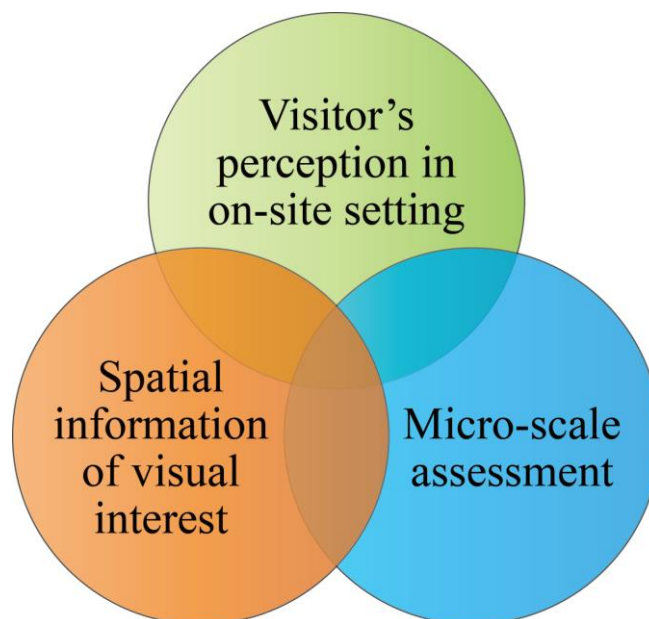
Figure 1-1. Research approach

Therefore, it is desirable that the targeted area is comparatively small and complex, such as an urban recreational space, or large and enclosed, such as a trail.

1.4. Thesis Goals

The goal of this thesis is to develop a computer-aided method for analysis and modeling of visitors' visual interest during their on-site experiences in geographic space. Combination of photographic methods, which have been mainly developed in landscape perception and assessment research, and geo-spatial information technologies are key factors. This hybrid method allows us to represent visitors' visual experiences as geographically distributed data and analyze them based on their positional relations in geographic space. In addition, the integration with physical landscape data is available, enabling us to analyze the relationship between person's visual perception and physical landscape quantitatively.

A series of data acquisitions, visualization, statistical analyses of spatial data of visitor-oriented photographs and modeling potential is at the core of this study. On-site field surveys are an essential part of data acquisition in this context. Acquired spatial data needs to be visualized using a map representation before or after analysis. Statistical analysis, especially statistics for spatial analysis, is used in this thesis to find significant data patterns that are buried in the complex datasets. Modeling potential is effective for the planning and management of tourism and recreation purposes, focused on modeling visual quality for sightseers. Based on this research, several approaches for analysis and modeling are presented in this work.

1.5. Structure of This Thesis

This thesis is organized into eight chapters. The research flow is described in Figure 1-2. While the primary area of focus is an analysis of spatial data representing visitors' visual interest, in this study it is also important to analyze the physical landscapes of a targeted site to assess visual resources from physical and psychological aspects.

Chapter 2 reviews existing research on scenic/landscape perception and assessment, tourist/recreational behavior and applied studies for planning and management of tourist/recreational sites. Subsequently, the advancement of these techniques by application of geospatial information technologies is addressed, and primary work is also described.

Chapter 3 mainly explains the field surveys and data acquisition methods. The field surveys were conducted for collecting several kinds of photographic data taken by visitors, indicating their interest during their on-site experiences. Thereafter, two types of spatial data representing the visitors' interest were generated; point data of photo-taking locations, and vector data of photo-shooting lines. In addition, the landscape structure of the study area is analyzed using 3-D digital landscape data to grasp the physical aspects of the targeted site.

Chapters 4 and 5 focus on the spatial data of photo-taking locations and their attributes. Chapter 4 explores the spot characteristics through analysis of the photo-taking locations, photo-taking directions, and preferences of visitor-experienced scenes. The similarity of spatial features, based on preference levels, is measured for evaluating "spot attractiveness" in terms of visitor consensus. Following this, the

7
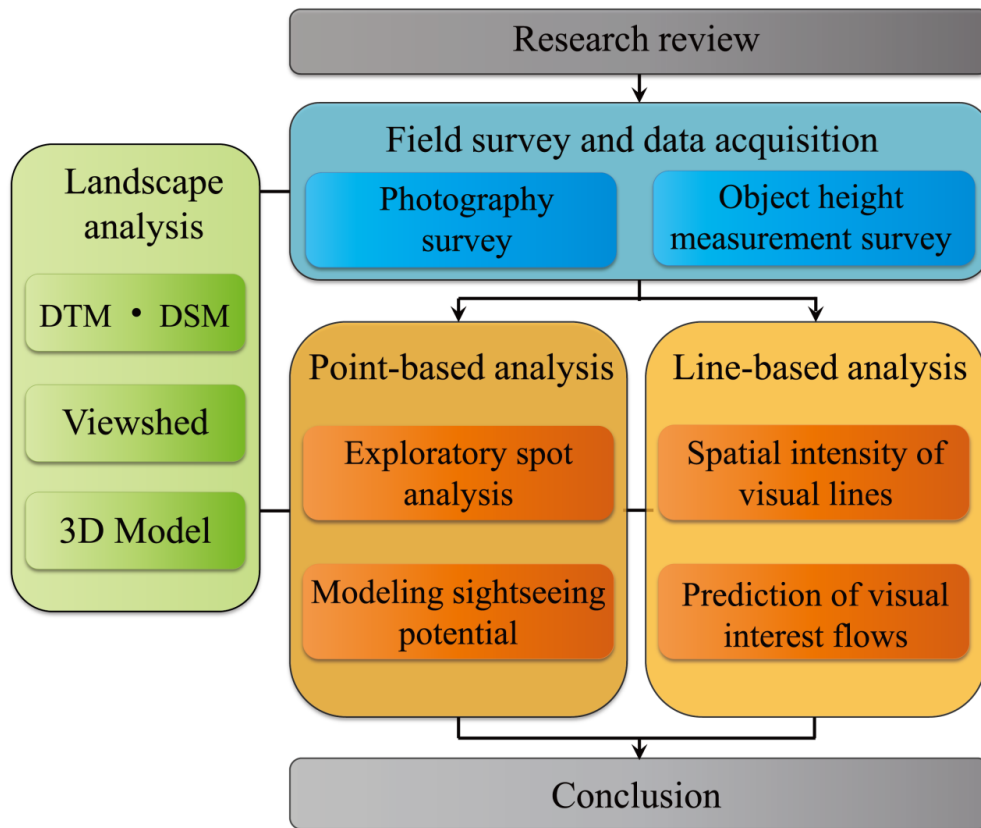
Figure 1-2. Research flow of this thesis

spatial ranges of these spots are determined, and each spot characteristic is statistically described through several indicators of photography-related data and the difference between actual observed field and potential viewshed.

Chapter 5 demonstrates GIS-based modeling and visualization of sightseeing potential. The density of photo-taking locations is computed, and treated as the potential degree of the spot. At the same time, the weighted scores are shown; these are processed using a density computation algorithm for reducing biases.

Chapters 6 and 7 focus on the spatial line data of associated with the photo-shooting lines. Chapter 6 describes effective methods to analyze and visualize spatial intensity of visitors' visual lines. Three types of map representation are demonstrated; line

density, grid-based aggregation, and flow data visualization. Advantages and disadvantages of each are compared. Thereafter, some are combined with the 3-D landscape models of the targeted site and its surrounding area to examine the effectiveness of geo-visualization.

Chapter 7 describes the creation of the mathematical models used for prediction of the flow patterns of visitors' visual interest. Models include both perceptual and physical landscape data in explanatory variables. The accuracy of the predicted values is tested by comparing with the observed values using goodness-of-fit and actual distribution on the map.

Chapter 8 concludes this thesis with a summary of major results and a discussion of future research in this field.

Chapter 2

Related Work

2.1. Existing Research in Landscape Perception and Assessment

When designing and managing tourist destinations, understanding both the type of space, and the scenery that people prefer, is important. "Tourist experiences are generated via a process of perceiving and recognizing a variety of sensory information obtained within a landscape" (Chhetri et al., 2004). Visual experiences have particularly profound effect on people, emphasizing the characteristics of the environment (Sugimoto, 2012). Therefore, knowing which scenery people generally prefer can be useful in understanding their experiences. This type of study, known as human-landscape perception research, has been developed within various fields including geography, forestry, tourism and recreation, environmental psychology, and landscape studies (Zube et al., 1982).

Many previous studies of landscape perception and assessment in several disciplines have attempted to clarify the types of scenes that are preferred by humans, to provide fundamental knowledge for environment design and management (Zube et al., 1982; Jacobsen, 2007). While there have been investigations carried out by experts and non-experts (Daniel, 2001), and perception-based research has mainly been conducted from the latter perspective (Figure 2-1).
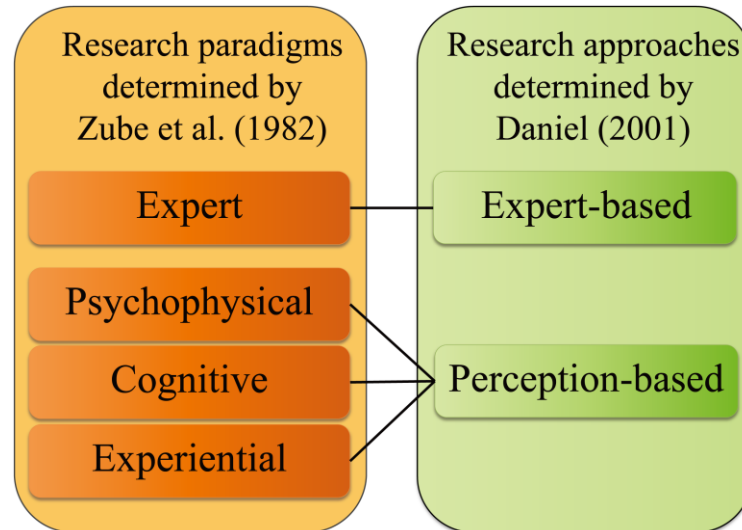
Figure 2-1. Types of landscape perception research determined by Zube et al. (1982) and Daniel (2001)

Landscape perception research has been subdivided further. Zube et al. (1982) have identified the four paradigms of landscape perception research from review of over 160 articles published during the period 1965-1980; expert, psychophysical, cognitive, and experiential (Figure 2-1). The expert paradigm involves evaluation of landscape quality by skilled and trained observers. The psychophysical paradigm involves assessment through testing general public or selected populations' evaluation of landscape aesthetic qualities or of specific landscape properties. The cognitive paradigm involves a search for human meaning associated with landscape properties. Finally, the experiential paradigm considers landscape values to be based on the experience of human-landscape interaction.

In recent trends, tourism and recreation related studies have been conducted from all paradigms. The findings of landscape perception research focusing upon the recreation settings can be applied directly to tourism (Fridgen, 1984). Applied studies related to the recreation planning typically adhere to the expert and psychophysical paradigm,

have aimed to resolve whether landscapes are significant and/or beautiful as the visual resource (Jacobsen, 2007). Typical research of expert paradigm evaluates the quality of various landscapes in tourism region from mainly their geophysical values and conditions, depending on the knowledge and experience of specialists (Mizoo et al., 1975; Mizoo & Osumi, 1983; Rangel-Buitrago et al., 2013). On the other hand, the cognitive and experiential paradigms have been concerned with theoretical issues, such as the character of landscape, the reason of public preference to specific landscapes and the meaning people attach to particular landscapes. The combined approaches of two or more paradigms, for example psychophysical and cognitive, will be further used to advance landscape perception and assessment research.

Strictly defining the paradigm of this thesis is involved is difficult. In simple terms, this study combines psychophysical and experiential approaches because of following reasons; firstly, this thesis uses quantitative measurement to assess the visual experiences of participants and the location potential of spaces, and secondly the acquired data are generated based on the participants' perceptions within the interaction with real environment during their on-site experiences.

2.2. Photographic Methods

Studies of landscape perception and assessment have usually relied on photographic data. Various types of perception-based research have been developed to evaluate visual elements. For example, photo-based questionnaire surveys as represented by Daniel and Boster's (1976) scenic beauty estimation (SBE) have widely been employed. SBE requires participants to evaluate the visual quality of landscapes in

slide photographs that researchers have prepared on Likert scales, in a laboratory setting. This technique is recognized as a reliable approach to evaluate the aesthetic qualities of a landscape, and to compare various landscapes presented in forms such as digital media (Bishop & Hulse, 1994). However, visitors' on-site perceptions of landscapes could be affected by contextual factors, such as their mood, interpreted meaning and novelty, and could thus be different from perceptions of photographed landscapes (Hull & Stewart, 1992). In addition, this kind of simulated landscape assessment causes problems arising from, for example, researcher bias in scene selection, photographs, panels, and respondents, as well as the inability of researchers to capture the qualities of a scene through their own photographs (Akbar et al., 2003). The prepared photographs may therefore not be representative of the target area (Chen et al., 2009).

Some techniques of photo-based research have recently been applied in field research (Jacobsen, 2007), requiring methods that take account of the contextual factors attributed to field settings that involve actual visitors. Fairwether and Swaffiled (2001, 2002) employed the Q-method with questionnaires that asked respondents to assess landscapes photographed in New Zealand so as to elicit favorable landscapes for visitors. Wong and Domroes (2005) assessed the visual quality of urban park scenes from the perspective of both tourists and residents via a questionnaire that asked visitors to sort and evaluate photographs. Naoi et al. (2006) interviewed students using photographs of various settings in a Japanese historical district as stimuli to evaluate their experiences. Fyhri et al. (2009) explored foreign tourists' perceptions, preferences, and assessments of agriculturally-related coastal landscapes by asking them to sort

landscape photographs in several themes and evaluate in terms of preference. Múgica and Lucio (1996) investigated landscape preferences of national park visitors by asking them to answer photo-questionnaires. Chen et al. (2009) evaluated aesthetic quality (visual, auditory, tactile, and olfactory factors) of urban green space using photographic stimuli and questionnaires. However, these investigations have failed to fully capture visitors' views about real landscapes of their own choice (Naoi et al., 2011).

In order to evaluate actual landscapes and elements that they encapsulate, some researchers have employed methods that analyze photographs taken by participants who actually visited the targeted sites. A concrete photographic technique called visitor-employed photography (VEP) has been used to analyze visitors' scenic perceptions during their on-site experiences. This is a method based on participants' own photography in the context of a real environment. Haywood (1990) describes VEP as a powerful tool that provides visual and evidentiary information to support reactions to, opinions about, and assessment of visitors' experiences in specific places or destinations. Moreover, VEP allows us to record the memory of the visitor's indistinct experience, which is difficult to capture using questionnaires (Chenoweth, 1984). Cherem and Driver (1983) used VEP to measure visitors' common perceptions of natural environments. Following their research, VEP has been used for various types of studies. Taylor et al. (1995) used VEP as a technique to quantitatively and objectively evaluate the importance of water resources in the Rocky Mountains. Oku and Fukamachi (2006) collected photographs from visitors in a forest recreation trail and analyzed the kinds of objects that visitors photographed in relation to the visitors' attributes and preferred activities. Haywood (1990) mentioned the possibility of using

VEP to assess an urban environment. MacKay and Couldwell (2004) used VEP to extract tourists' images that reflected their preferred landscapes. Dorwart et al. (2009) used VEP to determine visitors' perceptional affects with regard to their outdoor recreation experiences. Heyman (2012) assessed visitors' recreational preference of landscapes with different management conditions by VEP. Nielsen et al. (2012) researched factors affecting visitors' preferences in terms of the attributes of visual scenes, such as spatial configuration and content-based properties of landscape. Qiu et al. (2013) investigated the relation between preferences and biodiversity in the landscape using VEP in an urban green recreational space.

As befits the purposes or style of various researchers, this technique has been referred to by a number of names; it has instead been called volunteer-employed photography (Garrod, 2008), host-employed photography (Brickell, 2012), resident-employed photography (Stedman et al., 2004; Amsden et al., 2011), photo elicitation (Loeffler, 2004; Matteucci, 2013), caption evaluation (Naoi et al., 2011), and the photo projective method (Yamashita, 2002).

In most previous studies, the kind of scenery that people recognize as having formed part of their positive or negative experiences has been intensively studied. However, the spatial distribution of photo-taking locations has not yet been sufficiently analyzed, partly because many researchers have used disposable cameras for their investigations. If the photograph is merely used to extract humans' visual perception based on the specific theme and region, using a disposable camera alone seems to be sufficient. However, when we consider the use of photographic techniques in managing the environment quality, we must conduct our analysis with a technique that is more

15

effective at identifying locations that allow visitors to see attractive views or objects. If such an analysis is possible, the spatial evaluation structure of the site's specific area can be clarified from the perspectives of these visitors. Such analysis, which is based on the geo-spatial research approach, may be important to regional resource management.

2.3. Geographic Information System and Other Relevant Geo-Spatial Tools

2.3.1. GIS and tourism/recreation management

Geographic Information Systems (GIS) and other relevant geo-spatial technologies are regarded as effective tools for planning and management of recreational sites. A GIS is an information systems technology that can be used to store and retrieve geographical data, and it provides the tools for manipulating, analyzing, and presenting geographic information (Rigaux et al., 2001). Tourism and recreational features including both natural and cultural sites of interest, along with their attribute information, can be stored as spatial objects in a geographic database (Chhetri & Arrowsmith, 2008). Spatial information stored in a GIS provides the tools to gain an understanding of the geometrical and topological relationships of spatial objects in geographical space. A GIS also allows both spatial as well as attribute data stored in the database to be processed using geospatial statistical analysis techniques and mathematical operations. Numerous studies have adopted GIS to support decisions towards planning and managing tourist or recreational spaces. Chhetri and Arrowsmith (2008) identified four main themes of research that use GIS for different purposes (Figure 2-2), including the tourism carrying capacity modeling (Arrowsmith &

Inbakaran, 2002; Navarro Jurado et al., 2012), the recreational opportunity spectrum (Kliskey, 2000), visual resource assessment and modeling (Chhetri, 2006; Schirpke et al., 2013), and nature-based tourism modeling (Bishop & Gimblett, 2000; Gimblett et al., 2001). However, this theme classification tends toward researches in nature-based tourist destination. Other GIS-based studies for tourism/recreation planning and management have also developed in various settings, such as trail planning and evaluation (Chamberlain & Meitner, 2013; Tomczyk & Ewertowski, 2013), recreation value mapping (van Riper et al., 2012; Nahuelhual et al., 2013), site suitability modeling for recreation (Lwin & Murayama, 2011; Kienast et al., 2012), evaluation of spatial centrality of villages in rural area (Lee et al., 2013), analysis of beach availability using remote sensing technique (Yang et al., 2012), assessment of the geographical accessibility of recreational opportunities (Brabyn & Sutton, 2013), creating GIS database on cycle tourism infrastructure (Bíl et al., 2012), and simulating visitor behavior in urban recreational spaces (Moulin et al., 2004). My study is certainly involved in research of visual resource assessment and modeling, and this theme is significant in almost all settings involving tourism/recreation management.

2.3.2. Visual resource assessment and modeling

Visual resource assessment and modeling is used to evaluate the visual quality of landscapes from both objective and subjective elements of human-landscape interactions (Chhetri & Arrowsmith, 2008). Scenic or landscape perception research has contributed to the development of assessment indicators for visual resources. The outcomes have been used in the modeling scenic beauty, which is one typical research

17
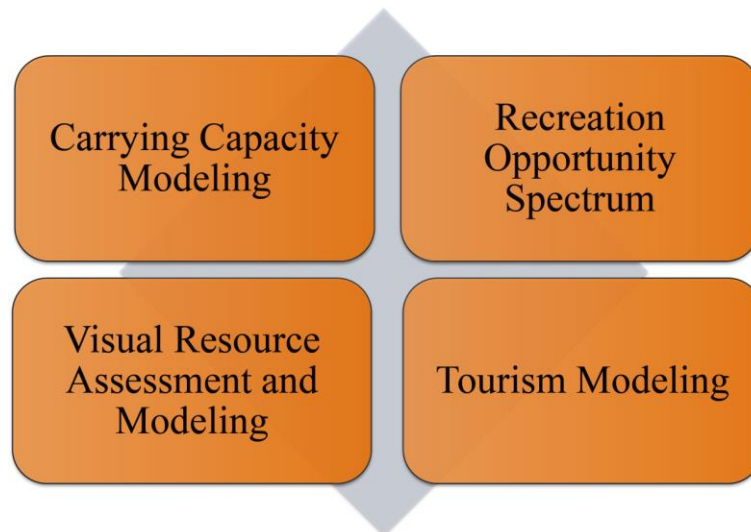
Figure 2-2. Four significant subjects for the GIS-based recreation planning management of a space (Chhetri & Arrowsmith, 2008)

theme of visual quality assessment. The majority of these studies have used a multiple linear regression to derive the predictive model of scenic beauty, attractiveness, or other types of visual quality (Bishop, 1996): in most cases such indicators have been set as dependent variables and estimated by independent variables composed of physical features of landscapes (e.g., Bishop & Hulse, 1994). The predicted results are often visualized on GIS, and the location of high or low visual quality areas may then be identified. Recent studies of model construction have tended to focus on the perception-based assessment or the integral assessment approaches, such as combination of perception-based and expert-based assessment. For instance, Chhetri and Arrowsmith (2008) modeled and predicted the recreation potential of landscape by combining scenic attractiveness modeling (constructed by multiple regression using indicators of landscape preference, collected interviewing predominant visitors) and a neighborhood operation that identified the potential distance from tourist facilities frequented by visitors. Schirpke et al. (2013) developed the scenic beauty model

combining objective methods, which assess spatial patterns of visible landscapes from viewpoints using GIS, with perception-based methods, which reflect the participants' perceptions including tourists at study sites to scenic quality. These studies have mainly focused on natural landscapes such as national parks, protected areas, and forest recreational sites, and assessed the large-scale areas. However, these GIS-based techniques for visual resource assessment in small areas have not been sufficiently developed.

2.3.3. Investigation of visitor behavior using geo-spatial tools

In recent tourism and recreation research, GIS-based micro scale investigations of visitor behavior such as movement and space use have been conducted using several approaches. Most of researchers have used Global Positioning Systems (GPS) for recording visitor behavior. Ostermann (2010) used a mobile GIS as a new tool to capture visitor activity patterns of an urban park, but this approach is not widely used. The Global Positioning System (GPS) is a space-based satellite navigation system that provides location and time information. By using GPS loggers, which are mobile devices capable of logging the location of moving objects such as people and vehicles, we can easily record the spatial and temporal data of movement trajectories of objects. For management purposes, GPS tracking has been widely accepted as a method for investigating visitors' spatial and temporal movements in geographical space (Shoval & Isaacson, 2007a; Chhetri et al., 2010; Shoval et al., 2011; Hallo et al., 2012; Orellana et al., 2012). To implement this technique, a researcher issues GPS loggers to many visitors in a specific place and collects them after visitors' recreational activities are

completed. GPS records high-resolution micro spatial data of visitors' current locations and other attribute data including time, elevation, and speed. Such complex data can help us to clarify not only movement patterns but also the characteristics of visitor behavior from various perspectives; for example, spatial intensity of visitor use (Shoval & Isaacson, 2007b; Shoval, 2008; McKercher et al., 2012), travel mode (Gong et al., 2012; Bolbol et al., 2012), and the effect of environmental influences on visitor behavior (Meijles et al., 2013). Thus GPS-based visitor tracking has diversified in recent times, and its effectiveness has been championed in many previous studies. The spatial patterns of visitors' logs may often reflect their environmental preferences. However, in a precise sense, visitors' logs cannot completely explain what objects visitors prefer, but show only physical conditions at specific times and locations. Researchers need to estimate visitor behaviors and preferences from distributions of GPS logs. A combination of GPS tracking and other surveys that query visitors about their actual experiences may overcome this problem. However, questionnaires are generally constrained by researchers and conducted before or after the experience, and are not able to record preferences directly. To acquire such location-specific experience data, I suggest the use of the spatial information with visitors' photography, which includes not only visitors' perceptions to scenes they encounter but also location and time.

Digital cameras have become popular nowadays (Sugimoto, 2011a). An image taken by a digital camera contains Exchangeable image file format (Exif) data, which can record various types of information. Moreover, geographic coordinates can be recorded if GPS are used in combination with the camera. If photo-taking locations are managed

as point data on a GIS, they can have various usages. On the Internet, photo-based community sites such as Flickr have been created. Many people enjoy such sites by sharing their travel photographs (Lo et al., 2011; Stepchenkova & Zhan, 2013), often managing geo-tagged photographs on Web-GIS. Those user generated geo-tagged photographs have recently been targeted for academic researches such as analysis of regional images (Hollenstein & Purves, 2010; Stepchenkova & Zhan, 2013) and development of information services (Kurata, 2012). It is also possible to extract point data on desktop-based GISs, such as ArcGIS. This software is an effective tool for spatial analysis and the visualization of geographical and spatial events, and has been used for modeling the scenic potential of space in previous studies on tourism and recreation (Chhetri, 2006; Chhetri & Arrowsmith, 2008). However, previous research has not been conducted assessing and modeling the potential of recreational spaces at the scale of small areas. The use of spatial data from visitor-oriented photographs could be an effective method to address this problem. Therefore, this thesis focuses on a spatial analysis and visualization of spatial data from visitors' photographs to assess the potential of recreational sites.

2.4. Outline of the Current Work

I have previously discussed existing work pertinent to the application of photo-taking location data to scenic preference assessment research. Some important findings have been provided from the results; presented here is the representative study from my primary work (Sugimoto, 2013), with reference to the limitations and implications leading the present study in this thesis.

The content of my primary study is related to the visualization of visitor reactions and their preferred stimuli using digital cameras, GPS loggers, and GIS instead of disposable cameras. This method enabled calculation of the spatial accumulation of photographs and, in so doing, helped to visualize such sites. With these tools, I examined the analysis of spatial and temporal patterns of photographing. Spatial analysis of photographs is useful for clarifying which locations visitors prefer, but it is insufficient for understanding visitors' changing awareness of the sequence of attractions. Therefore, I could also shed light on the effects of the sequences in which those scenes first appear to visitors. Examinations of such comprehensive evaluations of spaces could influence planning and design of recreational spaces.

2.4.1. O-site experiment using digital cameras and GPS loggers

I conducted the on-site experiment for capturing the spatial and time-related data of visitor-oriented photographs. The experiment was conducted at Inokashira Pond, which is a main part of Inokashira Park in Tokyo, Japan, as the case. The date was on Sunday, July 10, 2010, when the weather was fine. Participants were recruited from my university as part of the preparation for the experiment, and all were Japanese; there were 12 individuals total, including the students and social workers. Seven participants were males and five were females. Half of the participants were in their 20s, and the others were aged from 30 to 60. Two courses (see Figure 2-3) had been predetermined by the researcher for analysis of sequence patterns of reactions. The participants were divided into halves, each of which was instructed to walk each course. All participants received the camera at the same place, shown as "A" in Figure 2-3, and were asked to

Course 1: A⇒C⇒B⇒D⇒F⇒E⇒C⇒B⇒A
Course 2: A⇒B⇒C⇒E⇒F⇒D⇒B⇒C⇒A
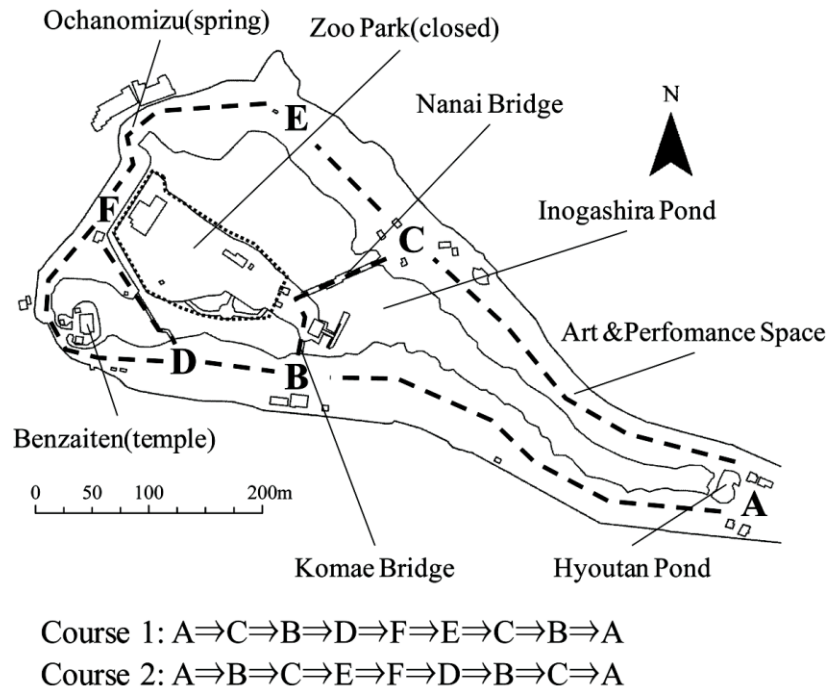
Figure 2-3. The two courses for the experiment

photograph what they viewed as positive scenes along the way using digital cameras and wearing GPS loggers. I did not limit the number of photographs taken by participants, because it is more natural for visitors not to restrict the number of their reactions to the stimulus—if the number of photographs is limited, some participants may not take very many. The operations of the data collection sets were followed by Sugimoto (2011b).

2.4.2. Spatial accumulation of photographs

In total, I collected 448 photographs as data; each participant took 37 photos on average (14 to 76 photos per person), with a standard deviation of approximately 23. I applied kernel density estimation (KDE) with all the photo-taking locations in order to identify spaces where many participants took photographs—in other words, spaces that

were thought to have impressed many participants. When the kernel density of photographs was calculated, the reciprocal multiplied 100 of the number of photographs taken by each participant was used as the weighted value, because the difference in the number of photographs among participants who walked the same course could cause noticeable biases. The maps in Figure 2-4 illustrate the density distribution of photo-taking locations and the distribution of categorized ones. The place that has the highest accumulation is the central Nanai Bridge—here, the field of vision is open on all sides, and we can see the landscape, which has abundant water and green coppices. Moreover, photographs taken there covered various elements such as fish, architecture, boats, and people.

The results show that the accumulative number of photographs varied depending on the locations. Furthermore, some objects were photographed by many participants at locations that showed a high density of photographs. The findings of an experiment by Sugimoto (2011b) revealed that the locations where many objects were preferred and photographed by visitors were almost the same as the locations whose overall impressions were highly rated by the same group of visitors after the experiment. This tendency was the same with this study case. Figure 2-5 shows the spatial preferences of participants evaluated by recording the circle signs after the experiment; this indicates the participants' overall evaluation to the park. In the places where many signs were recorded, the accumulation of the photo-taking locations was also very high. This indicates that we can extract the spatial potential of the place where participants' demonstrated interest and concern by analyzing the density distribution of the photo-taking locations.
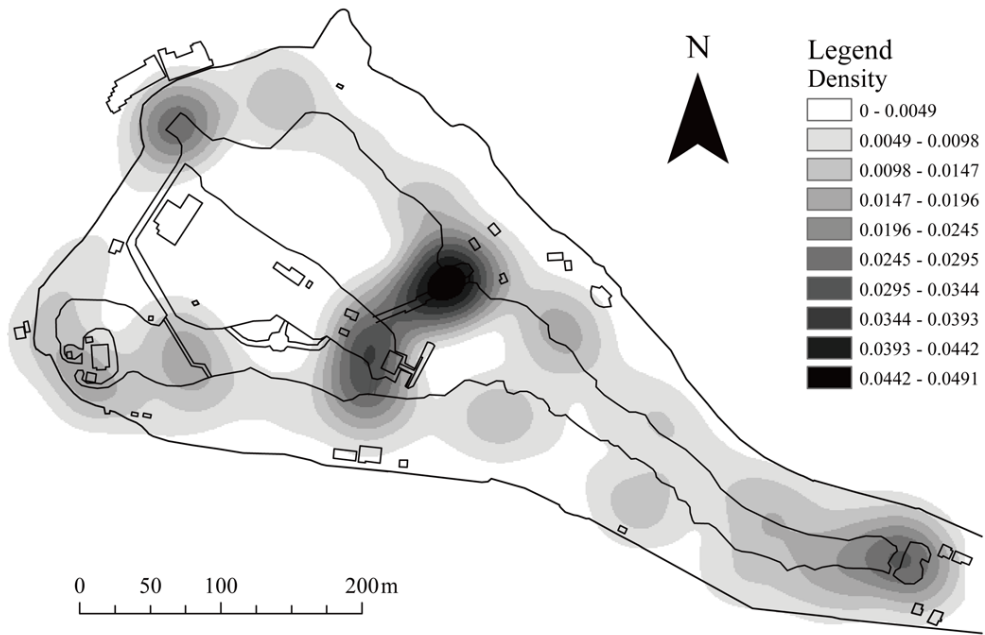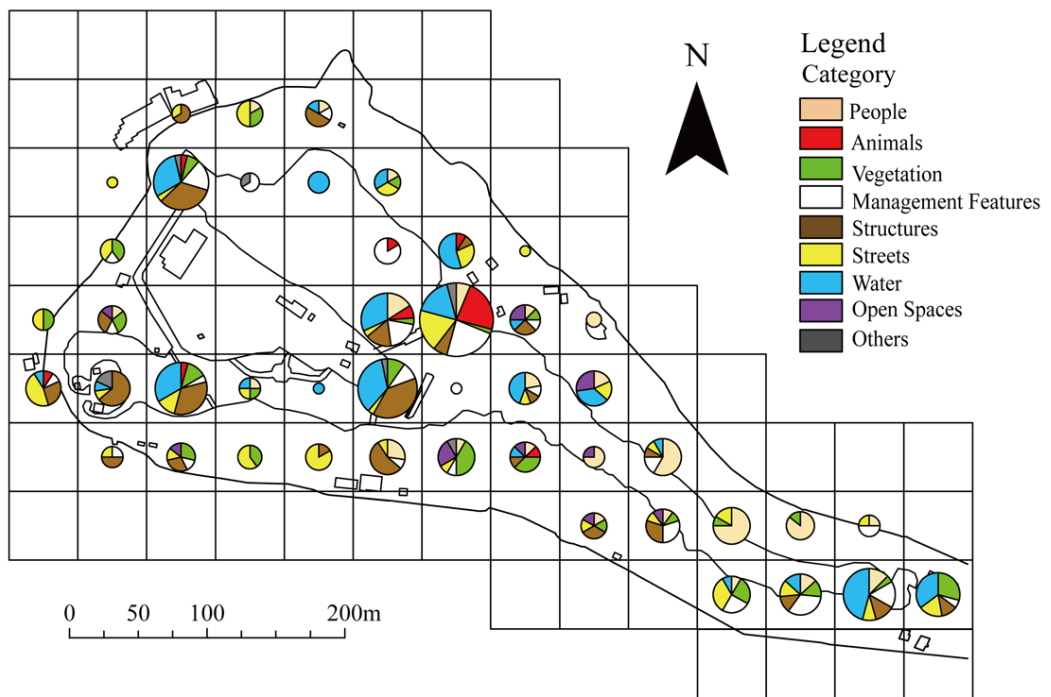
Figure 2-4. Distributions of photo-taking locations by: (a) kernel density estimation with 50-m bandwidth and (b) categorization in 50-m cells

Figure 2-5. The spatial preferences recorded by circle signs of participants

2.4.3. Temporal accumulation of photographs

In order to analyze the accumulation of photographs according to the time, the photo-taking locations were smoothed by calculating the density of photographs. First, the duration of each participant's walking was standardized from 0 to 1, and the point data for all the participants were then combined on the one common axis by each course. KDE on 1-dimensional space was adopted for calculating and visualizing the density of points. The reciprocal of the number of photographs each participant took was used as the weighted value in the calculation of the density in the same manner as in the spatial density computation. The bandwidth was set to 0.03, which is considered suitable for the analysis. When the density of photographs reached its peak in Figure 2-6, almost all participants made their first move to the center of Inokashira Pond on one of the bridges. Therefore, the centers of the bridges could be considered to be "hot spots" in view not only of spatial density of photographs but also of the changes in the

density of photographs over time. Interestingly, though, when the center of the same bridge was passed by participants more than once, they rarely took photographs on the second occasion. This suggests that the participants did not remain interested in the same objects, possibly due to the effects of changing expectation, boredom, and fatigue (Oku & Fukamachi, 2003).

The density of photographs was found to change quite considerably over time; density peaked during the first half of the touring period and showed an overall decline after the peak. Most participants were moving on the center of a bridge when the density of photographs reached its peak; therefore, spaces around the center of a bridge can be argued to have high potential as sightseeing resources. Several landscape assessment studies have found that water is one of the most important attributes (Zube et al., 1982), demonstrating why spaces around the central bridge were preferred. Moreover, the reason many participants were found to take the largest number of photographs earlier in their tours may also be explained by the upsurge in feelings like the sense of freshness when visiting a new place (Markwell, 1997). After the peak, the density of the participants' photographs decreased as their interest in the visited places fell over time. Oku and Fukamachi (2003) illustrated that the pace of visitors' photographing gradually slowed, possibly owing to their increased fatigue and boredom and decreased expectation of attractions. In addition, Hull et al. (1992) have also considered the implications of the sequential characteristics of visitor boredom. They asked the hikers to a national forest to fill out a questionnaire to ascertain their current emotions about 12 landscape views during hiking. According to them, some hikers felt bored when they met the same landscape view (mountain and lake) to one
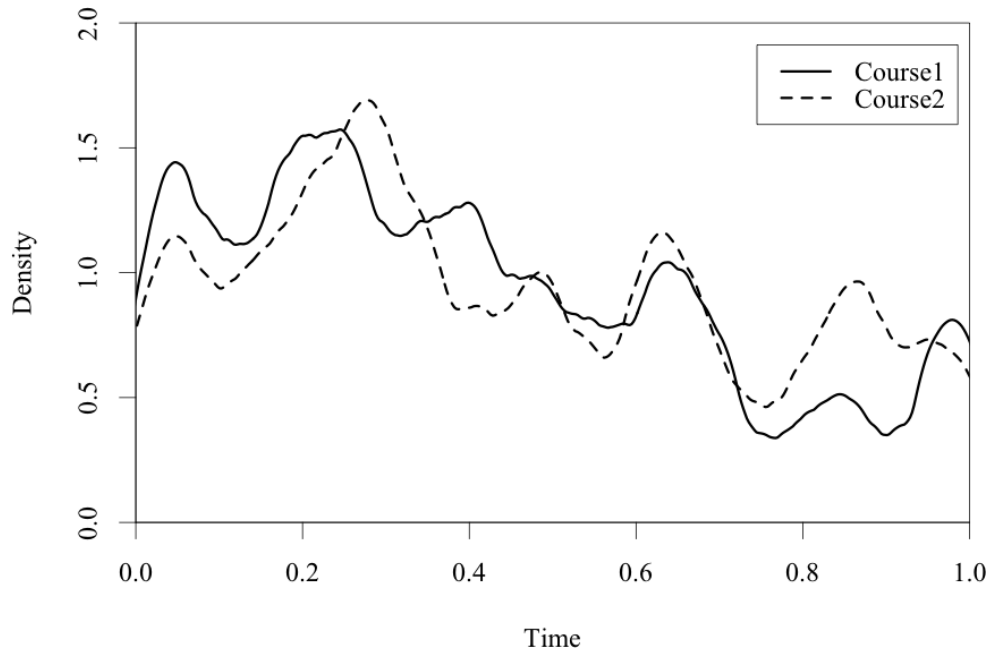
Figure 2-6. The change in the density of photographs for Course 1 and Course 2; the Epanechnikov kernel function and the 0.03 bandwidth

observed previously. Finally, they concluded that visitor's experience patterns seemed to be dependent on the relationship of a person's current state of mind and site characteristics. Although this study found results similar to those from the earlier studies, this study suggests the effects of the sequence in which objects are encountered by visitors. Such an implication may benefit planners who wish to design touring routes that could enhance visitors' satisfaction in light of the sequence of attractions.

Thus, I attempted to examine the spatial patterns and time-series of visitors' interest in elements of an urban park by analyzing photographs taken by participants at Inokashira Pond. The method enabled spatial and time-series analysis of photographs, and, in so doing, could help to identify attractive scenic resources.

2.5. Limitations of the Primary Work

As can be seen from my primary works, the combination of digital camera data combined with geo-spatial tools has great potential to develop an analysis method for assessing on-site scenic preference. It is useful to know the precise location that stirs visitor interest during his or her experience. Large amount of spatial photographic data obtained from visitors were aggregated, which enabled us to evaluate the whole target area. Such analysis also provided insight into location-specific attractiveness by comparing several locations that visitors photographed. However, the primary work is still of fundamental importance. Various statistical and visualization techniques for spatial data have been developed today, and will assist in the advancement of the research. Other traditional statistical techniques, different from density estimation, will also be worthwhile to identify visitors' reactions to scenic features in specific spaces from another perspective. This application of more advanced statistical methods is future work.

The development of research is also possible through the addition of different data types. The primary study used only the spatial data of photo-taking location (spatial object) and visual object category (attribute value) for representing the visitors' reactions in geographic space (the photo-taking time was handled in separate with spatial analysis). Visitor's visual interest occurs in the interaction between visitor and scene he or she encounters. This phenomenon is a complex system of human behavior, so it may be considered difficult to represent it only as spatial point data; the data should be composed of multiple elements such as the photo-taking location, direction, and distance to the scene. Recent rapid progress of spatial tools, including the

increased functionality in digital cameras, has the potentiality to enable us to acquire, analyze and visualize the spatial data of visitor's interest in greater detail. The examination of new types of data is the second area recommended for further work.

This thesis presents several research advances in acquisition, analysis, and visualization of spatial data derived from visitor-oriented photographs. In particular, I examine the use of multiple data types and various spatial analysis and modeling techniques; I then refer to the potential contribution of my studies to the tourism or recreation planning and management sectors.

Chapter 3

Field Survey and Data Acquisition

The process of data acquisition is one of the most essential parts of this thesis, because the data quality depends on the setting of the survey. Many considerations must be addressed in a field survey for collection of behavioral or social science data. Moreover, this study should utilize proper use of digital tools, which are very sensitive, to suppress any mistakes or error occurrences. Sections 3.1 and 3.2 describe the performance of digital cameras as used for measuring visitors' reactions, and show the characteristics of data which need to be collected. Section 3.3 explains a study area as a tourism/recreation site and analysis its landscape structure with 3-D landscape data. The processes of field surveys and data clearance are then explained in the following two sections (Sections 3.4 and 3.5), and Section 3.6 describes estimation of photo-shooting distances. Finally, the spatial data representing visitors' visual interest are generated.

3.1. Understanding Digital Camera and Exif

A digital camera records images taken by an image sensor and stores them for later reproduction. A digital camera utilizes an optical system, using a lens with a variable diaphragm, to focus light onto an electronic image pickup device. Features integrated

into digital cameras enable the immediate display of images on a screen and provide the ability to store and delete images from memory after recording.

Exif is a standard image file format used to record digital images captured by digital cameras. It specifies the existing file format, such as JPEG or TIFF, with the addition of specific metadata tags. The metadata tags defined in the Exif standard can store a broad range of information, including date and time stamps and static information about the camera's settings such as orientation, aperture, shutter speed, focal length, metering mode, and ISO speed. Exif data can also contain the geo-spatial information acquired by the GPS and the electronic compass. The geographic coordinates may be the most common additional spatial information for Exif data, which many users have used for displaying the location and image of photographs in a GIS environment. The process of adding geographic information to a photograph is known as geo-tagging. Another new wave is the addition of directional information to the photograph metadata. This brand-new development in digital camera technology enables us to know the exact value of photo-taking direction, which is included in the Exif-format data.

Combining physical information such as the photographed object (visual scene), the photo-taking location and the photo-taking direction has great potential to expand our ability to analyze the sightseeing behavior of tourist/recreationist in geospatial context. This evolution will impact on the behavioral science in the field of tourism, leisure and recreation and also the traditional scenic/landscape perception research. Moreover, the methods used to acquire such spatial data and the analytical techniques for

manipulating the data into useable metrics can contribute significantly to the research field of geographic information sciences.

3.2. Data Elements

Visual interest occurs in the complex system of spatial interaction between a person and environment. The data used to quantify visual interest is acquired through a person's photography behavior, as recorded by the digital camera and its embedded information technologies. In spatial data representation, person's perceptual response to visual stimuli is composed of multiple elements, which are based on physical and psychological aspects.

The physical side, such as location and time of geographical space, determines the spatial characteristics of visual interest. The positional relation of the observer and visual object is especially important to represent the interaction. This relation can be simply represented by spatial information such as point or linear vector data; for example, the observer's standing location and the object's representative location correspond to point vector data, and their perceptual interaction is represented as line vector data. I use the photo-taking location, photo-taking direction, photo-shooting distance, photo-taking time, and photographic image to construct and provide detailed information about the experience of visual interest in a geo-spatial context.

The psychological side depends on an observer's feeling and impression perceived from a scene. This type of data is collected through investigation of the person's state of mind, such as via a questionnaire, interview, and other methods. Quantification is required to enable statistical analysis of the psychological data. The likeability index is

used for measuring the person's evaluation of visual objects in this study. Likeability represents a psychological construct that provides favorable emotions and meanings experienced in relation to scenes, and this contains visual aspects of scenes and human evaluative responses (Wong & Domroes, 2005). Wong and Domroes (2005) investigated not only liked scenes but also disliked scenes to clarify the scenic preference of urban park visitors, but I do not employ the disliked or negative scenes because it is complex for participants to evaluate scenes by such multiple aspects during on-site experiences.

Table 3-1 shows the seven data elements for configuring the visual interest as spatial data. The photo taking location, photo-taking direction, photo-taking time, and visual scene can be captured by equipping visitors with digital cameras with the necessary with spatial information technologies. The photo-shooting distance needs to be

Table 3-1. Data characteristics and method for data acquisition

Data	Unit	Equipment	Recording	Data generation
Photo-taking location	Geographic coordinates	Digital camera	GPS	Photography by persons
Photo-taking direction	Angle	Digital camera	Digital compass	Photography by persons
Photo-shooting distance	Distance	Laser distance meter Photographic image	Calculation	Estimation
Photo-taking time	Time	Digital camera	Digital Clock	Photography by persons
Visual scene	Photographic image	Digital camera	CCD image sensor	Photography by persons
Object category	Category symbol	Questionnaire	Evaluation by respondents	Questionnaire method
Likeability score	Point scale value	Questionnaire	Evaluation by respondents	Questionnaire method

computed by the specific estimation formula. The variables required for this estimation are collected through the several on-site investigations including a photography survey by visitors. The likeability score and the object category of each scene are evaluated by visitors through questionnaires. The object category reflects visitors' intention with regard to the elements they targeted.

3.3. Study Area

3.3.1. An urban park as a tourism resource

In order to conduct the assessment method of my study, I selected Hibiya Park, an urban park in Tokyo, Japan, as the case. An urban park is a functional place for residents to escape from stress and for tourists to go sightseeing (Wong & Domroes, 2005): The aesthetic, historical and recreational values of urban parks increase the attractiveness of the city and promote it as tourist destination (Chiesura, 2004). Of the
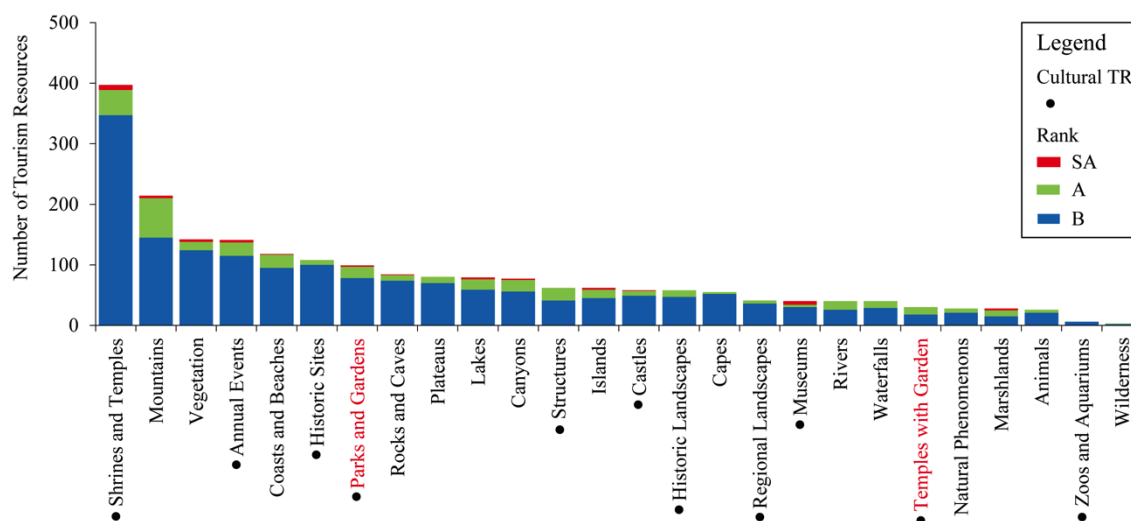
Figure 3-1. Number of Japan's representative tourism resources by category (Tourism resources were evaluated by the Japan Travel Bureau Foundation. The evaluation rank is higher in order of SA, A, and B.)

four grades used to assess Japan's tourism resources (Special A, A, B, and C), as evaluated by the Japan Travel Bureau Foundation (http://www.jtb.or.jp/en), Hibiya Park is rated as Grade B, deemed to be one of the representative tourism resources that can characterize the prefecture (the largest administrative divisions of Japan) in which it is located.

An urban park and similar sightseeing spots such as a garden are popular types of tourism/recreational resources worldwide; most cities have attractive urban parks and gardens, which are often promoted as tourist sites by city governments in their tourist information outputs. Japan boasts many parks and gardens that attract mostly foreign tourists. As represented by the term "Japanese Garden," Japanese traditional landscapes in parks and gardens are regarded as important and effective resources to promote Japanese formal beauty and culture. In addition, compared to other types of tourism resources, the number of parks and gardens represents their significance and popularity in Japan's tourism sectors. According to the database of Japan's representative tourism resources, provided by the National Land Information Division, National Spatial Planning and Regional Policy Bureau, MILT of Japan (http://nlftp.mlit.go.jp/ksj-e/index.html), "parks and gardens" rank 7th of 26 types of natural and cultural tourism resources in Japan in terms of number, and 4th of 11 types of cultural resources (Figure 3-1). This figure is even greater when combined with the category "temples with garden."

3.3.2. Hibiya Park

Hibiya Park is a western-style urban park that opened in 1903. It is adjacent to

streets lined with office buildings in the central business and political districts of Tokyo, such as Kasumigaseki, Nagatacho, Yurakucho, Ginza, and Marunouchi (Figure 3-2). This park has various facilities, including the Hibiya Public Hall, the Music Bowl, the Tokyo Hibiya Public Library, tennis courts, and the Matsumotoro restaurant. In addition, it boasts of natural features such as pine trees, plum trees, azalea gardens, flowerbeds, and ponds, and cultural features such as sculptures, monuments, and bronze statues, which are located all over the park. On the weekend, various types of events are held at the Second Flower Garden and its surrounding environs. Hibiya Park is suitable for examining the new research approach provided in this thesis because the park covers a comparatively small area.

Hibiya Park is constructed with five large zones and over twenty spaces that have different unique characteristics such as gardens, ponds, forests, grasses, restaurants, music halls, libraries, etc. This spatial diversity is one of the reasons that I selected Hibiya Park as a study area, as it enabled the comparison of scenic perceptions in different space characteristics.

3.3.3. Landscape structure

For the visual resource assessment, it might be desirable to grasp the physical and visual aspects of landscape from not only planar mapped information but also stereoscopic spatial data. To understand the physical landscape characteristics of Hibiya Park and its surround area, I used DSM (Digital Surface Model) and DTM (Digital Terrain Model), which are 3-D landscape models created from LiDAR (Light Detection and Ranging) data (Figure 3-3). These data have been provided as the name
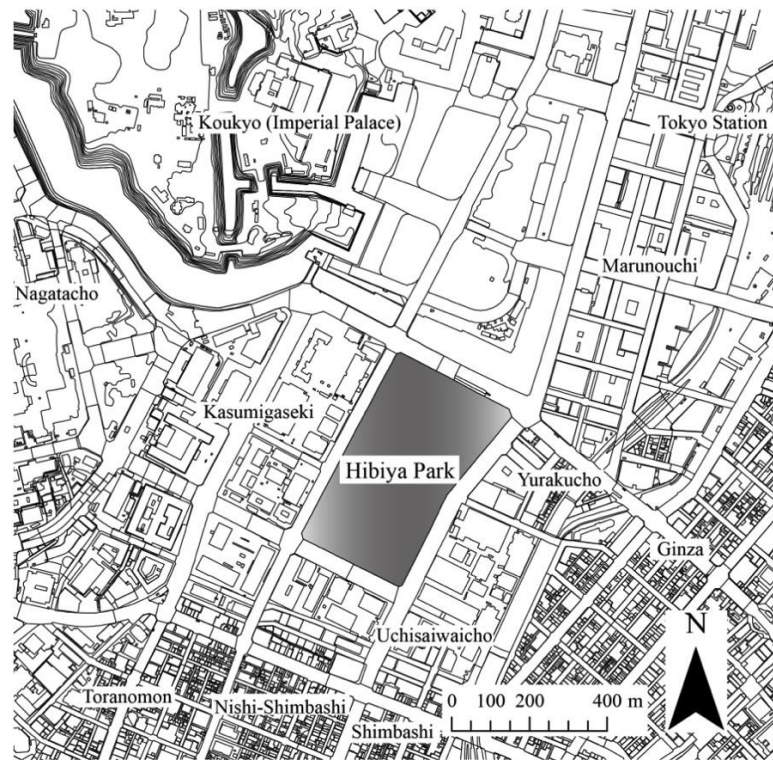
(a)
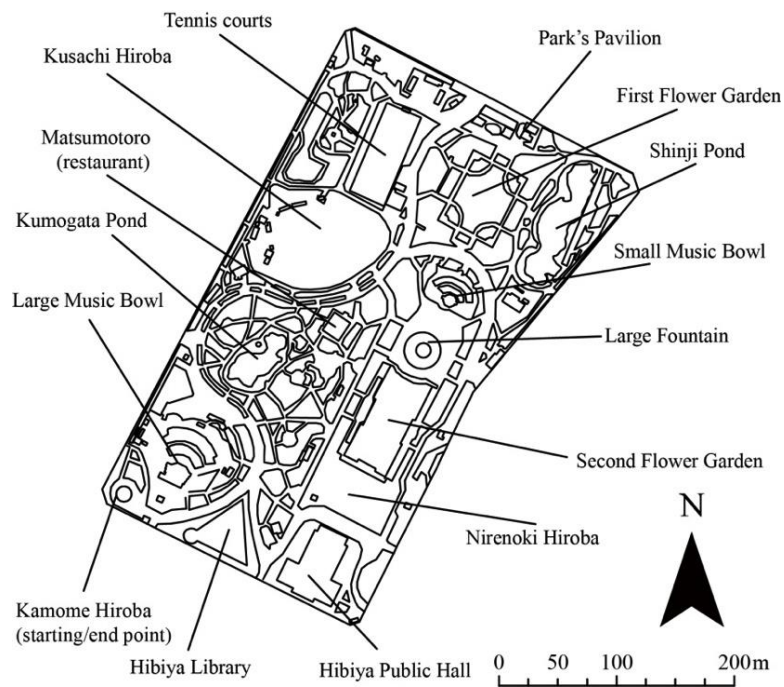
(b)

Figure 3-2. Study area: (a) the location of Hibiya Park and (b) the map of Hibiya Park
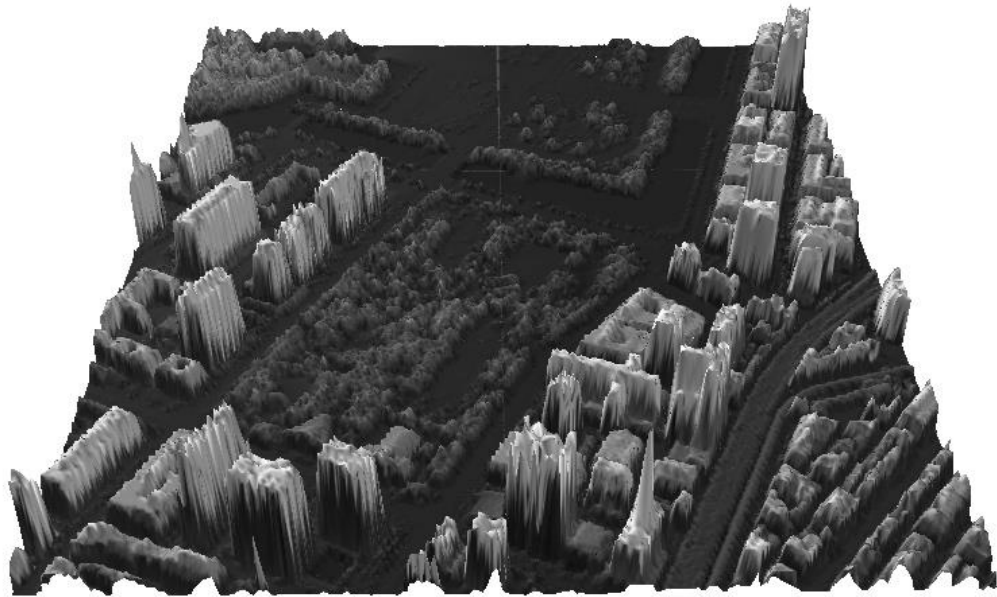
(a)
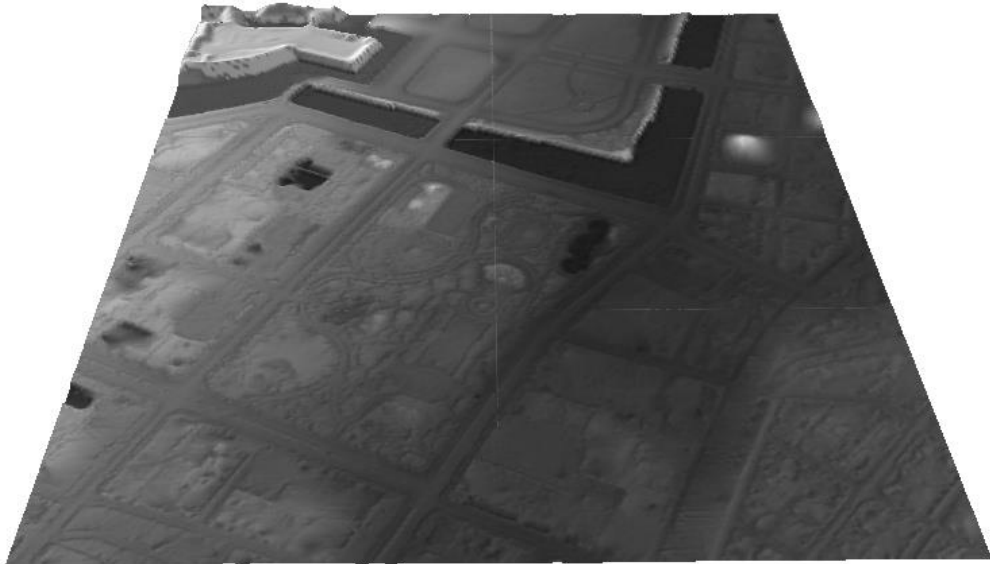
(b)

Figure 3-3. 3-D landscape model of Hibiya Park and its surrounding area with the 2-m grid raster: (a) Digital Surface Model and (b) Digital Terrain Model

"good-3D" by Aero Asahi Corporation. LiDAR is an optical remote-sensing technique that uses laser light to densely sample the surface of the earth, producing mass point

cloud data sets with highly accurate location measurements, including geographic coordinates and heights (ArcGIS Resource Center, n.d.a). The DSM stores the height of earth surface, including the objects existing on the earth ground such as architectures and trees, whereas the DTM stores the height of earth ground in the case with such objects reduced. If such points are transformed into raster data, it is possible to three-dimensionally visualize 3-D model in a good expression. When comparing Figure 3-3 (a) and (b), we can clearly understand the difference between DTM and DSM. The DSM of targeted area describes the location, figure, and volume of buildings and trees precisely, but such spatial information is not in the DTM. From these data, we can confirm that Hibiya Park is surrounded by a lot of skyscraper, and is located on the even ground.

By separating landscape elements in types, more detailed landscape analysis is available. Figure 3-4 shows the raster image of landscape combined with four types of landscape elements; the water surface of ponds and rivers, trees that are higher than 5 meters, buildings, and terrain surface. This map was made through the several spatial operations on ArcGIS (ver.10) to kinds of spatial data including DSM, DTM, DHM (Digital Height Model), which is the data deducted DTM from DSM, and polygon vector data of spatial objects of buildings and water. The spatial distribution and volume of each element can be grasped easily with the representation with changing colors in the kind and height of each grid. As Figure 3-4 is showing, about a half and more area of Hibiya Park is covered with middle and tall trees, but at the same time, the open spaces with high opening degrees, ponds with unique shapes, and some low-height architectures exist.
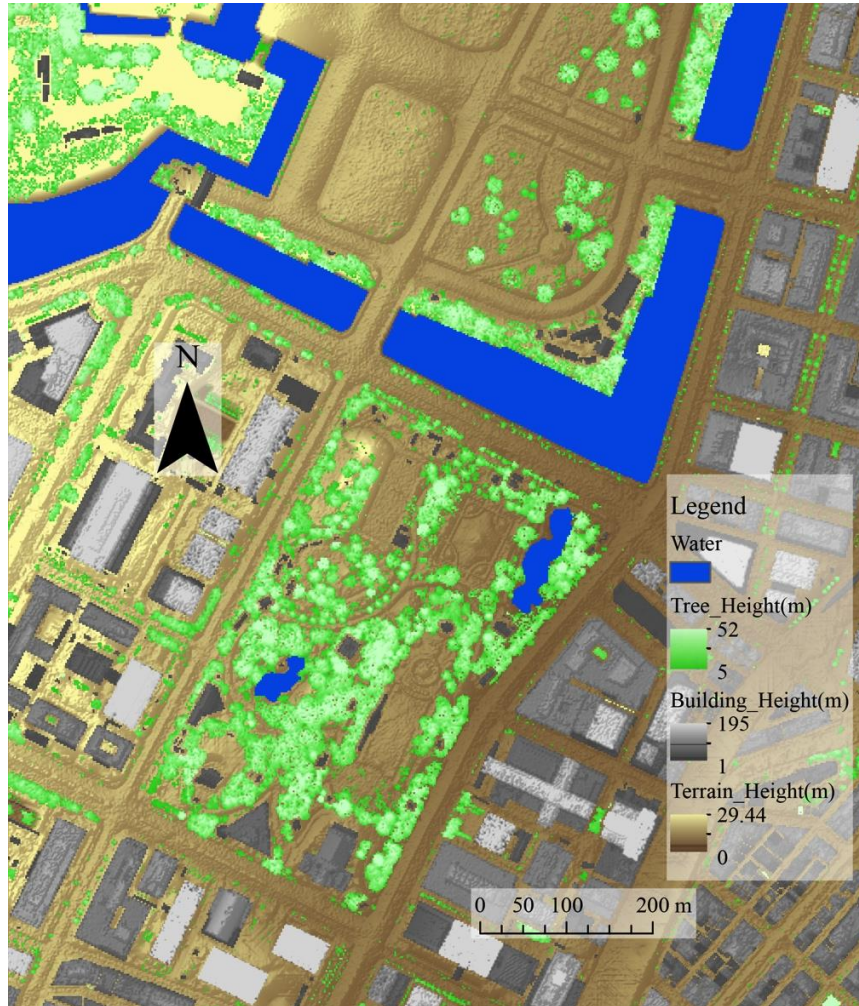
Figure 3-4. Landscape elements constructed by DSM, DTM, and DHM

3.4. On-Site Field Surveys

In order to acquire the attribute values of spatial data of photographs, two surveys are conducted; (1) the photography survey by visitors and (2) the object height measurement survey. The first was achieved through collection of photographs and other relevant data reflecting the persons' visual interest on their scenic perception during sightseeing experiences. The photo-taking locations, the photo-taking directions, the categories of photographed objects and the likeability scores of visual stimuli are included in these. The second was achieved by measuring the height of real objects in

photographs taken by visitors; this information is required to calculate the height of filming coverage in each photograph, and hence the calculation of photo-shooting distance.

3.4.1. Photography survey

The photography survey was conducted on Sunday at 16th October in 2011. The 21 recruited participants, whose ages ranged from their 20s to early 30s, were asked to photograph the positive scenes during walking around the park freely. The number of participants was relatively few, but specifically selected; I chose the younger-generation park users to ensure the reliability of acquired data. Naoi et al. (2011) mentioned that the small sample size utilized in their study necessitated the exclusion of subject attributes such as socio-demographic and psychological characteristics from the scope of investigation; because of this generalization, the results are somewhat compromised. Naoi et al. (2011) recruited a group of 30 university students for the photography surveys in an on-site setting; Chhetri et al. (2004) also selected a group of university students in their research of on-site landscape perception during hiking experiences. In my study, it was difficult to gather large samples due to the length of time required for participants to complete both the photography exercise and the subsequent questionnaire (as per previous studies).

Each participant was handed one digital camera, and map of Hibiya Park; all participants started from Kamome Hiroba located at the southwest end of the park. I prepared Casio's Exilim EX-H20G, a compact digital camera with embedded GPS and electronic compass, for recording the photo-taking location and direction automatically

(Figure 3-5 (a)). After the participants finished their tours and came back to Kamome Hiroba, they were asked to answer the questionnaires about their visual experiences immediately so as not to forget their impressions to each scene they encountered. Specifically, the following measures were taken; firstly, the visual object categories in each photograph were selected and described using at most three categories, from a list of nine. The object type names were also described as auxiliary information to support the accurate determination of photographed objects. The detail of this process is explained later. Secondly, the participants evaluated the preference degree of each scene using a five-point likeability score. The respondents answered these questions looking the photographs projected on the screen of digital camera. The equipment was retrieved after the questionnaires were complete.

3.4.2. Object height measurement survey

The survey of object height measurement was done over two days, the 31st July and 7th August, 2013. The heights of over two hundred objects noted in the photographs taken by participants were measured using the laser distance meter. However, the 116 object heights of these are actually used for calculating the photo-shooting distances. The object height includes both the full length of an object, and the length of key object parts. I used Leica's laser distance meter (model DISTO-D510) combined with a tripod and a support angle adjuster designed for this meter (Figure 3-5(b)). Observers can measure the distance between the bottom and top of object by targeting the laser at these two points. When aiming at the desired point on a distant object, the mounted camera zoom function was found to be useful for targeting a precise point. The

<center>(a)   (b)</center>

Figure 3-5. Equipment; (a) the digital camera, Casio EX-H20G and (b) the laser distance meter, Leica DISTO-D510

measured height of each object was recorded on the paper sheet displaying the image of the object being measured. When it was difficult to measure the object height, the object width was used as the variable for estimation of photo-shooting distance in few cases.

3.4.3. Categorization of photographs

The photographs were classified into nine categories (Table 3-2). Four of these, labeled "people", "animals", "vegetation", "management features", and "structure" are based on their subjects, and the remaining three, which are "streets", "water", and "open spaces", are identified in light of the spatial extension of scenes. The remaining photographs did not share common elements, and were therefore labeled as "others". This classification was identified in my primary works (Sugimoto, 2011b, 2012).

When conducting the questionnaire sessions after the photography survey was

<center>44</center>

Table 3-2. Categories of visual objects in the photographs

No.	Category	Example
1	People	Walking, resting, chatting, taking a picture, festival
2	Animals	Bird, fish, cat, dog, turtle
3	Vegetation	Tree, flower
4	Management Features	Monument, bench, sign, bronze statue
5	Structures	Architecture, building, bridge, stone wall, fountain
6	Streets	Scenery centered on vista of street
7	Water	Scenery centered on water element
8	Open Spaces	Scenery centered on open space
9	Others	Non-categorized to Nos.1-8

complete, I asked the participants to specify the category of photographs in the manner stated above, and also to describe the feature name, which they took as the main object in each photograph. In most studies, the author classified the photographs, but there is some risk of rift between the researcher and actual observer in classification. If photographs taken by participants include multiple elements, it is difficult to know which object was most important for the participant who took the photograph; if classification is conducted by the researcher, it is possible to select a different thing from the person who really photographed it. To obtain good data precision, it is desirable to know the observers' intention whenever possible. This is important to evaluate the visitors' experiences.

3.5. Data Clearance

The original dataset obtained can include some data that is unsuitable for use in the analysis phase. There are two types of data requiring removal or modification; the first

is images generated by user mistakes during photographing, and the other is location information with large positioning errors caused by the condition of the GPS integrated into the digital camera. This thesis took following steps for inappropriate data.

If there were multiple photographs that targeted the same object, I removed the photos taken later from the analysis, and included only the one that had been taken first. This reason is to regard one specific scene projected in photograph as one visual experience. Moreover, I removed the photos that had a negative object or were the result of mistakes in the operation of the digital camera. Next, only the point data confirmed the large gap from an original position because of the error margin of GPS that was corrected to the proper position by corresponding to the photographic imagery.

3.6. Estimation of Photo-Shooting Distance

3.6.1. Lens, object, and real image

To derive an estimation formula of photo-shooting distances, the fundamental principles of thin lens and rays tracing method are introduced. Figure 3-6 (a) shows the relationship between a thin lens, an object, and a real image. This relation holds when using a camera.

When a lens and object are given, three principal rays can be traced from a point on the object through the lens and beyond. First, the "parallel ray" travels parallel to the axis after starting at the object point, and it passes through the image's focal point after refraction by the lens. The second "focal ray" starts at the object point and passes through the object's focal point, traveling parallel to the axis after refraction by the lens.

46

The third "central ray" starts at the object point and passes through the center of the lens, but it is not refracted and continues forward in the same direction. For identifying the place, size, and orientation of an image, it is necessary to trace rays from only two points on the object because the positions of all three corresponding image points cross at one point (Brandl & Effects, 2002).

For the case of a thin lens and paraxial rays, triangulation of the central ray produces the magnification that indicates the ratio of image size to object size.

$$M = \frac{d_i}{d_o} = \frac{h_i}{h_o} \qquad (1)$$

This transverse magnification is most useful in photography (Ray, 2002).

"The thin lens equation," a well-known equation in optics (Born & Wolf, 1999), is

$$\frac{1}{d_o} + \frac{1}{d_i} = \frac{1}{f} \qquad (2)$$

This equation represents the relation among the focal distance, the distance from a central point of lens to an object or a real image in the case of thin lens.

3.6.2. Photo-shooting distance

The object distance d_o and the image distance d_i can be formed by combining the magnification and the thin lens equation.

$$d_o = f \left(\frac{h_o}{h_i} + 1 \right) \qquad (3)$$

$$d_i = f \left(\frac{h_i}{h_o} + 1 \right) \qquad (4)$$

The shooting distance d_s is the sum of d_o and d_i and its calculation formula is given as below.

$$d_s = d_o + d_i = f\left(\frac{h_o}{h_i} + \frac{h_i}{h_o} + 2\right)$$

$$= f\left(\frac{1}{M} + M + 2\right) = f\frac{(M+1)^2}{M} \qquad (5)$$

We can estimate the shooting distance if three variables such as the focal distance, the object height and the image height are known. The image distance is actually much shorter than the object distance (Figure 3-6(b)) so it is possible to omit h_i or replace h_i with the focal distance f. However, I used the equation shown above to estimate more accurately the shooting distance. The necessary input variables were acquired in practice as explained in next section.

3.6.3. Acquisition of variables of the estimation formula

The photo-shooting distances are estimated by substituting the data variables collected by the two surveys for the estimation formula (5). Here, the focal distance f is contained in the Exif data, and the image height h_i is related to the height of the image sensor. In the case of this study, the 1/2.3 inch type CCD is mounted in the digital camera EX-H20G, and accordingly 4.6 mm is used as the image height if horizontal photography or 6.2 mm is used if vertical photography. Because the image height is set as same as the image sensor height, the object height h_o needs to be calculated and set as same as the height of the filming range. The operation for calculation of the filming range height is as follows.

The photographic image data is adjusted to 150 mm on PC, and then the height of object aimed by the participant is measured using the ruler with 150 mm long. Here,

48
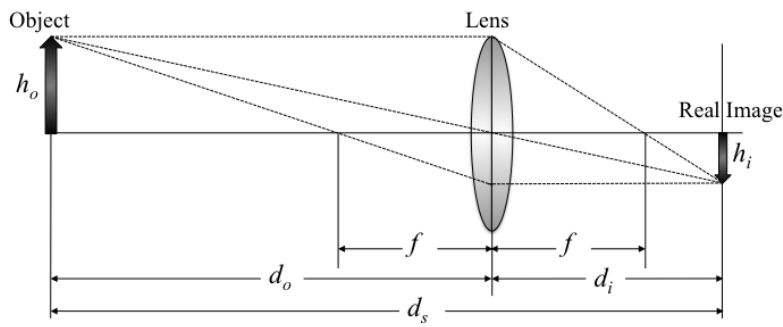
h_o : the object height
h_i : the image height
f : the focal distances

d_o : the distances from the lens to the object
d_i : the distances from the lens to the image
d_s : the shooting distances

(a)
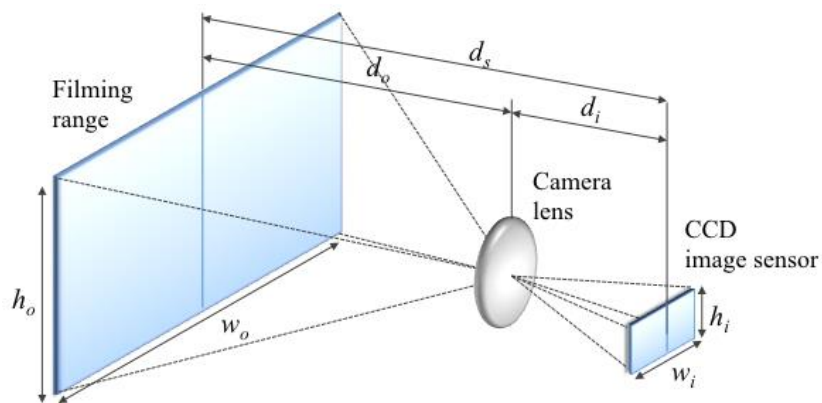
(b)

Figure 3-6. Relationship between the lens, object, and real image in an optical system; ray tracing (a) in the cross section and (b) in the structure of digital camera

the objects that can be clearly recognized as containing a specific element such as "people", "animals", "vegetation", "management features", and "structures" are measured based on the full length or the length of a part of the element. On the other hand, in case of the scenes which sizes or amounts are difficult to be perceived clearly such as "streets", "water", and "open spaces", the things that seem to locate at the end of the person's visual line are used for the measuring objects instead, because of difficulty in measuring the scenes in those categories. As a exception, if there is a landmark object that is important in the composition at the center of the scene, for

49

instance the monument standing at the center of pond, this is used as the end point of visual line. When the filming range height is h_o, the real object height measured in the survey is h_o', the vertical height of the photograph range is h_p (=150mm) and the object height in the photograph image is h_p', h_o is computed by the following formula.

$$h_o = h_o' \frac{h_p}{h_p'} \qquad (6)$$

After this, I computed the photo-shooting distances by their estimation formula. The estimation is also available by using the width of image sensor w_i and the real object width w_o instead of the height in estimation formula (5). As stated above in Section 3.4.2, this processing was applied to few visual objects in this study.

3.6.4. Modification of photo-shooting distance

A correction operation was applied to some photo-shooting distances, as described below. First, shooting distances in scenes categorized in "streets", "water", and "open spaces" are decreased by multiplying the original value by 2/3. This is necessary because the distances of almost all such scenes are calculated based on the distance between the participant's standing location and the end point of his or her visual line (Figure 3-7 (a)). For example, in the case of a scene of pond that is mainly categorized in "water", the distance between the standpoint and the opposite bank is regarded as the first calculated distance. This distance is not appropriate to be used for the reason that the person who took the pond scene has no interest in the object at the opposite bank but is interested instead in the composition of the pond scene. Therefore, the end point of the shooting distance is managed to be included within the pond range so that
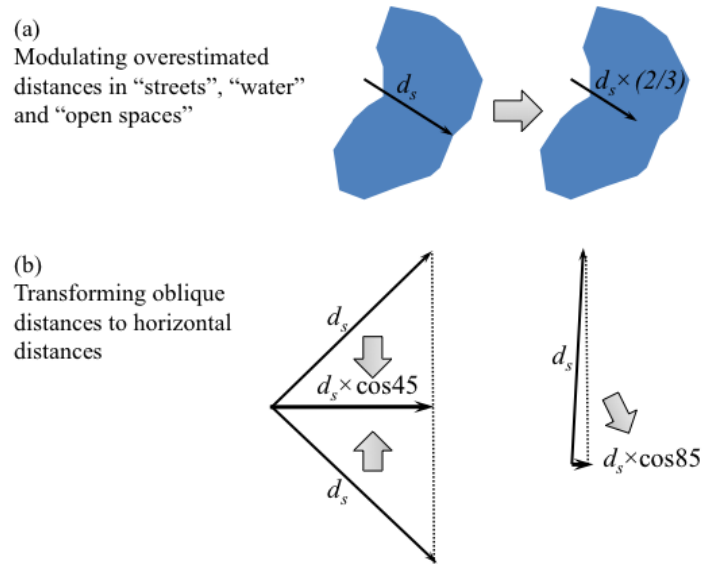
Figure 3-7. Modification of shooting distances; (a) shortening the over estimated distance and (b) transforming an oblique distance to horizontal distance

the calculated distance become more appropriate.

Second, if there are the photographs tending towards oblique directions, the shooting distances of corresponded data are corrected to horizontal directions by multiplying by $\cos(45°)$ or $\cos(85°)$ (Figure 3-4 (b)). The $\cos(85°)$ is only applied for photographs directing at the near right, above such as the scene which looking up to the top of a tree or building from right under them, but the $\cos(45°)$ is used for any photographs clearly tending diagonally upwards or downwards. The authors judged which parameters for correction should be used while assessing a photographed scene.

3.7. Generating Spatial Data of Visual Interest

3.7.1. Points of visual interest

The point data of the photo-taking locations were extracted. I captured the Exif data of the digital photographs in ArcPhoto, an ArcGIS function, and extracted the point

vector data of the photo-taking locations. The point data that was farthest away from the original position was brought back to the original position by identifying it from the photographic imagery corresponding to each point (Sugimoto, 2012). This dataset of spatial point features is referred to as "points of visual interest", or PVI

3.7.2. Lines of visual interest

The line vector data of visitors' visual lines are extracted by using the "Bearing Distance To Line" tool in the Data Management tools of ArcGIS10. This tool creates a new linear feature based on the values in a coordinate field of a line's starting point, bearing field from the north zero degree indicating line's direction, and the line's distance field within a table. In this study, the coordinates of the photo-taking locations (modified in extraction of PVI), the photo-taking directions, and the photo-shooting distances are used as their field values. This dataset of spatial linear features is referred to as "lines of visual interest" or LVI. The starting point of each LVI is equal to the PVI.

3.8. Summary

In the Chapter 3, the methodology of field surveys and data acquisition was explained. The field-based GIS tools described have developed rapidly, and have been applied in various spatial disciplines. The digital camera has become one important tool, allowing us to analyze the sightseeing behavior and scenic/landscape perception in geographical terms.

To acquire the spatial data of visitor's visual interest, two on-site surveys were conducted. First, through a photography survey in which participants used digital cameras with embedded GPS and digital compass functions, I collected digital information such as photo-taking location, photo-taking direction, photo-taking time, and photographic image of visual scene. The likeability score and the category of main targeted visual object in the photograph were captured from the questionnaire after the photography survey. Second, an object-height measurement survey was conducted using the laser distance meter to extract the data variables for use with an estimation formula, derived from the optics for thin lens, for the photo-shooting distance. I then computed the photo-shooting distance of each photograph and modified the distance measurement in some cases.

Finally, spatial data representing the visitors' visual interest were derived from the collected data from the field surveys. Points of visual interest (PVI) were used to identify the visitors' standing locations at the moment the photo was taken. Lines of visual interest (LVI) describe the perceptual interactions between visitors and visual objects in space. Analytical methods for assessing these spatial data are described in Chapters 4 to 7.

Chapter 4

Exploratory Spot Analysis

Human-perceived landscapes have often been researched considering the multi-sensory nature of observer's perception. The focus in this type of research is the difference in characteristics between various perceived landscapes. In ranking several types of scenes and/or scaling, some adjectives representing the person's impression of the visual components have determined such a difference. Hull et al. (1992) and Chhetri et al. (2004) evaluated hikers' experience patterns to natural landscapes by multiple emotional indicators in questionnaires. Fiarwhether and Swaffield (2001) investigated the different types of visitor experiences of landscape by scoring several photographs of regional tourist sites with interviews. Wong and Dormorse (2005) assessed the urban park scenes perceived by residents and tourists in terms of likeability, by asking the respondents to rank prepared photographic scenes. These could clarify not only the differences in scenic preference of each visitor type, but also the hierarchy of scenes, providing important suggestions for designing and managing recreational spaces. This approach can apply to my studies, enabling us to clarify the spatial characteristics of visitors' visual interest by their emotional levels.

This chapter suggests an analysis method for assessing the emotional indicators within visitors' scenic preferences and photo-taking directions, and then clarifies the spot characteristics based on visitors' preference levels. First, the fundamental dataset

of collected photographs and its spatial distribution are explained in Section 4.1. I then explore the spatial distribution patterns of PVI based on visitors' preference levels to visual stimuli, extracting PVI clusters that are of similar or dissimilar likeability based on statistical significance (Section 4.2 and 4.3). Next, the spatial ranges of "spots" are identified based on accumulation patterns of PVI in Section 4.4, and the characteristics of each spot are described using statistical indicators (derived from visitors' evaluations) in Section 4.5. The photo-taking directions and the indicators of preference level at each PVI are used for analysis in detecting the spot characteristics. Finally, based on these results, this study discusses the interpretation of clusters and the hierarchy of spot attractiveness (Section 4.6).

4.1. Distribution of PVI and Their Attributes

The 517 photographs/points utilized in this study is the total valid data for analysis, excluding photographs labeled "others" that were regarded as inappropriate in the previous chapter. Each participant took 25 photographs on average (11 to 54 photographs per person), with a standard deviation of approximately 11.

The spatial distribution of PVI with likeability scores and the histogram count of each score are shown in Figure 4-1. The photographs of score 4 was in the largest number and seen in 143, and the number of score 1 was the smallest and in 68. It is difficult to understand the spatial patterns of PVI distribution with likeability scores from the map in Figure 4-1 (a). The exploratory analysis is required for specifying significant features.

Figure 4-2 shows the distribution of PVI according to eight categories and the count
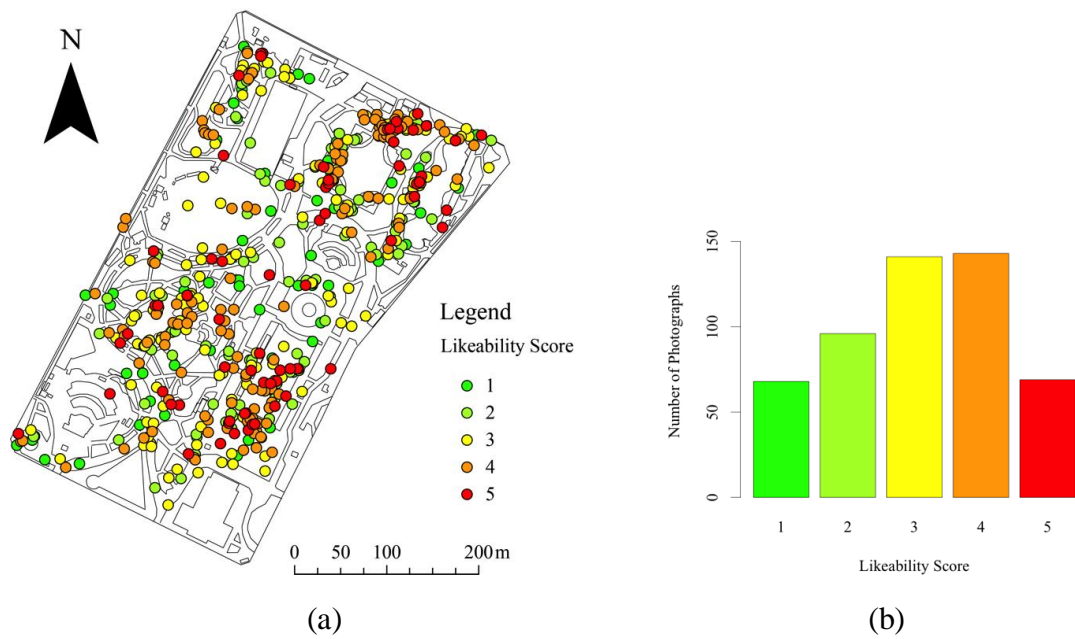
Figure 4-1. Distribution of all PVI according to likeability scores; (a) the map representation and (b) the histogram count

in each category. The results revealed that "people" were seen in 111 photographs, "animals" in 34, "vegetation" in 60, "management features" in 76, "structures" in 105, "streets" in 50, "water" in 41, and "open spaces" in 40. This study found that it was easier to recognize objects of interest if they belonged to "people", "structures", or "management features", while recognition of objects with a spatial extension, such as "streets", "water", and "open spaces" were difficult to recognize. This indicates the reaction of visitors to the complicated spatial characterization presented by the various elements in Hibiya Park.

4.2. Spatial Feature Similarity Based on Preference Levels

4.2.1. Spatial autocorrelation

This study applies the spatial autocorrelation analysis to the likeability scores of
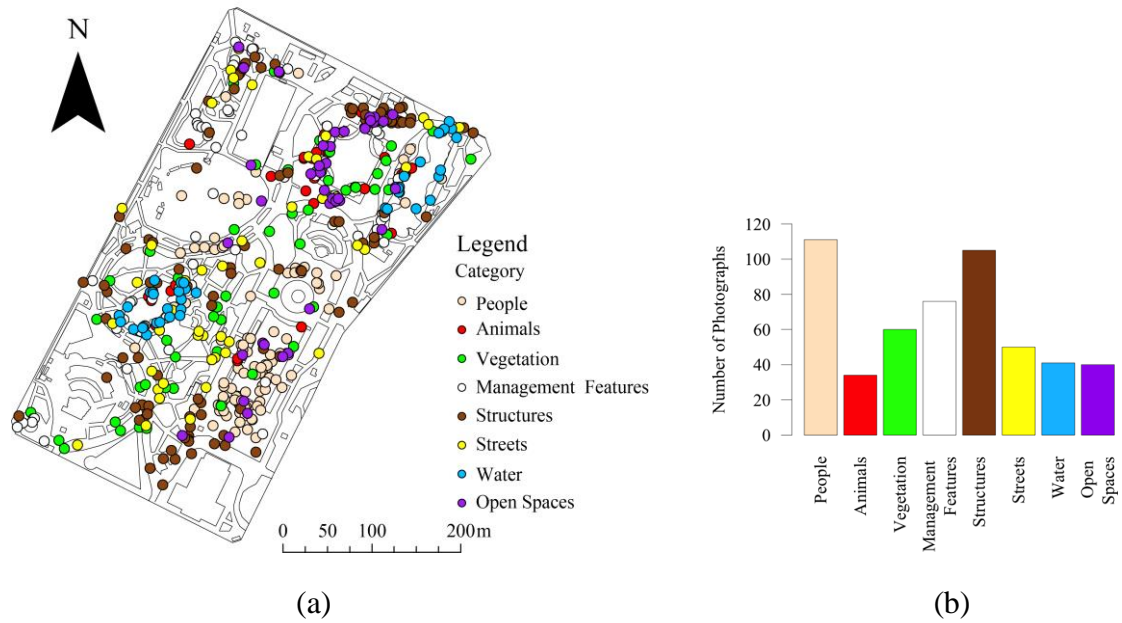
Figure 4-2. Distribution of all PVI according to categories; (a) the map representation and (b) the histogram count

PVI, and extracts the point clusters and outliers based on the similarity of preference levels. Spatial autocorrelation statistics measure the spatial dependency among spatially distributed observations and indicate the degree of self-correlation of observed values in space. There are indicators for global and local spatial autocorrelations.

Global spatial autocorrelation, measured by Moran's I in this study, captures the extent of overall clustering that exists in a dataset. The formulation of global Moran's I is given by

$$\text{Moran's } I = \frac{N}{\sum_{i=1}^{N} \sum_{j=1}^{N} w_{ij}} \cdot \frac{\sum_{i=1}^{N} \sum_{j=1}^{N} w_{ij}(x_i - \bar{x})(x_j - \bar{x})}{\sum_{i=1}^{N}(x_i - \bar{x})^2} \qquad (7)$$

where N is the number of observations, x_i is the attribute value of location (region) i, x_j is the attribute value of neighbor location (region) j, $\bar{x}$ is the mean of observed values

and w_{ij} is the spatial weight matrix. This formula is very similar to the coefficient correlation in standard statistics. The large difference with the correlation coefficient is the spatial weight matrix, which defines the spatial relationships among targeted locations (regions). Where spatial data are distributed so that high values are generally located near to high values and low are near to low, the data are regarded as exhibiting positive spatial autocorrelation (Anselin, 1995; Fotheringham & Brunsdon, 1999), operationalizing Tobler's First Law of Geography, whereby closer areas are more similar in value than distant ones (GeoDa Center, n.d.). However, where the data are distributed such that high and low values are generally located near each other, the data are said to exhibit negative spatial autocorrelation (Anselin, 1995; Fotheringham & Brunsdon, 1999), which exists when high values correlate with low neighboring values and vice versa (GeoDa Center, n.d.). Global Moran's I generally takes a value from minus 1 to plus 1; a positive value indicates the spatial clustering of similar values, and a negative value the clustering of dissimilar values (Anselin, 1995). However, the range of global Moran's I coefficients are not constrained by the range minus 1 to plus 1, depending on the choice of the weights matrix (GeoDa Center, n.d.).

Local spatial autocorrelation indicates the location of local clusters and spatial outliers. Local Moran's I statistics is used for local indicator for spatial autocorrelation (LISA) in this study.

$$I_i = \frac{N \cdot (x_i - \bar{x}) \cdot \sum_{j=1}^{N} w_{ij}(x_j - \bar{x})}{\sum_{i=1}^{N}(x_i - \bar{x})^2 \cdot \sum_{i=1}^{N} w_{ij}} \qquad (8)$$

Generally, the sum of LISAs for all observations is proportional to a global indicator of spatial association (Anselin, 1995). This study provides pseudo-significance levels for

local spatial autocorrelation by comparing the observed spatial distributions to spatially randomized reference distributions.

I apply these global and local Moran's *I* statistics to the likeability scores of PVI, and thereby classify the spatial patterns of PVI distribution in terms of their preference levels. The statistical computation and visualization was achieved with the original programs, which were developed with R (ver. 3.0.1).

4.2.2. Spatial weight matrix

Before the calculation of Moran's *I* statistics, I need to formulate the spatial weight matrix w_{ij}. In this study, to avoid pointless clusters accidentally being created, I used the original method for making the weight matrix (Figure 4-3). A binary matrix was first created based on the relation between a base point *i* and neighbor point *j* on the geographical space. If a point *j* exists in the circle range taking a distance from point *i* as a radius, a point *j* is regarded as an adjacent point with point *i* and w_{ij} give a value 1, and if not, w_{ij} give a zero value. Thereafter, whether two adjacent points satisfied with three conditions are searched, and then the weighted values are changed according to these results.

The first condition is whether the categories of visual objects are the same between two points. If the category of point *i* matches that of point *j*, a one value is added to the weight for point *i* and *j*. If the condition is not satisfied, the weight value is not changed. Next, if the photo-taking direction of point *i* is within the range of plus-minus 22.5 degree from point *j*, w_{ij} increases by one. Finally, if the participant who took point *i* is

Start

$W_{ij} = W_{ji} = 0$ or 1
$(i, j = 1, 2, \ldots, n)$

$i = 1, \ j = k = 2$

$i \leq n-1$ — No

Yes

$j \leq n$ — No → $i = i+1$ → $j = k+1$

Yes

$W_{ij} = 1$ — No

Yes

$X_{ci} = X_{cj}$ — No → $W_{ij} = W_{ij}$

Yes → $W_{ij} = W_{ij} + 1$

$X_{di} \leq X_{dj} \pm 22.5$ — No → $W_{ij} = W_{ij}$

Yes → $W_{ij} = W_{ij} + 1$

$X_{pi} \neq X_{pj}$ — No → $W_{ij} = W_{ij}$

Yes → $W_{ij} = W_{ij} + 1$

$W_{ji} = W_{ij}$

$j = j+1$

End
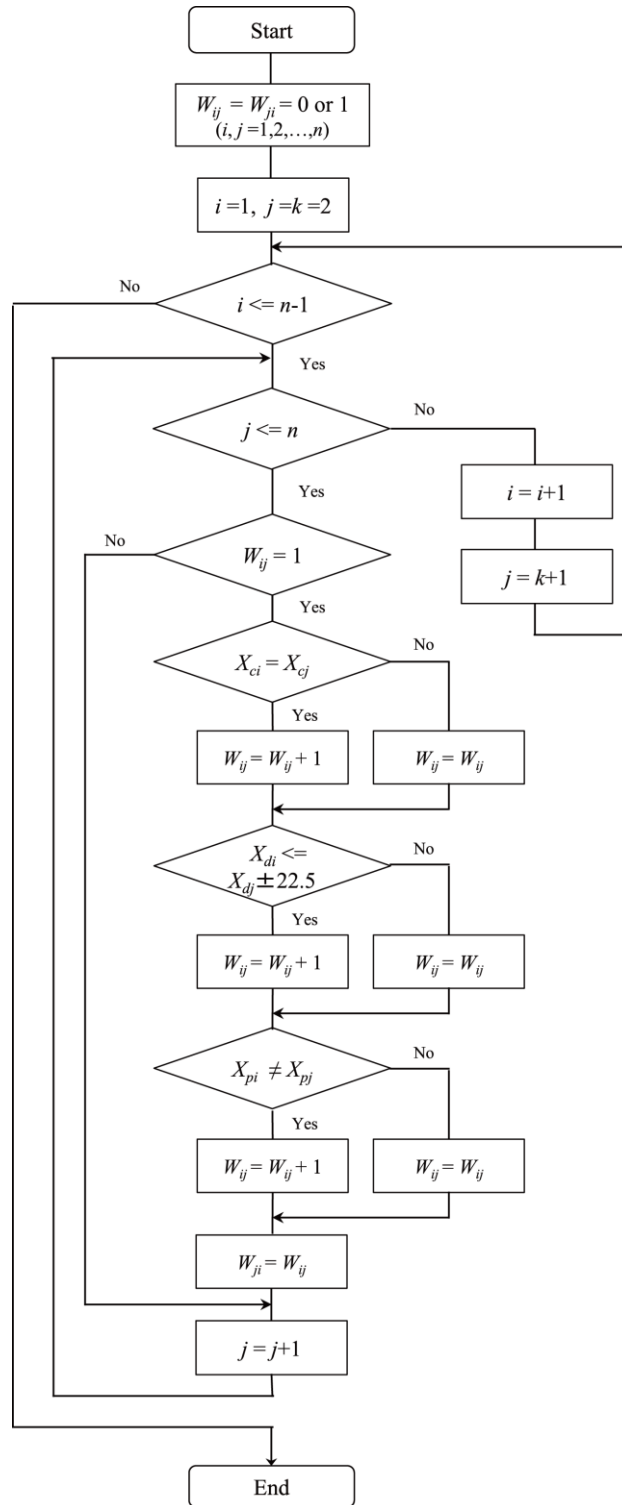
W_{ij} : the weight value for point i and j
X_{ci}, X_{cj} : the visual object category of point i or j
X_{di}, X_{dj} : the direction of point i or j
X_{pi}, X_{pj} : the participant ID of point i or j

Figure 4-3. Flow of making original spatial weight matrix

different with the one of point j, the weight take more one value. The purpose of setting the third condition is to reflect the view that the case in which different people show their interest at a specific spot is more important for evaluation than the case in which the same person shows ongoing interest. When all conditions are fulfilled, the weighting may be up to four.

The size of the value to be added is determined based on following conditional expression.

$$max\left(w_{ij}+1\right)\cdot min\left(x_j\right)\leq min\left(w_{ij}+1\right)\cdot max\left(x_j\right) \qquad (9)$$

x_j is the likeability score of neighbour point j. This expression limits the excessive weight setting.

4.2.3. Determining search bandwidth

I need to determine the search distance from points to make the spatial weight matrix. Here, I focus on the relationship between the Global Moran's I and the Local Moran's I.

$$I=\sum_{i=1}^{N}\frac{I_i}{N} \qquad (10)$$

Thus, the Global Moran's I is given by the mean of Local Moran's I (Anselin, 1995). This relation suggests that the absolute value of Local Moran's I become higher overall, or locally as the Global Moran's I is higher, increasing the possibility to extract more clusters (Anselin, 1995). Therefore, I examined several patterns of search distance and used the distance where the Global Moran's I take the maximum value from several patterns. The search distance is increased by 1-m from 36-m to 136-m, which is the
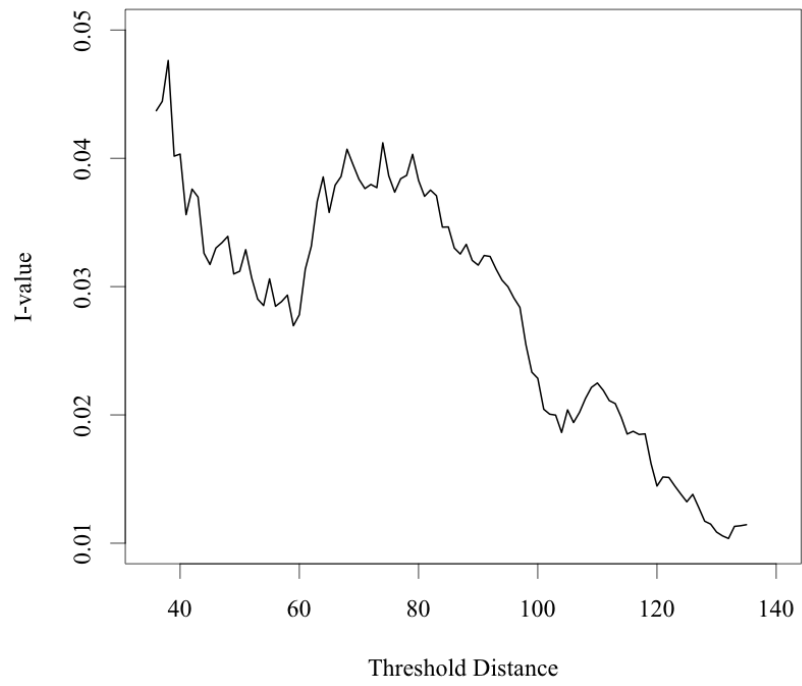
Figure 4-4. The change of global Moran's *I* value in threshold distances
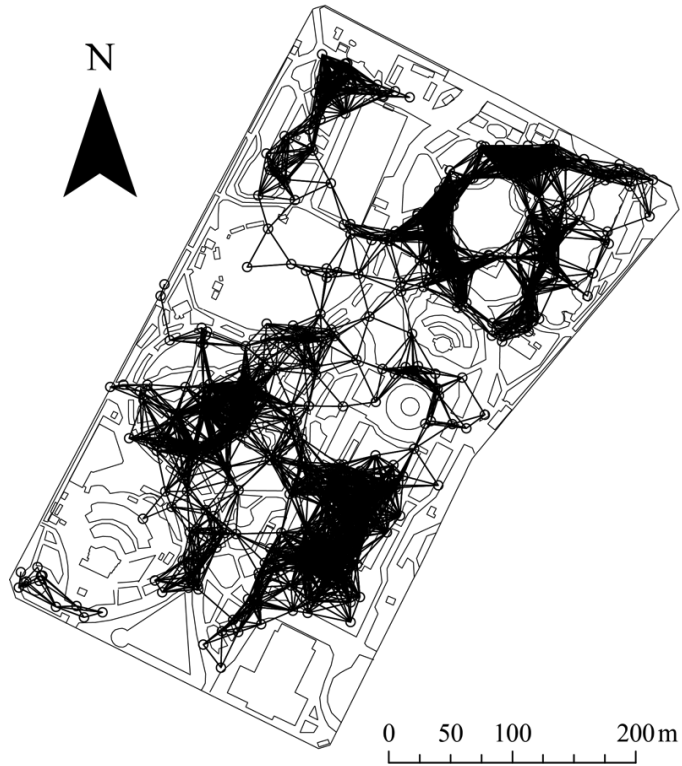
Figure 4-5. Neighborhood relation among PVI

shortest distance that permits each point to have a neighbor relationship with at least one other point. The result is shown in Figure 4-4. The Global Moran's *I* statistic takes the maximum value 0.048 when the search distance is 38-m. This distance was chosen to compute the Local Moran's *I* values. The original spatial weight matrix was made intending to be suitable for clustering points based on the short search distance, and we can consider this 38-m distance as suitable for analysis on such an intention. Figure 4-5 shows the spatial neighborhood relationship among points in the case of 38-m distance, which are represented by black lines that connect points in neighborhood.

4.3. Local Spatial Clusters of PVI

4.3.1. Extraction of point clusters

This section shows the derivation of the Local Moran's *I* value of each point using the original spatial weight matrix and the search distance 38-m, and describes the computation of the significant spatial cluster outliers for each point based on this Local Moran's *I* value.

A randomization approach is used to generate a spatially random reference distribution in order to assess statistical significance. A numeric permutation test is conducted to describe the computation of pseudo significance levels for local spatial autocorrelation statistics. To determine how likely it would be to observe a specific spatial distribution, actual values are randomly reshuffled at a given number of permutations (GeoDa Center, n.d.).

The likeability scores in all points were reshuffled at 999 numbers, and the randomly simulated Local Moran's *I* values were generated. The permutation tests in this study

63

follow those of Anselin et al. (2006), so the significant statistic is computed as $(M + 1)$ $/ (R + 1)$, where R is the number of replications and M is the number of instances where a statistic computed from the permutations is equal to or greater than the observed value (for positive local Moran) or less or equal to it (for negative local Moran). The tests are applied to all 517 observed Local Moran's I values. The points with p-values that are lower than 0.05 (positive local Moran) or higher than 0.95 (negative local Moran) are regarded as the spatially significant clusters or outliers. Therefore, this study use two-sided significance tests.

A Moran scatter plot (Anselin, 1996) is used for clustering the extracted outliers. The Moran scatter plot visualizes the type and strength of spatial autocorrelation in a data distribution (GeoDa Center, n.d.). This provides the linear association between the
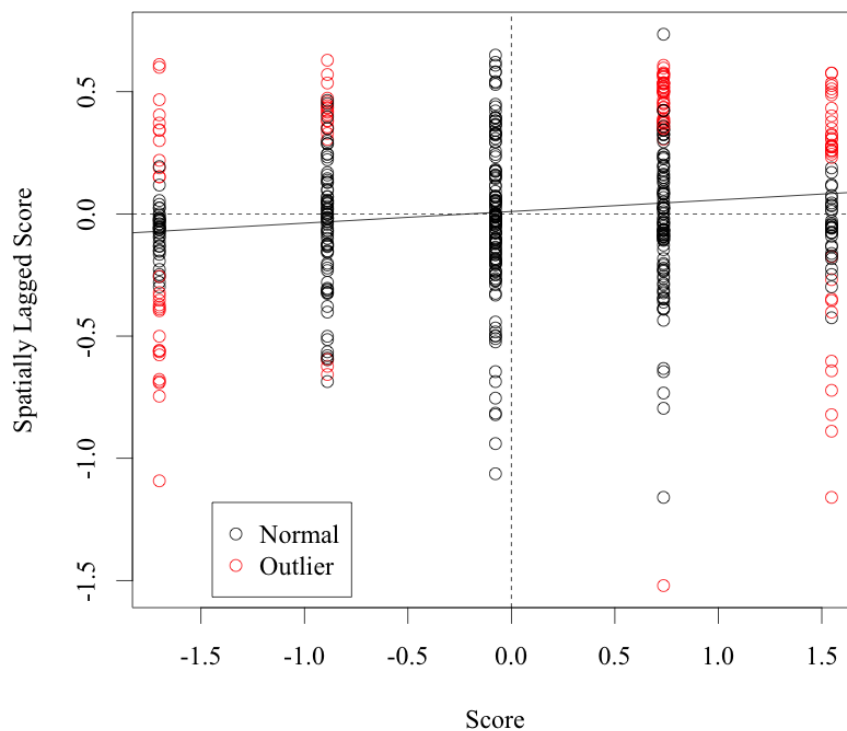
Figure 4-6. Moran scatter plot

64

variables of observations (x-axis) and those in the spatially lagged transformations from observations (y-axis). The slope of the scatter plot corresponds to the value for Global Moran's I (Anselin, 1996). The four quadrants of the scatter plot describe an observation's value in relation to that of its neighbors and correspond to the clusters and spatial outliers in the LISA maps: Clusters of high-high or low-low values for positive local spatial autocorrelation and high-low or low-high values for negative local spatial autocorrelation. Figure 4-6 shows the Moran scatter plot of likeability scores (x-axis) and the spatially lagged scores (y-axis); these are variables used to average the neighboring point values. We can find that the outliers are distributed away from zero.

4.3.2. Spatial distribution of PVI with local spatial autocorrelation statistics

Figure 4-7 (a), (b), and (c) show the spatial distributions of points with attribute values of the Local Moran's I values, p-values and the cluster outliers based on the four quadrants of the Moran scatter plot. The points with high Local Moran's I values are concentrated in specific locations, since this indicates the accumulation of points with similar high values on preference levels, while the points with low values are dispersed (Figure 4-7 (a)). According to the distribution of p-value (Figure 4-7 (b)), the points with low p-values for the positive spatial autocorrelation accumulates as the same tendency with the high Local Moran's I values distribution. These results do not show the cluster distributions, but the degrees of Local Moran's I values or significance are described in detail.

The distribution of cluster outliers is shown in Figure 4-7 (c). The locations of
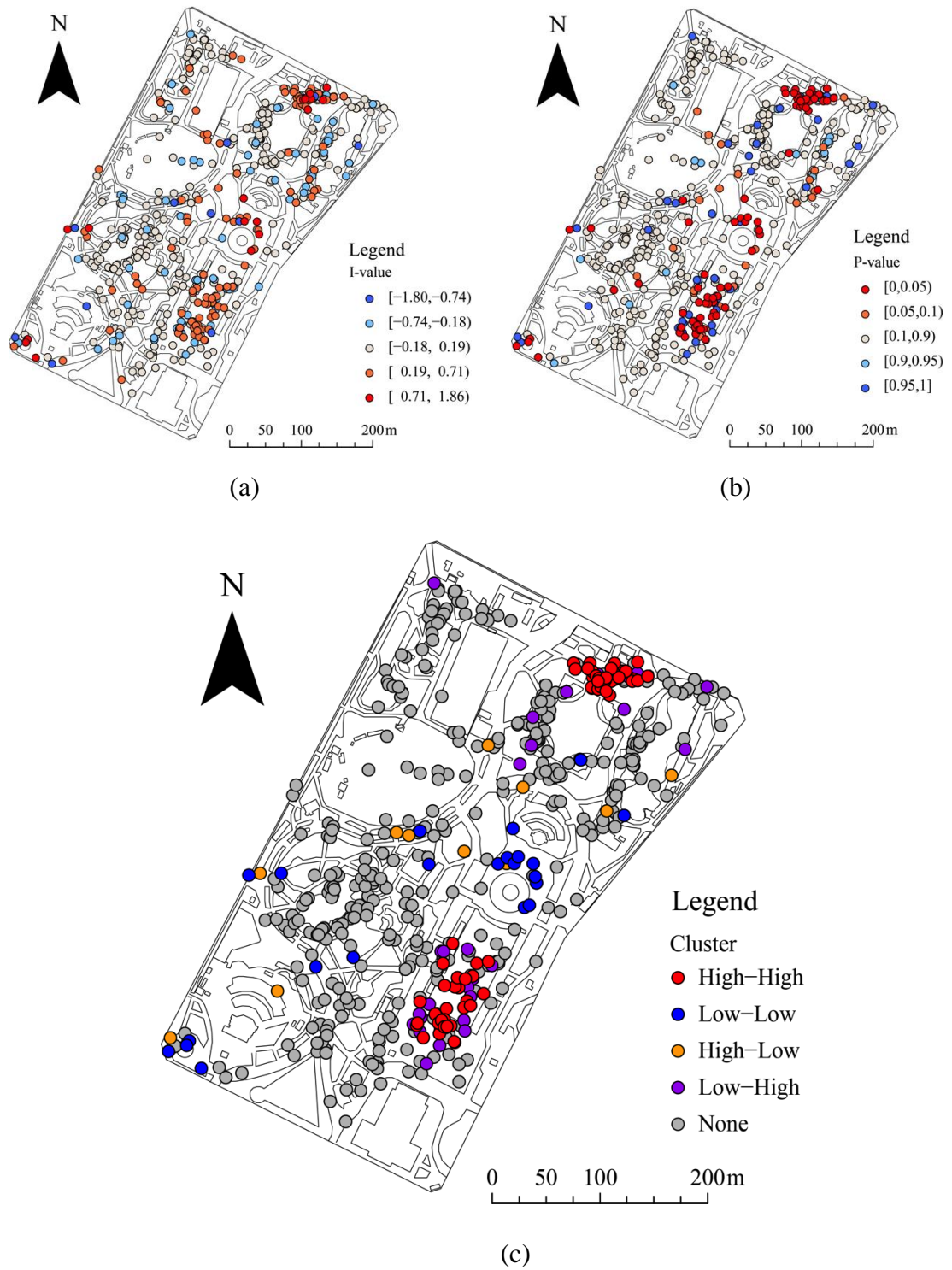
Figure 4-7. The results of the local Moran's *I* statistics: (a) *I*-value, (b) *p*-value, and (c) significant clusters

high-high (the high value in observed score and spatial lagged score) cluster, regarded as the high attractive spots, were found near the First and Second Flower Garden, which have different characteristics for sightseeing. The locations of low-low cluster existed around the common fountain. Moreover, the points of high-low clustering were randomly scattered, and the low-high points distributed surrounding the points of high-high clustering.

4.4. Detecting Spatial Range of Spots

In this work, I applied density contours as the extraction method of spot ranges. First, the density of all the PVI is calculated and the raster data of density map is obtained. The kernel density estimation is used for density computation; the bandwidth is set as 38-m and the raster cell size is set as 1m-square grids. Thereafter, the raster data is transformed into the polygon vector data of density contour using ArcGIS10 Spatial Analyst extension tool (Figure 4-8). The interval between the contour line was set to 0.001. The spatial ranges of the density with high values are the places where the visitors' interest is focused and can be regarded as the important spots. The spatial ranges surrounded by the contour lines having high values 0.01 are extracted as the polygon data of spots. Moreover, the spatial ranges over which the points accumulate locally, and separately from the high density values, are also extracted (the values of contour lines are 0.004).

Using the density contour representation is useful to extract the location and range of spots in a flexible manner. We can determine the spatial range by looking the contour lines and confirming whether their spatial ranges are suitable as the spot candidates.
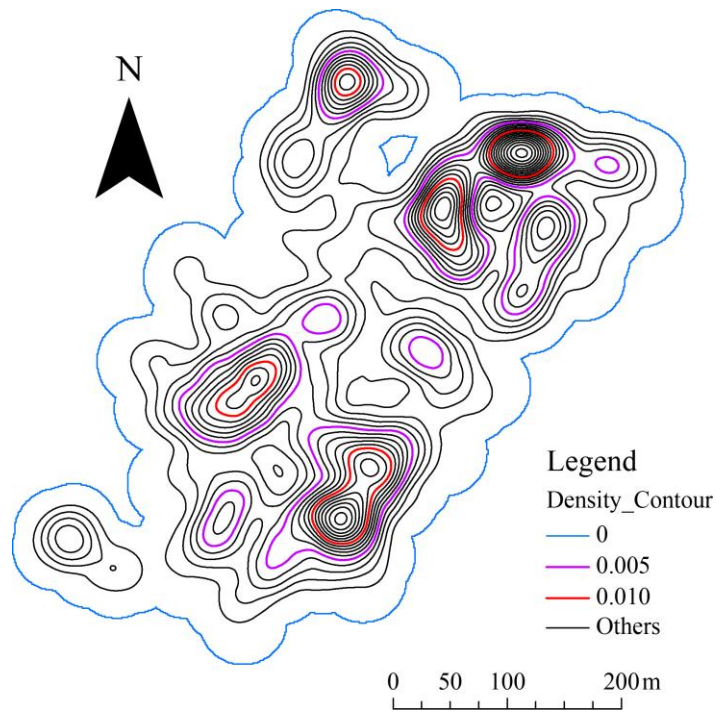
Figure 4-8. The kernel density of all points with a 38 m bandwidth and a 1 m×1 m raster cell size
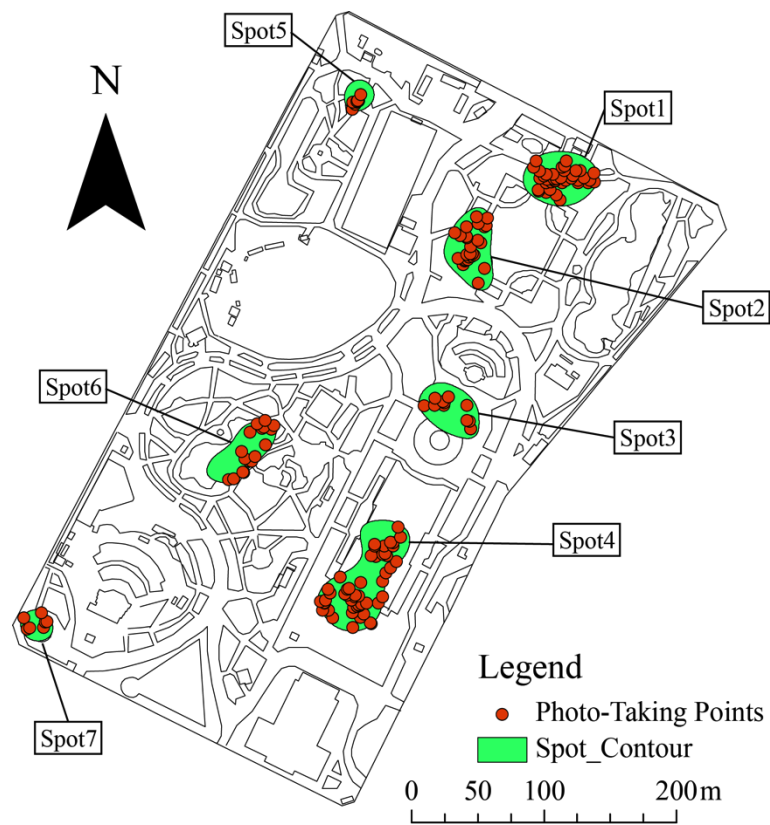
Figure 4-9. Seven spots determined by the density contour

The spots extracted by the density contour are shown in Figure 4-9. There are total seven important spots in the park. The spatial range of each spot has not a simple shape but a unique shape. The reason for this result is that the spot range reflects the spatial pattern of point accumulation. The creation of flexible spot shapes is one of merits of spot extraction using density contours.

4.5. Analysis of Spot Characteristics

4.5.1. Spot profiles

In order to clarify the characteristics of each spot, I suggest making "a spot profile". The spot profile expresses an evaluation of a certain spot from visitors' views, according to a set structure. It can be considered that the value of a given spot (or view spot) is mainly formed by physical aspects such as location, visual objects observed in the landscape when viewed from that site, or social or behavioral aspects such as visitors' evaluation. A spot profile, or representation, based on these aspects would be useful to understand spot characteristics in detail. I created spot profiles containing (1) geo-spatial related data, (2) quantitative data of visitor's evaluation to visual objects at each spot, which are described as several kinds of graphs, and (3) mixed data of both types. The first data type includes a location and spatial range of each spot (Figure 4-9) and representational scenes at each spot (Figure 4-12). The second data type has the behavioral data of visitors' photographing and preference levels to visual scenes at each spot (Figure 4-10 and 4-11), analyzed by the descriptive methods of circular statistics and basic statistics. The last data type is the spatial difference between participants' observed fields and the viewshed from each spot (Figure 4-13).

Circular statistics is the subfield of statistics that deals with cyclic or periodic data, such as direction or time, on a circular scale (Fisher, 1995; Mardia & Jupp, 2009). Circular scales do not have a true zero point. There are several disciplines of social and behavioural science that have applied circular statistics; for example, in the assessment of direction taken during journeys to work (Corcoran et al., 2009), directional distortions of cognitive maps (Cadwallader, 1977), temporal movements of park visitors (Chhetri et al., 2010), and crime incidents (Brunsdon & Corcoran, 2006). This study uses circular statistics to describe the frequency of visitor viewing orientations at a specific spot.

The circular plot is used to describe the photographer's direction, intended subject and shooting distance (Figure 4-10). For a specific spot, the photo-taking direction of each PVI is plotted along the circumference of a unit circle, and the point's color indicates the category of a visual object. In addition, the kernel density for circular data is used and visualized around a unit circle in order to represent the intensity of directions. The two summary quantities of circular statistics, the mean direction and the mean resultant length, are also calculated and visualized on the circular plot. The mean resultant length is a quantity of dispersion for circular data and lies in the range from 0 to 1. In the circular plot of this study, the mean resultant length is represented as the length of the red arrow, from the center point of a unit circle (the direction of red arrow is defined by the mean direction). R=1 implies that all directions are coincident, but on the other hand, R=0 does not imply uniform dispersion around the circle and is not a useful indicator of dispersion or spread of the data. The difference in mean resultant length from 1 is called the sample circular variance, being similar to the variance of

linear data. As the last indicator in the circular plot, the photo-shooting distances are combined and visualized. The black lines, which extend from the center of a circle to the points in the circumference, are the photo-shooting distances for which length is normalized from 0 to 1.

The data are organized according to the eight visual object categories at each spot; this information may be visualized using the histogram (Figure 4-11). Total aggregation in each category is subdivided into the clusters of preference similarities extracted by the Local Moran's *I* statistics. This graph helps us to know which type of visual object is more significant at each spot.

The viewshed analysis is a popular GIS-based technique that identifies the locations of visible objects from a particular point or line, outputting the raster image that contains visible cells. The tool is normally set in the extension of ArcGIS Spatial Analyst. The DSM points in each spot are used as the observation points, and the raster image that contains the height of DSM in the study area is used as the base for identifying the viewshed. Computed raster records the height of the top of objects above the ground surface, such as the architecture and vegetation at each location. The limitation of the region is possible by specifying various items in the feature attribute dataset (ArcGIS Resource Center, n.d.b). By applying this function, the observed fields of photographed scenes can be identified. I gave the specification to the following items; the elevation values of observation points, vertical offsets, horizontal and vertical scanning angles, and scanning distances. The elevation values of observation points are set as the heights of DSM at the same location. The vertical offsets are identified at a 1.5-m height, which indicates the Japanese's average eye position, from

the ground surface height of the park, which equals the DTM height. The horizontal and vertical scanning angles are regarded as the same as the angles of view of photographs and can be computed by the following formula.

$$\theta_{w,\,i},\,\theta_{h,\,i} = \frac{180}{\pi} \times 2\tan^{-1}\left(\frac{x}{2f_i}\right) \quad (x=w,\,h\,) \qquad (11)$$

$\theta_{w,\,i}$ and $\theta_{h,\,i}$ are the horizontal and vertical angles of photograph i; f_i is the focal distance of photograph i; w and h are the length of wide and height of CCD image sensor of a digital camera. The scanning distances are set as the photo-shooting distances. Here, the photographs of "people" and "animals" are given zero value in the scanning distances because the consideration of such moving objects is meaningless in this physical assessment. Therefore, the computed observed fields target the static objects such as "structures," vistas of "streets," or views of "water" and "open spaces." In addition, the scanning distances of photographed scenes in "open spaces" were given an extremely large value because the buildings surrounding the park, which can be seen at a distance from the spots within the park, were perceived as the important landscape elements or backgrounds for the participants. The photo-shooting points in each spot are used as the observation points for calculating the observed fields. Then, both the viewshed and the observed field are displayed on the same map (Figure 4-13).

4.5.2. Characteristics of each spot

I explain the characteristics of seven spots by Figure 4-9, 4-10, 4-11, 4-12, and 4-13. Spot 1 is located on the north trail of the First Flower Garden. The evaluation of this spot reveals that the visitors' interest is mostly toward the visual objects of "structure",

"management features", and "open spaces". The number of "structure" photographs taken is the largest in all categories. The participants took photographs of the architectural features in north direction and the sculptures of twin pelicans or the opposite open space at south direction. The mean direction tends toward the north direction but the mean resultant length shows the high variance because of the multimodal distribution of data. The photo-shooting distances are different at north and south directions; the distances at south are longer than the ones at north. Although the viewshed contains the area in the long distance at various directions, except north from the spot, the observed fields have spread to the southerly direction within a comparatively small angle, including the buildings behind the park as the borrowed scenery, not mainly focused on by the participants. In terms of preference level, as many high-high clusters were found in a number of photographs in almost all categories, it can be surmised that visual objects were evaluated highly from this spot.

Spot 2 is the space on the southwest trail of the First Flower Garden. The "animals", "vegetation", and "open spaces" are the main visual objects evaluated by the participants. The clusters extracted by the Local Moran's *I* statistics cannot be seen for Spot 2, except for a few low-high clusters. This indicates that the PVI do not exhibit similar preference levels in the neighborhood relations. In the circular plot, the variance of directional data is very high, but focusing on the category and distance of data, I can find there are roughly two patterns in distribution; the visual interest towards "open spaces" at the directions from southeast to northeast and those towards "vegetation" and "animals" at the directions from southwest to northwest. The former's observed field is by far wider than the latter's. This tendency is similar to
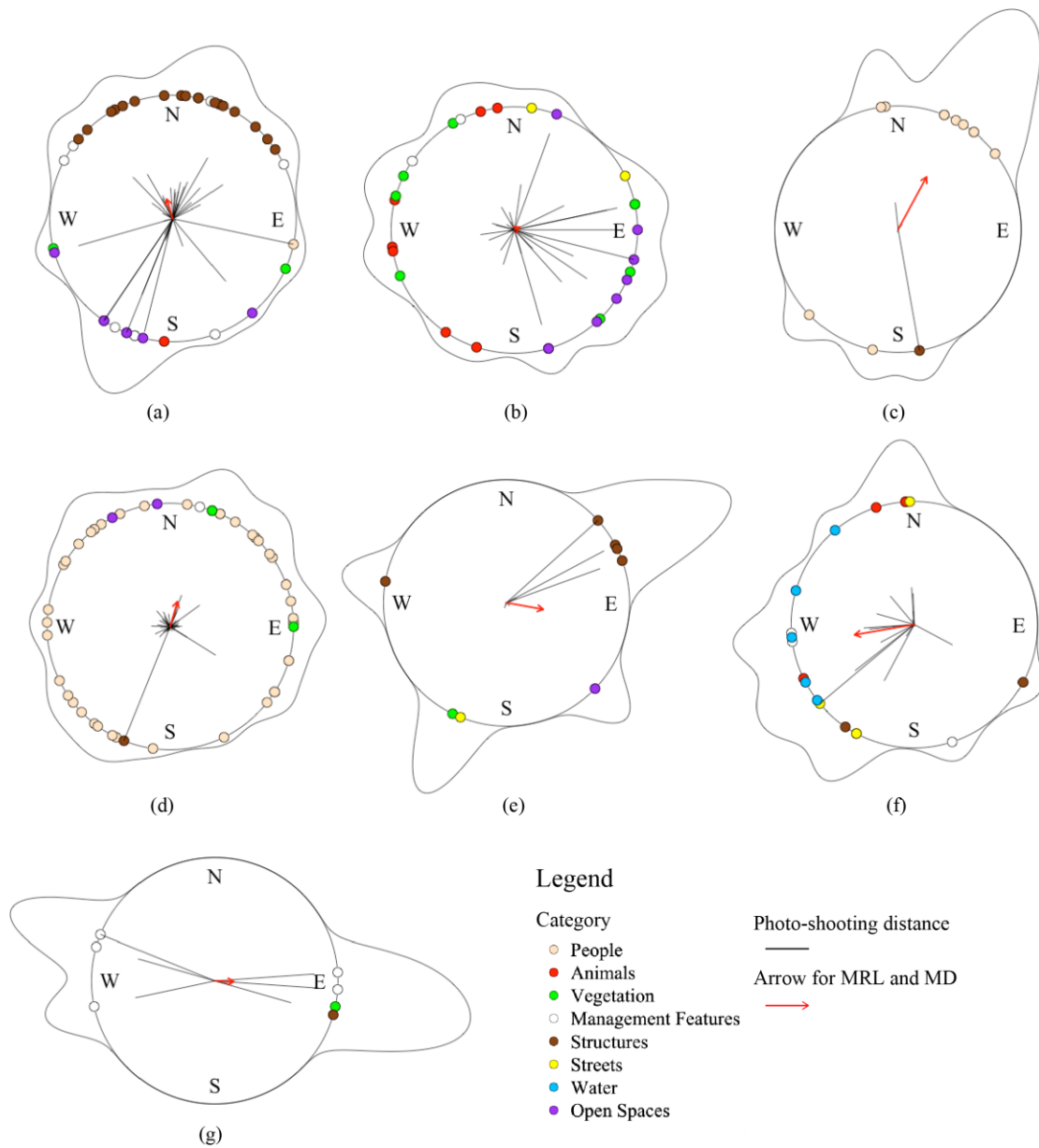
Figure 4-10. Spot profile–Circular statistic of photograph-related data: (a)–(g) corresponds to the results of Spot 1–7

Spot 1, although the kind of objects evaluated in the opposite direction, toward the open space, is different.

Spot 3 is generated by the PVI at the north space of the Large Fountain. The photographs of "people" are taken mainly in this place, so the observed field is little or nothing. However, the low-low clusters occupy the high ratio of the number of
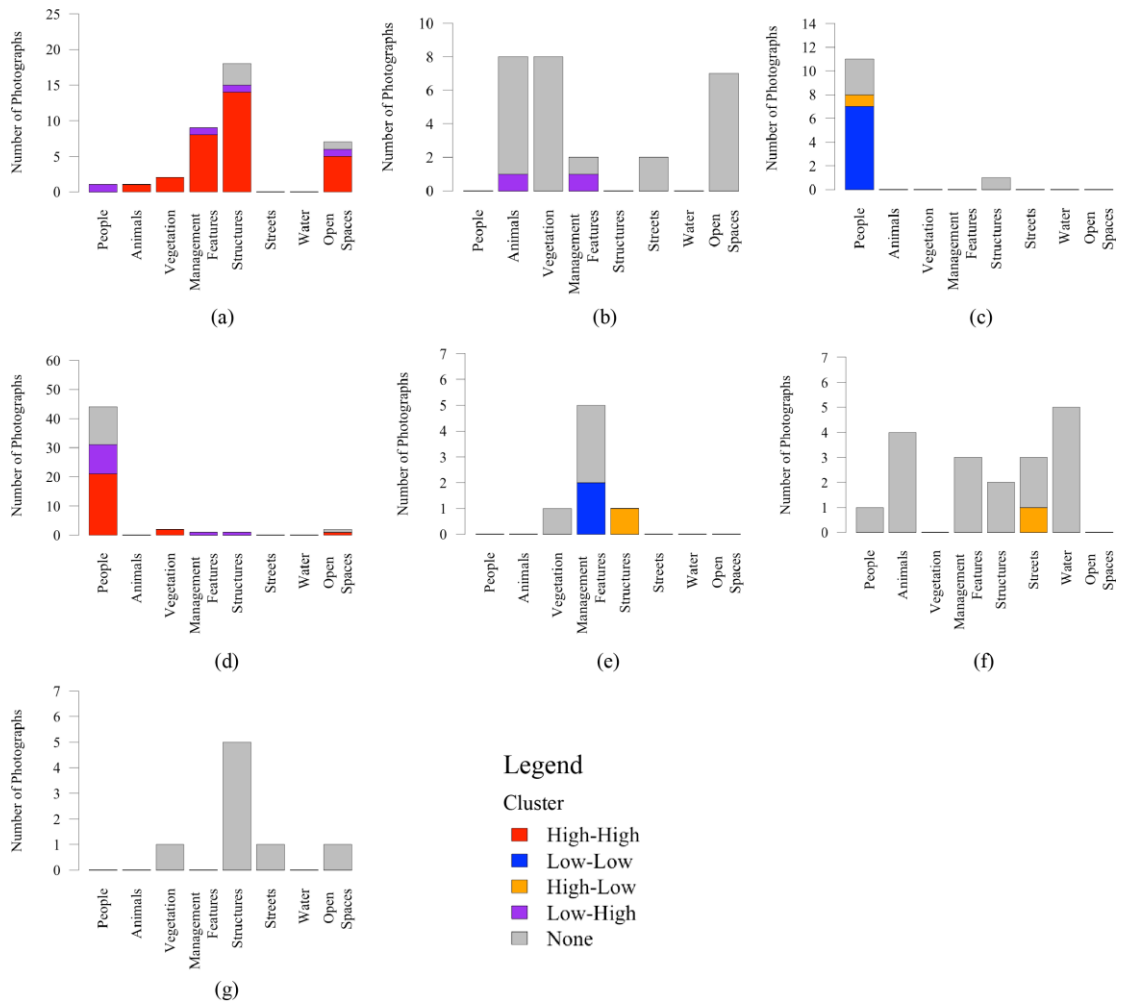
Figure 4-11. Spot profile–Number of photographs in each category and cluster: (a)–(g) corresponds to the results of Spot 1–7

photographs so the likeability score is low in almost all PVI. The scenes are event photographs that are cheap-looking but nevertheless unique.

Spot 4 is constructed of regions ranging from the Second Flower Garden to the Nirenoki Hiroba. Many photographs of "people" are taken at this site, and almost are the scenes of the crowds and the performances during the event. In contrast to Spot 3, about half are belonging to the high-high clusters. In addition, the dispersion of the photo-taking directions is very high, having a nearly uniform distribution.

Spot 5 is located at the northwest end of the park, an area with high elevation. The

Figure 4-12. Spot profile–Representative scenes photographed by participants: (a-1) and (a-2) is the scenes viewed from Spot 1, and (b)–(g) corresponds to the scenes viewed from Spot 2–7

number of photographs is comparatively small and the "structure" is the main component of object categories. According to the circular plot, the views of "structures" with a specific direction (northeast) and a long distance are seen. These indicate the interest directed towards the tower buildings, seen at the distant place outside the park.

Spot 6 is located on the east side of the Kumogata Pond. Here, various kinds of photographs were taken by the participants; the largest number is in "water", the second is in "animals", and the third is in "management features" and "streets". The

76
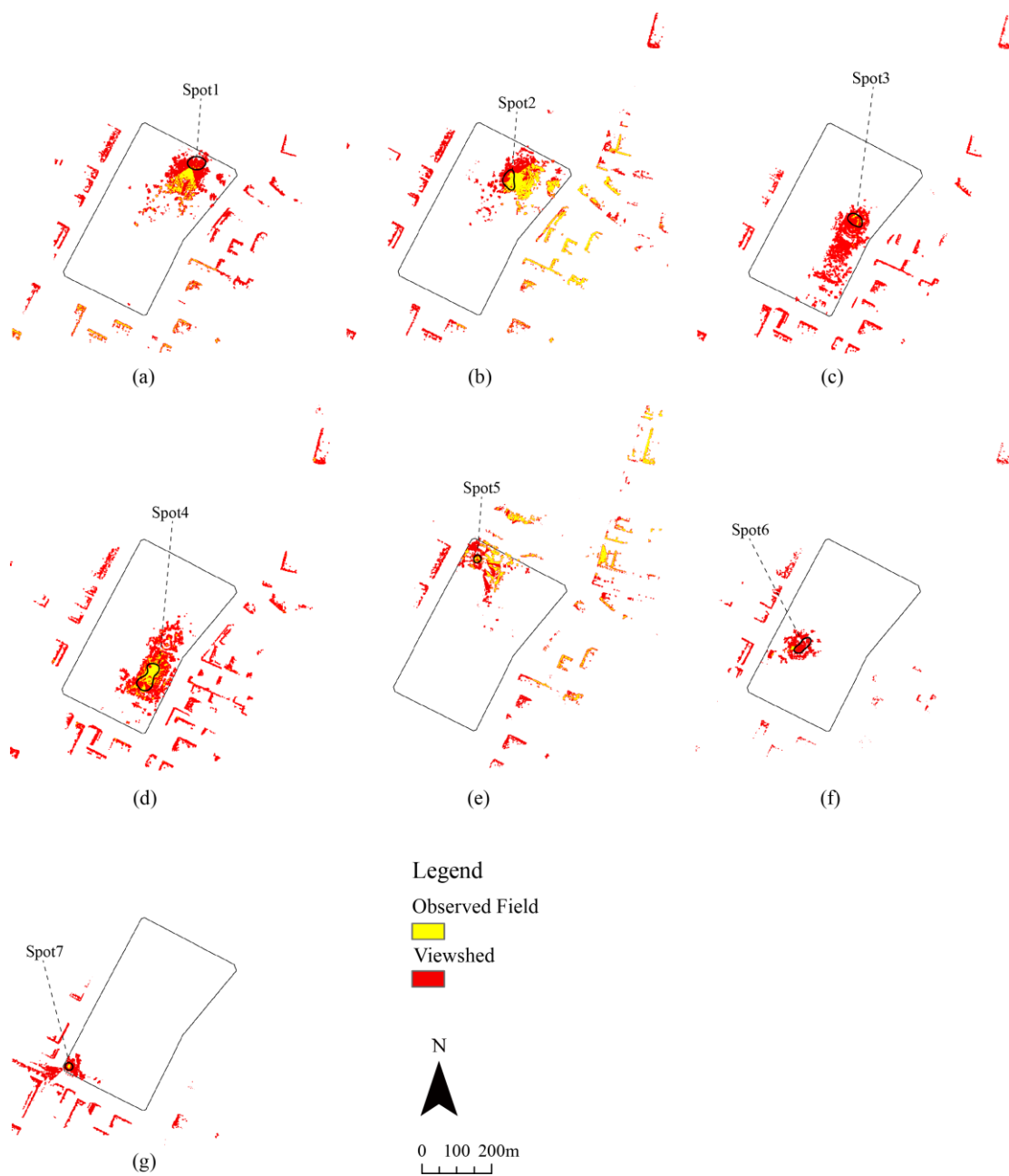
Figure 4-13. Spot profile–Difference between the actually observed field and potential viewshed: (a)–(g) corresponds to the results of Spot 1–7

photo-taking directions are biased towards the west and the mean direction is also in this direction. The water feature and the crane statue rising in the center of the pond are the main features that attracted the participants. However, the preference levels vary in spite of the similarity of photographic data. The observed field is small and distributes

at the center of the pond and the nearby house, since the spot is covered with and surrounded by tall trees.

Spot 7 is located in the Kamome Hiroba, which is at the southwest edge of the park. This place was used as the start and end point of the participants' movements during the photography investigation. Many "management features" photographs were taken, but two of them are in the low-low cluster. The photo-taking directions clearly tend towards the east and west. The data seems to indicate contradicting directions of interest, however the PVI in Spot 7 is distributed around a fountain that has a gum sculpture inside, and photo-taking directions are generally toward this sculpture. The circular plot cannot represent the accurate result in this case.

Thus, each spot has unique characteristics in terms of the visitor evaluation.

4.5.3. Examination of biases in each spot

To evaluate the importance of spots in terms of visitors' emotional consensus, I need to examine how the bias related to the number of participants, or photographs of one participant at each spot. I show the indicators for searching such biases in Table 4-1.

First, the variety of participants is examined by using the number of participants who took the photographs in each spot. If many participants took photographs at the same spot, we can regard this as having a low bias but a high consensus level. Five of seven spots have a low bias, as evaluated by more than 40 percent of the total 21 participants, but two remaining spots are in middle level bias. Those spots having a large number of photographs exhibit a low bias.

Next, the influence of one participant data is investigated. The max number of one

Table 4-1. The indicators for searching the bias in each spot

		Spot1	Spot2	Spot3	Spot4	Spot5	Spot6	Spot7
Number of participant	Number (ratio to all)	16 (76%)	11 (52%)	10 (48%)	17 (81%)	6 (29%)	9 (43%)	4 (19%)
	Bias[※1]	Low	Low	Low	Low	Middle	Low	Middle
Number of photograph in each participant	Total	38	27	12	50	8	18	7
	Max (ratio to total)	7 (18%)	6 (22%)	2 (17%)	13 (26%)	2 (25%)	3 (17%)	2 (29%)
	Mean	2.38	2.45	1.20	2.94	1.33	2.00	1.75
	SD	1.96	2.02	0.42	2.82	0.52	0.71	0.50
	Individual Bias[※2]	Low	Low	Low	Low	Low	Low	Low

※1 Strength of the bias is determined by the variety of participants in each spot; Low: 40-100%, Middle: 10-30%, High: 0-10%

※2 Individual bias is Low if the max number of one participant's photographs is less than 30% of total number in each spot

participant's photographs in each spot is not high according to their percentage to the total number of photographs in each spot; every percentage is less than 30 percent. The average number of photographs of each participant is comparatively low, ranging from 1.33 to 2.94. In addition to it, the standard deviation is not very great. I conclude that the bias level for one participant's data is low in seven spots.

4.6. Discussion about spot attractiveness

I explored the spatial characteristics of Hibiya Park in terms of visitors' perceptual interest by analyzing the PVI with several techniques. The spatial significant clusters of PVI were extracted based on the similarity of participants' preference levels. In the seven derived spots, some spots have many PVI that belong to one specific cluster, but some have a few PVI which belong to multiple clusters. Clarifying this difference is important to understand not only the spatial characteristics of tourist sites but also the

perceptual system of visitors' evaluation to the visual stimuli. In this section, I discuss the interpretation of clusters on emotional consensus at spots, and clarify the "hierarchy" of spot attractiveness.

4.6.1. Interpretation of clusters

The interpretations of four clusters of PVI are defined by their statistical characteristics and spatial distributions. The meanings of the four clusters might be interpreted from the list shown in Table 4-2.

In the cases of high-high and low-low clusters (for the positive autocorrelation), the PVI tended to concentrate at specific spaces such as Spot 1, 3, and 4. In other words, the PVI for which likeability scores were similar values are distributed locally. Spots 1 and 4 were places where many high-high points were located. Spot 3 was characterized by the PVI in a low-low cluster. These specific cases show the "consensus of preference level", meaning that many participants perceived and evaluated the scenes in almost the same emotional level on likeability. The accumulation of high-high cluster points can indicate the existence of the "best spot". Conversely, the concentration of low-low cluster points can indicate the location of "ordinary spot" that may not provide an important experience to visitors overall.

On the other hand, the cases of high-low and low-high cluster (for the negative autocorrelation) indicate the reliable dissimilarity on preference level among the PVI that are adjacent one another. The results imply the possibility of interpretation that the high-low and low-high clusters show unique patterns of visual interest, which are different with the neighboring PVI. The high-low cluster points can be considered as

the strong "individual preference" that occurred at a certain moment, or at a location that is hard to find. The distribution of this type is scattered widely in the park, and this tendency supports the interpretation. The low-high cluster is the most difficult pattern to interpret. The locations of PVI in low-high clusters were mostly seen near the high-high cluster points. Here, I might assume that a site of "secondary interest" is associated with the deeper impression, using interpretation from previous research. Oku and Fukamachi (2003) investigated the temporal pattern of visitors' photography during recreation in linear trail environment and have suggested the idea of human's perceptual system adjusting awareness levels to landscapes from the results. They have argued that the high awareness level is derived from an encounter with an attractive spot. Thereafter, while the awareness level is maintained in high state, visitors tend to intensively photograph various kinds of scenes. According to the actual results of their study, when visitors reached the attractive spot, they photographed similar scenes from various angles and many kinds of scenes, including wide views such as vistas but also small objects such as animals and vegetation. Here, we can suppose different emotional levels in each visual experience. Some scenes had might have been photographed due to high preference but some had been taken from sudden impulses. The low-high cluster can be regarded as this latter case. However, the high-low and low-high cluster points are possibly mere outliers that were extracted accidently, influenced by a set of the statistic parameters during the Moran's I calculation such as the searching distance and the spatial weight matrix.

Finally, consideration is given to the PVI that did not belong to any clusters. However, the notable point is not the characteristic of each PVI but the spots at which

the non-clustered points highly accumulate. Spots 2, 5, 6, and 7 have a lot of the non-clustered PVI. The likeability scores took a variety of values though these spots that attracted many participants. A reason can be proposed from the complex interaction of two aspects, both the visitor's perception and the design issue of spot's space. The visitors' perceptual interest will be changed by the spatial characteristic of spot. Spots 1, 3, and 4, which were characterized by many PVI with positive autocorrelation, tend to depend on the large number of photographs in one specific category. On the other hand, the spots having many non-clustered PVI are derived from PVI in various categories. The former spots drew the participants to view similar scenes and be mostly interested in those views. Therefore, those spots depend on specific views and events that have the highest attractiveness. The latter spots directed the participants' interest to the various scenes or a few scenes from various locations. It is proposed that there were several choices of locations and angles to photograph for the participants.

Table 4-2. Interpretation examples of clusters

		Likeability Score	
		Low	High
Spatially Lagged Score	High	Secondary interest associated with big impression	Consensus on preference levels with high evaluation → Best Spot
	Low	Consensus on preference levels with low evaluation → Ordinary Spot	Strong individual preference at the moment View spot that is hard to find

4.6.2. Hierarchy of spot attractiveness

The results of cluster distribution demonstrate the hierarchy of spot attractiveness. The previous studies have concluded that the spaces having high accumulation of PVI were the spots with high sightseeing potential (Sugimoto, 2011b, 2013) so the hierarchy was implied from only the spatial intensity of PVI, as evaluated by the density values. Therefore, the difference of attractiveness level among the high potential spots has not been considered. My study results suggest the importance of more sub-divisional classification of spot attractiveness in terms of different preference levels. For example, Spots 1 and 2, which are located around the First Flower Garden, have the same density values of PVI but they were clearly different in likeability scores. Most of the PVI at Spot 1 had high values in likeability and also belong to the high-high cluster. In contrast, the PVI at Spot 2 were variable in terms of likeability scores and did not belong to any clusters. Identifying such differences permits more acute understanding of the spatial characteristics, and will be useful for the management of tourist/recreational spaces.

The hierarchical relationships of spot attractiveness derived from my research were summarized and shown in Table 4-3. First, the attractiveness level was roughly divided into two classes, based on whether or not there was an accumulation of PVI. The spaces with no PVI are regarded in the lowest class of spot attractiveness. Next, the spots with PVI accumulation can be further divided into three classes from the clustering results of PVI; best spots, spots with various preference levels and ordinary spots. The best spots, perceived by visitors in consensus of high preference levels, are the most attractive spots among the targeted sites. The ordinary spots show a consensus

Table 4-3. Hierarchy of spot attractiveness

Hierarchy		Criteria	(Cluster)	Attractiveness
Accumulation of interest	Best spots	Consensus in high preference	(High-High)	High
	Spots in various preference levels	Individual preference Spot that is difficult to find Secondary interest Others	(High-Low) (Low –High) (Not Significant)	↑ | Middle | ↓
	Ordinary spots	Consensus in low preference	(Low –Low)	
No accumulation of interest				Low

of low preference levels and are therefore not important for most visitors, but may interest few visitors. All other types of spots are evaluated by PVI accumulation with varying preference levels including high-low clustering, low-high clustering, and non-clustered PVI.

4.7. Summary

This chapter provided an exploratory analysis method for detecting spot characteristics, focusing on the likeability score and the photo-taking directions of each PVI. Spatial autocorrelation analysis and circular statistics were mainly applied to explore the spot characteristics. Firstly, global and local Morans' I techniques were used to measure overall spatial feature similarity and to search for the significant spatial clusters for each point. As a result, four clusters (high-high, low-low, high-low, and low-high) were extracted. Next, the seven spots were determined by the density contours of PVI. The characteristics of each spot were identified by making a spot profile, composed of a spot location and a range, a circular plot embedded with

photo-shooting distance, the histogram counting the number of photographs in each category and cluster, a representative photograph, and the difference of the viewshed and the observed field. Finally, on the basis of these statistical analysis results, I suggested the interpretation for examples of each of the four cluster types. The PVI of high-high and low-low clusters were generated by consensus of preference levels, and tended to concentrate at specific locations. The spots with accumulation of high-high clusters are regarded as the best spots in the park, and the low-low cluster define ordinary spots. The low-high points were found to be distributed around regions of high-high clustering. This fact possibly means that the low-high points are of secondary interest after encountering highly attractive visual scenes. The points of high-low clustering were randomly scattered, and this phenomenon seems to be driven by strong personal preferences or the existence of scenic spots that are hard to find. By combining these classified regions with the results of non-clustered point distribution and spaces that attracted no interest, the hierarchy of spot attractiveness was revealed.

Chapter 5

Modeling Sightseeing Potential

The opportunity for sightseeing is provided by the environment of a destination. Identifying the potential for providing such opportunities in specific locations can contribute significantly to the planning and management of tourist/recreational spaces. The potential of a destination to attract visitors can be determined by location-specific characteristics of the environment (Chhetri & Arrowsmith, 2008). The previous chapter identified the hierarchy of spot preferences in detail, but focused on a small number of representative spots. The potential of these modeling techniques is to provide an insight into the potential of the whole area, so the overall trends in spatial characteristics can be discussed.

This chapter describes the modeling and visualization of the "sightseeing potential" of locations using PVI and GIS. Section 5.1 defines sightseeing potential and describes the modeling used; next, Sections 5.2 and 5.3 explain the implementation of the modeling techniques. Section 5.4 outlines the results of potential modeling, and presents the data on a map for visualization. Finally, Section 5.5 covers the methodological limitations of this study.

5.1. Definition of Sightseeing Potential

The general meaning of "potential" can be described as either (1) the possibility that development will occur in a particular way, or (2) in the case of people or things possessing potential, the tendency to develop and improve (Longman English Dictionary Online, n.d.). In addition, "sightseeing" is the act of visiting and seeing places or objects of interest. Based on these definitions, this study defines the "sightseeing potential" of locations as having qualities that could attract many visitors, and the possibility that visitors can see attractive scenes. Therefore, the sightseeing potential indicates the spot-based potential at a destination. To measure the location specific sightseeing potential, this study utilizes density estimation to obtain PVI. The estimated density provides the possibility of identifying how many PVI are found in a specific location; in other words, the identifying occurrences of visitor interest in a location.

In one of my primary works (Sugimoto, 2011b), I conducted experimental research of potential modeling of visitors' interest using digital cameras, GPS loggers, and GIS. I clarified the relation between visitors' visual preferences and its spatial tendencies by estimating the kernel density distributions of PVI and visualizing the types of photographs in nine categories. However, Sugimoto's method is insufficient for visualizing the sightseeing potential of locations because various biases were not removed during the creation of the density map. In the case of Sugimoto (2012, 2013), the reciprocal number of each visitor's photographs was used as the weighted score for removing the bias that occurred because of the varying numbers of photographs taken by each participant. Sugimoto (2012, 2013) previously set the two courses specifically

for evaluating the difference between visitors' perceptions of each trail, with visitors keeping to these specific courses. Therefore, a method for removing biases in cases when visitors walk freely in a particular environment has not been examined. Moreover, any biases regarding the types of evaluated objects and the differing degree of emotions that each object elicits have not been considered. This study computes and visualizes the potential maps for sightseeing purposes while bearing in mind these multiple biases.

5.2. Data Analysis for Estimating the Potential of Location

The analytical method of this study mainly focuses on analyzing the distribution of photo-taking locations. Kernel density estimation (KDE) was applied to all the photo-taking points to visualize their density. Spatial analysis of point events, known as point-pattern analysis (PPA), has been widely examined by researchers targeting spatial phenomena and the resolution of spatial problems. KDE is one of the most commonly used methods for analyzing the point-event distribution (Bailey & Gatrell, 1995; Xie & Yan, 2008). KDE aims to produce a smooth density surface of point events over space by computing event intensity as density estimation (Bailey & Gatrell, 1995). It is effective for finding the locations where a peculiar value is seen. The kernel estimator $\lambda(\ )$ at the point s is given by

$$\lambda(s) = \frac{1}{h^2} \sum_{i=1}^{n} k\left(\frac{s-s_i}{h}\right) \qquad (12)$$

Here, s-s_i is the Euclidian distance between the zero point s and the ith event point s_i on 2-D space. h is known as the smoothing parameter, also called the bandwidth. The

various accumulation patterns can be found by changing the search bandwidth. If the bandwidth is small, density shows a local accumulation pattern of point events. If the bandwidth is large, density shows a spatial tendency on a larger scale. $k(\ )$ represents the kernel function, and several kernel functions are implemented using different GIS algorithms. I used the quadratic function, which is useful for calculating density estimates on a 2-D space (Silverman, 1986), and set it in the extension of ESRI's ArcGIS Spatial Analyst.

$$k(u)=\begin{cases} \dfrac{3}{\pi}(1-u^2)^2 & u^2=\left(\dfrac{s-s_i}{h}\right)^2<1 \\ 0 & \text{otherwise} \end{cases} \qquad (13)$$

In this study, I apply KDE tools in ArcGIS (Ver. 10) to visualize the potential of spaces that appeal to many participants.

KDE can be attached to the weighted values in its computation. If a weighted value of a point is n, this point is calculated as n points. The weighted values change the density values; therefore, it is possible to remove biases when the weights are properly set in each point. I design the weights according to the multiple indicators in the next section.

5.3. Designing the Weights

The comprehensive weighted score (W_i) of photo-taking point $i(i=1,2,\ldots,517)$ is determined by the following formula (3). W_i is considered to be the product of the five factors.

$$W_i = L_i\, C_i\, R_i\, D_i\, T_i \qquad (14)$$

First, L_i is the likability score. This index is the most important weighted value for considering the potential of locations and denotes the differing degrees of emotions that the photographs elicit in each participant. Likeability score is the only indicator through which the participants can evaluate themselves. The product method is chosen for designing the overall weighted score because L_i is regarded as the basic weight, while the other four indicators are solely treated as parameters to eliminate inequalities in conditions among participants. With L_i, the range of values extends from one to five. Five is the highest on likeability and one is the lowest, although it does not indicate active dislike.

Second, C_i refers to the weighted value for removing the bias regarding the types of objects the participants took photographs of. If the category of the photograph is "people" or "animals," the weighted score is less than 1, and in the range of 0 to 1. In addition, other types of photographs are assigned a score of one. The reason why the score of the photographs in the "people" and "animals" categories is reduced is that these types of objects move around the study area. As a result, the number of these types of photographs and its spatial distribution across the park are predicted to be move varied than with other categories.

$$C_i = \begin{cases} [0,1) & \text{("people" or "animals")} \\ 1 & \text{otherwise} \end{cases} \quad (15)$$

Third, R_i indicates the reciprocal number of photographs taken by each participant. This weight removes the bias caused by the difference in the number of photographs taken by each participant. When the number of photographs taken by participant $k(k=1,2,\ldots,21)$ is N_{ik}, R_i is defined as below.

$$R_i = 1/N_{ik} \quad (16)$$

Fourth, the distance between photo-taking point i and starting point is calculated as one of the weighted values. The Euclidian distance after logarithmic conversion is used for computing the distance weight D_i. The Euclidian distance before logarithmic conversion is represented in meters. This weight is used to remove biases regarding the selection of a starting point. A photo-taking point farther away from the starting point is assigned a higher value. Because the farther points from the starting point are in lower probabilities of participants' visits. When the geographic coordinates of point i and the starting point are represented to (X_i, Y_i) and (X_{start}, Y_{start}), D_i is defined in the following formula (17).

$$D_i = log\left(\sqrt{(X_i - X^{start})^2 + (Y_i - Y^{start})^2}\right) \qquad (17)$$

Finally, the fifth weighted value is the reciprocal of the photo-taking time. This value has two functions; the first suppresses the excessive effect of D_i on the overall weighted score, and the second adds the effect of a person's sequential emotional change to the overall weighted score. Some researchers have revealed that the pace of photography has declined over time, indicating that a person's interest in photography has gradually decreased (Markwell, 1997; Oku & Fukamachi, 2003; Sugimoto, 2013). Higher values are assigned to the photo-taking points taken in the early segment because the persons tend to be fresh during that time. On the contrary, lower values are given to the points in the late segment. The starting time of each participant is set as zero, and each photo-taking time is shown in seconds. When t_i is the photo-taking time of point i, T_i is computed as follows.

$$T_i = log\left(10^4/t_i\right) \qquad (18)$$

5.4. Results

5.4.1. Weighted scores

In total, the number of points is 517, not including the photographs labeled "others". As the result of the computation of the comprehensive weighted value W_i, the distribution of W_i is shown in Figure 5-1. I assign weighted scores of 0.5 and 0.3 to C_i ("people" or "animals"). In both cases, the distributions of these weighted scores are skewed toward a low value, but several points have relatively high values that score more than 3. However, these high weighted points would not possibly become a bias in the computation of a density distribution.
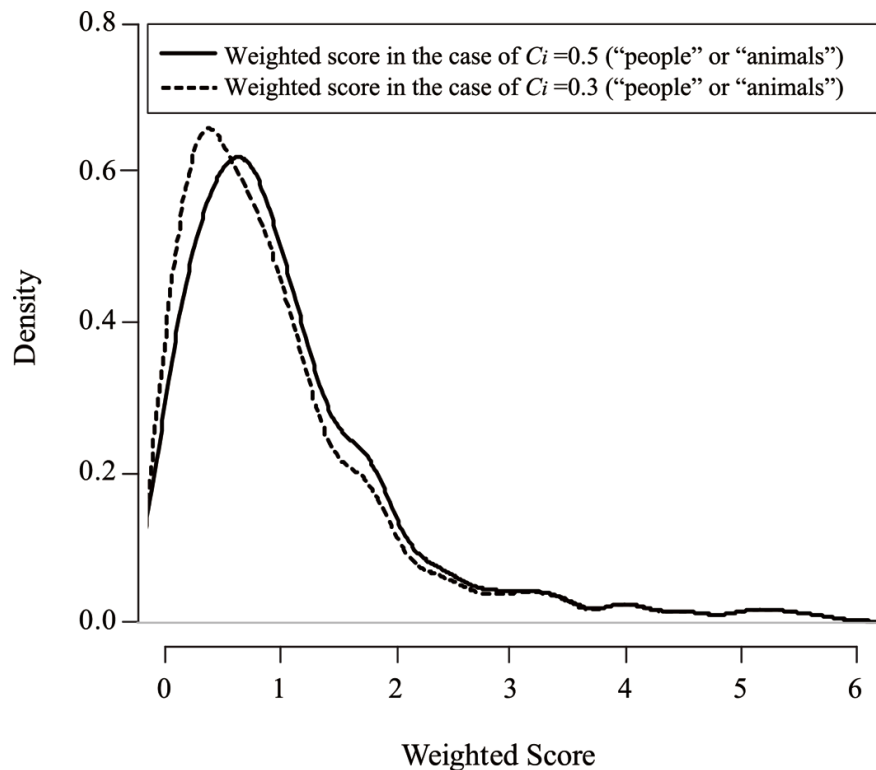
Figure 5-1. The distribution of weighted scores in two different cases

5.4.2. Visualizing the potential of locations

I calculate the three types of scores in density distribution of photo-taking locations; the non-weighted score, the weighted score in the case of C_i = 0.5 ("people" or "animals"), and the weighted score in the case of C_i = 0.3("people" or "animals"). All density maps are drawn on the basis of an equidistant classification. Two density maps with a 30-m bandwidth and a 70-m bandwidth are shown in Figures 5-2 and 5-3.

In the case of the 30-m bandwidth shown in Figure 5-2 (b), it is found that the points accumulate around the attractions and on the park roads. For example, the density is high at the park trails near Shinji Pond, Park Museum, and the First Flower Garden, and also surrounding the Kumogata Pond, the Second Flower Garden, and the Large Fountain. The density maps with the weighted scores shown in Figures 5-2 (c) and (d) do not show any significant differences. However, the density at the area surrounding the Second Flower Garden and the starting point is lower than that of the density maps with the non-weighted scores. There is very high accumulation of points in "people" at the Second Flower Garden and its nearby surroundings. The extent of this accumulation can be reduced by attaching the weighted scores C_i based on the categories of objects.

For the 70-m bandwidth and the non-weighted scores in Figure 5-3 (b), I found that the density is especially high within the Second Flower Garden. I also found a high accumulation of photo-taking locations at Kumogata Pond. However, there are too many photographs in the "people" category taken during the festival event at the Second Flower Garden. I do not consider this event as a potential location because its characteristics will change according to the date. Moreover, the density at the north

93

trail of the First Flower Garden is too low despite the location having high likeability scores. After performing an operation to reduce these biases, a large difference occurred between the density map with the non-weighted scores and the one with the weighted scores shown in Figures 5-3 (c) and (d). The density values of the latter cases were high at the north trail of the First Flower Garden and the Kumogata Pond compared to those of the former case. This indicates that the potential of the locations
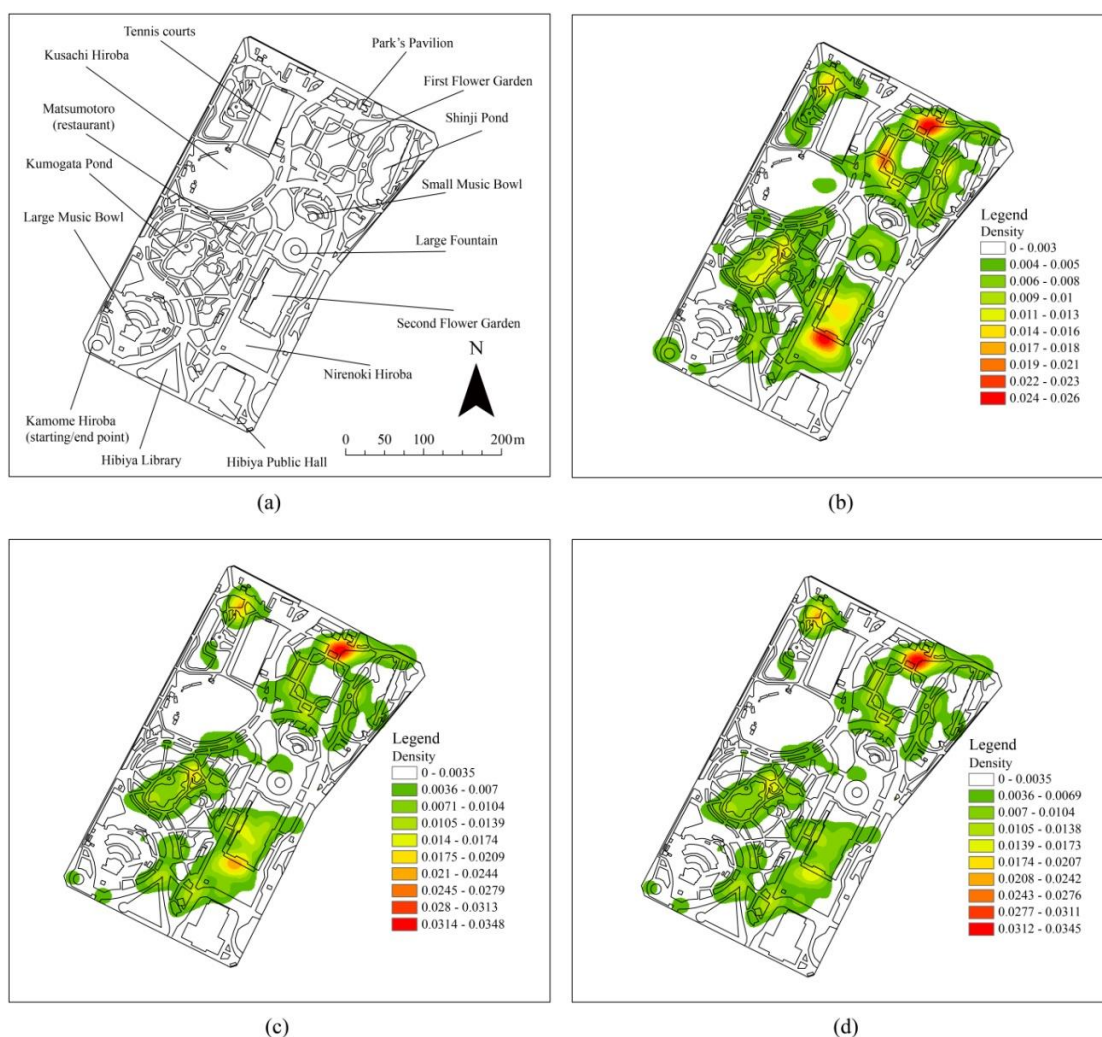
Figure 5-2. The kernel density distribution of photo-taking locations with 30-m bandwidth and 1m×1m cell size;(a) the map of Hibiya Park, (b) the density map with non-weighted score, (c) the weighted score in the case of $C_i = 0.5$("people" or "animals"), and (d) the weighted score in the case of $C_i = 0.3$("people" or "animals")

represented in the former case is underestimated. The densities at the First Flower Garden are as high as those in (Figure 5-3 (c)) or higher than those in (Figure 5-3 (d)), which represents the Second Flower Garden. These density values seem to indicate the proper potential of locations, as both gardens present with high density values. Because many photographs located at both of the gardens have high likeability scores. We can say that the density map with the weighted scores is a good result from those
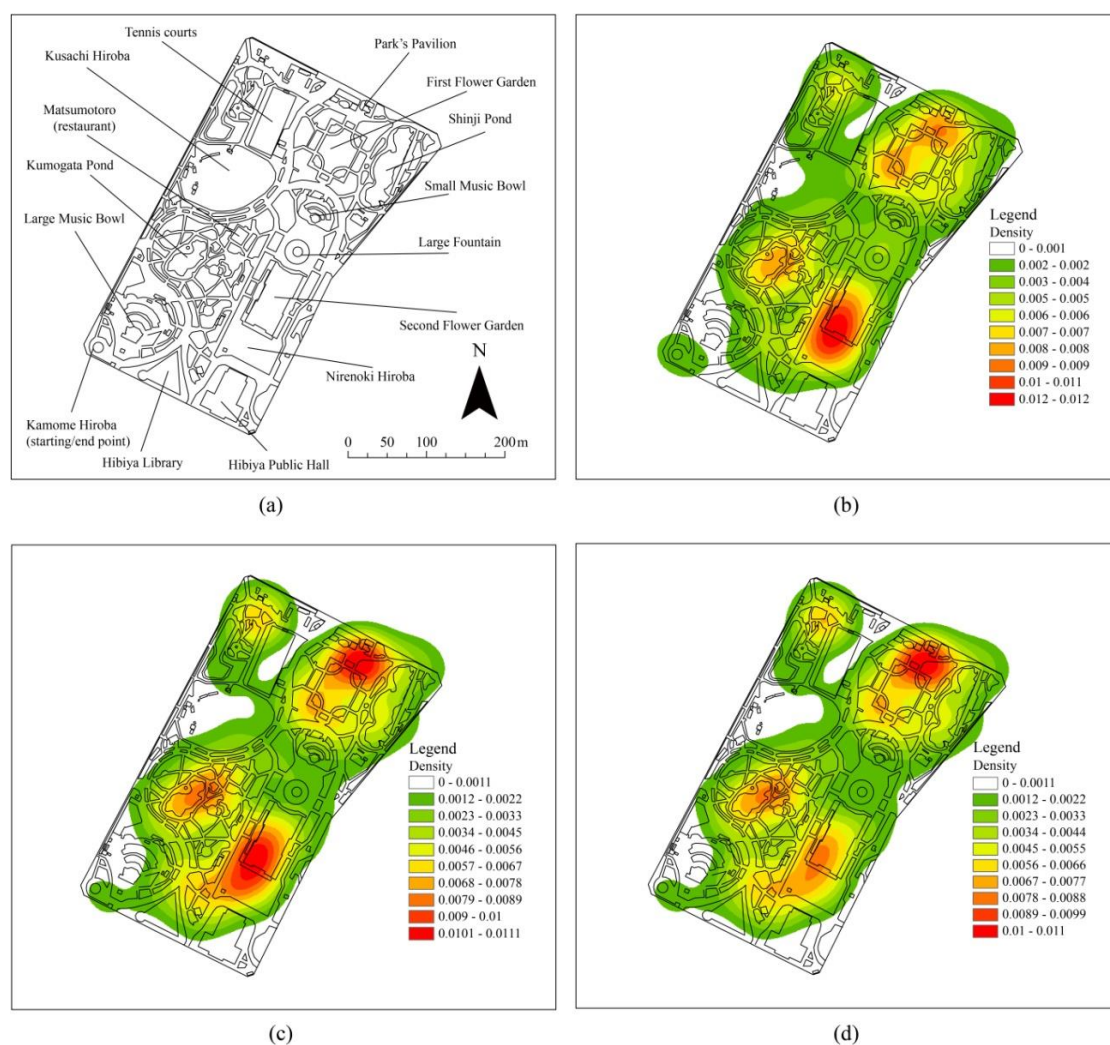
Figure 5-3. The kernel density distribution of photo-taking locations with 70-m bandwidth and 1m×1m cell size;(a) the map of Hibiya Park, (b) the density map with non-weighted score, (c) the weighted score in the case of C_i = 0.5("people" or "animals"), and (d) the weighted score in the case of C_i = 0.3("people" or "animals")

perspectives. The difference between the density at the Second Flower Garden in Figures 5-3 (c) and (d) occurs as a result of the weighted value C_i ("people" or "animals"). Changing this value largely influences the density value at the Second Flower Garden, and this is due to the accumulation of "people" photographs, which have a low weighted value at this location. Of these two results, I cannot unconditionally judge which result is better, but if I emphasize on removing the unstable factors, Figure 5-3 (d) is the more appropriate result.

Thus, by considering the weights theoretically regarded as the biases, the spatial patterns of density distributions could be different in the case with non-weighted scores and that with the weighted scores, thereby providing more accurate results in the sightseeing potential of spaces.

5.5. Methodological Limitation

The result of this study, limited in the density map with non-weights, is little different from Sugimoto's (2011b) research, which was conducted in the same study area. Most pertinently, the location with the highest density value of photo-taking locations was not the same in both studies. This seems to be caused by the difference in the sample size, the variance in participants' social background and the irregular movement of people and animals through the photographed locations. This study's participants are all from a younger generation, but the previous study's participants were of various generations and were fewer in number. The photo-taking locations in "animals" tended to accumulate around the First Flower Garden in the previous study. Moreover, the space with the highest density value was constructed using many animal

photographs. Potential changes in conditions are the methodological limitation of the on-site experiment. However, such a limitation is not a serious problem because, when viewed overall, the density maps in both studies demonstrate very similar results.

5.6. Summary

This chapter addressed the construction of a density map showing preferred photo-taking locations, for the purpose of evaluating the sightseeing potential of spaces based on people's visual preferences. In particular, this study focused on using the KDE method to reduce some of the biases that typically occur when the potential maps are studied. The weighted scores, which were multiplied by the five indicators, created more suitable maps of potential sightseeing preferences than the non-weighted density maps.

Chapter 6

Visualization of Spatial Intensity of Visual Lines

The PVI-based analysis and visualization were presented in the previous chapters 4 and 5, showing great results and potential for clarifying the spot characteristics and modeling the sightseeing potential of a given location. However, these assessments were mainly based on spatial information of photo-taking locations. Visitor's visual interest during his or her on-site experience occurs in the spatial interaction with the visual object, and this phenomenon involves aspects of the spatial context such as a position of the observer, and the visual object. Such spatial relationships can be represented in spatial data as a distance between the observer and the visual object, described as the LVI in the Chapter 3. The LVI is also regarded as the spatial indicator of visual distance on scenic/landscape perception (but in some cases, the estimated visual distances were modified). There is a small amount of existing research regarding the quantification and analysis of visual distance; however, the required data generation, spatial analysis and visualization of the spatial data related to visual lines has not yet been performed. Therefore, this study will contribute to the advancement of research in the field of landscape perception and assessment.

This chapter demonstrates effective methods for the analysis and visualization of the spatial intensity of LVI, which are the spatial line data representing visitors' visual lines. The studies are conducted as follows; the spatial distribution of LVI is visualized on

GIS environment, with some limitations as explained in Section 6.1. Next, three approaches to the analysis and visualization of LVI intensity are suggested and examined (Sections 6.2, 6.3, and 6.4). Map representation is an important consideration in the analysis of spatial data, and displaying results effectively. Therefore, the characteristics of the three types of analysis and visualization are described, with thorough discussion of the advantages and disadvantages of each approach. Moreover, visualization in a 3-D landscape model is suggested, and its effectiveness is argued in Section 6.5.

6.1. Lines of Visual Interest

6.1.1. Spatial distribution of LVI

The spatial distribution of LVI of all participants is shown on the map (Figure 6-1 (a)). Maps of the start and end points of the LVI are also plotted in order to compare with LVI's map (Figure 6-1 (b) and (c)). The former is equivalent to the location maps of points of visual interest (PVI), which indicates the spatial data of photo-taking locations, and the latter indicates the locations of visual objects that the participants photographed. Comparing with three maps, the map of LVI distribution is clearly more informative than the other two maps. Though the point-based maps have only location information about the standing point or visual objects and describe no other information, the LVI clarifies not only those but also the visual lines and directions at the same time. From this, we are possible to know where the participants viewed the scene, from and which place they targeted. The distances of visual lines are completely different according to the place where the participants' interest occurred. At the

99
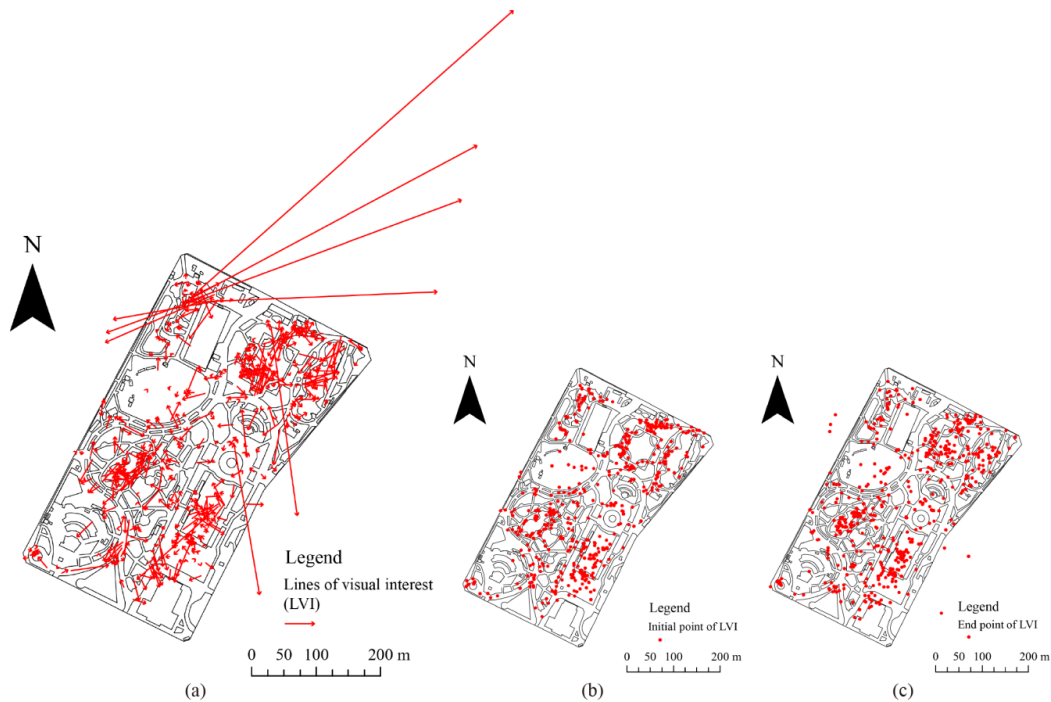
Figure 6-1. Distribution of (a) LVI, (b) the starting points of LVI, and (c) the end points of LVI

northwest of the park, there are some LVI of great length; these LVI show interest directed towards buildings exterior to the park. Spatial information of the PVI only, or the estimated location of visual objects, cannot describe such interaction between the visitor and the visual object.

Thus, LVI represents the interaction of visitor and visual object more precisely than using point features. However, because many lines of different length are distributed in the same area, the map of LVI is a little complicated to understand; an effective way to solve this visualization problem is shown in next section.

6.1.2. Spatial intensity of LVI

As a technique for effective visualization and pattern finding within discrete spatial features, the intensity of certain features' accumulation is often computed. If point data

is targeted for analysis, the Exploratory Point Pattern Analysis (EPPA; Bailey & Gatrell,

1995) is one well-known approach, and various spatial intensity computation methods

have been developed on EPPA. However, few exploratory analysis methods applicable

to discrete line data such as LVI have been developed. Network analysis is based on

linear features, but focuses on the connectivity among lines and processes them like

continuous data. To describe the spatial intensity of the LVI, I suggest three approaches

of geo-visualization; density estimation, grid-based aggregation, and flow data

representation.

6.2. Density Estimation

6.2.1. Kernel density estimation for linear features

   To visualize the intensity of spatial features, I initially used the kernel density

estimation (KDE). KDE is a technique used to generate a smooth density surface by

estimating the probability density function of a data variable. In spatial analysis using

GIS, KDE calculates the density of spatial features around each output raster cell.

Many previous studies have applied 2-dimensional KDE to point features for

identifying hot spots, where data points are concentrated. I can also apply KDE to

linear features using ArcGIS10 Spatial Analyst tools. The density surface value is

largest on the line and diminishes as this move away from the line. When the distance

from the line reaches the search bandwidth, the surface value becomes zero. This

procedure is adapted from the quadratic kernel function (Silverman, 1986) as the

kernel function for lines. The density at each output raster cell is calculated by adding

the values of all the kernel surfaces. It is defined so that the volume under the surface

equals the product of the line lengths where they overlay the raster cell center (ArcGIS Resource Center, n.d.c).

6.2.2. Density distribution of LVI

The density maps of LVI are shown in Figure 6-2 (a). The quadratic kernel is used as a kernel function and the 30-m bandwidth is set. In addition, I show the density maps of the starting and end points of LVI with the same parameter in the case of LVI density formula in Figure 6-2 (b) and (c). The density of starting points equals that of PVI, representing the potential of view spots (but actually requires the addition of the weighted value on the density computation for visualizing the perfect potential map). The density of end points of LVI shows the accumulation of estimated locations of visual objects that attracted participants' interest upon viewing. These two point densities simply show the accumulation of a single kind of feature. On the other hand,
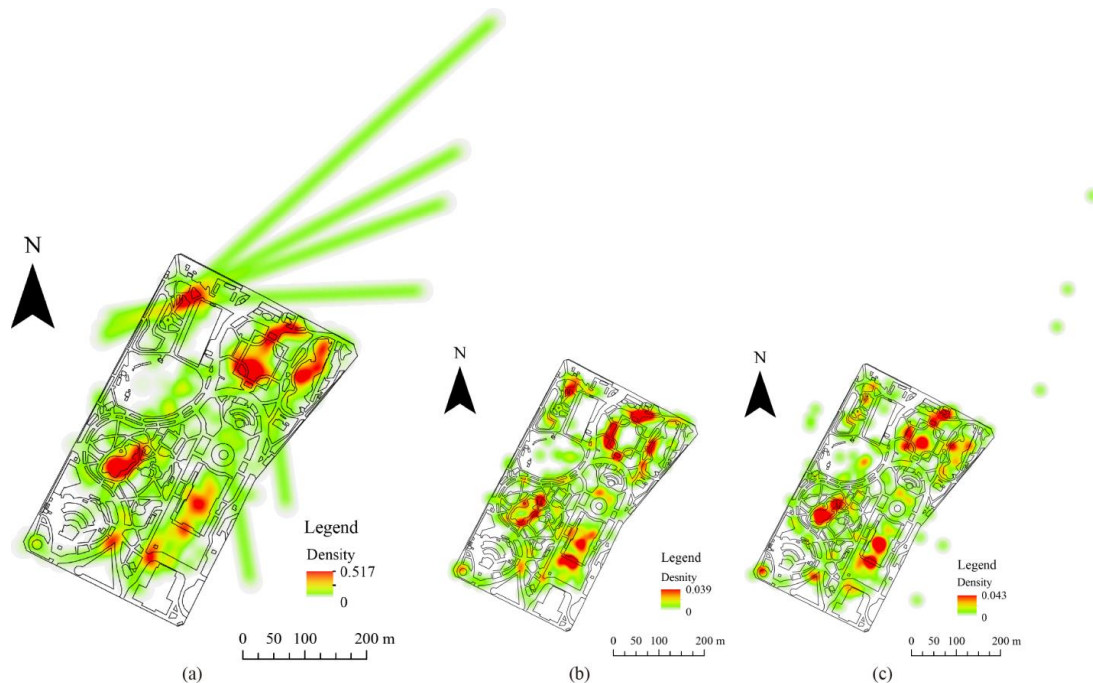
Figure 6-2. Density distribution of (a) LVI, (b) the initial points of LVI, and (c) the end points of LVI

102

the LVI is constructed with the complex elements including not only start and end points, but also a line linking both points. This indicates that the density of LVI represents the mixed accumulation of such plural spatial features.

Comparing the three density maps, I observe that the distribution patterns are clearly different. For example, the high values of the LVI density (Figure 6-2 (a)) are distributed "on" the two ponds of Hibiya Park but the ones of the starting points (PVI, Figure 6-2 (b)) locate "around" the ponds. The density distribution of the end points (Figure 6-2 (c)) has the similar tendency to the LVI density. The density value of LVI and end points of LVI may be regarded as the potential level of space as same as the case of starting point (PVI) intensity. However, each has the different meaning upon interpretation. The density of LVI indicates "the spatial intensity of psychological interactions" that occurred between persons and visual objects on the geographical environment. In contrast, the density of starting and end points of LVI indicate only location information of either subjects or objects of interactions.

The problem of visualizing LVI accumulation using density estimation is that the directional information of LVI is entirely abstracted. By overlaying the LVI distribution on a density map, it is possible to address such problems; however, the map retains a high degree of complexity.

6.3. Grid-Based Aggregation

6.3.1. Count and mean direction of LVI based on grids

To represent plural variables such as the spatial intensity and direction of LVI on one map, a grid-based aggregation method is used. First, the square grid polygons are

generated and overlaid in the range of the study area and LVI distribution using ArcGIS10 Cartographic tools. I show the cases of 20m×20m and 30m×30m grids. These grid sizes were selected such that the mean value of shooting distances, corrected on horizontal axis, was 22.3; therefore, the integral round value of 20 m was selected. Moreover, to study the effect of grid size on the analysis results, 30 m square grids were also made. The number of grids is 574 for 20 m and 294 for 30 m. As the size was increased by 10 m, the number of grid squares essentially halved.

Each grid joins the number of LVI existing inside the spatial range of them. The mean direction of LVI in each grid is also calculated using circular statistics programming by Python. The mean direction of grid i is computed as following formula (Arai, 2011):

$$\bar{\theta}_i \begin{cases} \tan^{-1}(S_i/C_i) & \text{if } C_i>0,\ S_i\geq0 \\ \pi/2 & \text{if } C_i=0,\ S_i>0 \\ \tan^{-1}(S_i/C_i)+\pi & \text{if } C_i<0 \\ 3\pi/2 & \text{if } C_i=0,\ S_i<0 \\ \tan^{-1}(S_i/C_i)+2\pi & \text{if } C_i>0,\ S_i<0 \end{cases} \qquad (19)$$

Here, C_i and S_i are the sum of directions transformed by the trigonometric function in each grid. When the LVI's direction k in grid i is represented as θ_{ik}, C_i and S_i can be calculated as shown:

$$C_i = \sum_{k=1}^{n} \cos\theta_{ik} \qquad (20)$$

$$S_i = \sum_{k=1}^{n} \sin\theta_{ik} \qquad (21)$$

Point data showing the locations of grid centers were made, and the values of mean directions are attached to them as attribute values.

6.3.2. Map representation of LVI intensity based on grids

After these operations, the calculated results are visualized spatially using statistical map representation techniques, combining the choropleth mapping method and a point symbol plot (Figure 6-3 (a) and (c)). The count number of LVI is represented by the color intervals and the arrow symbol is used for showing the mean direction. I can well understand where the count value is high or low, and in which direction the LVI tend to point, on average. However, though the color interval is effective for visualization, the spatial features of park infrastructure are hidden within the grids and the relation to LVI distribution is difficult to understand. Therefore, I show another type of map representation using only the arrow symbol. The size of symbols was changed to fit the number of LVI in each grid, and the polygon of grid range was removed on the map (Figure 6-3 (b) and (d)). This type is simpler than the first type of map, but it cannot emphasize the cumulative value as in the earlier map.

Comparing the 20 m and 30 m size square-grids, the mean directions between these two types are similar in many places, but differ in some locations. For example, the arrows around the Second Flower Garden completely differ in size type, though the ones at other places are generally the same. This is due to the different variance levels of LVI directions in grids. The LVI around the Second Flower Garden have a large variance on their directions. Therefore, the grid size affects the outcome at specific spaces that exhibit large dispersion in the LVI directions.

Grid-based aggregation enables representation of the degree of accumulation and mean direction of LVI in each grid. However, the limitation of this approach is that there is a problem in that the spatial relationship between two important locations of an
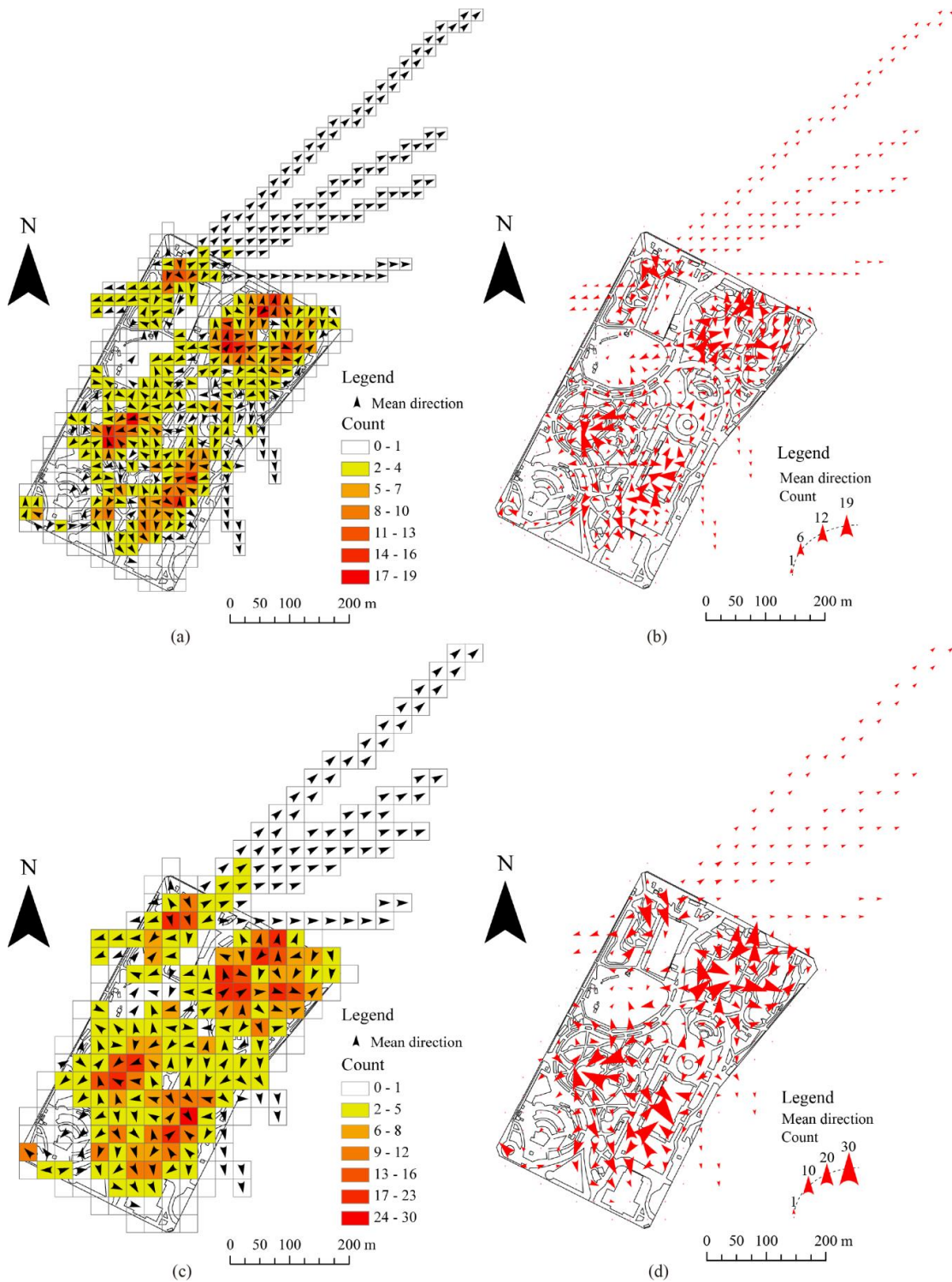
Figure 6-3. Visualization of aggregated LVI based on (a)-(b) 20m×20m grids and (c)-(d) 30m×30m grids

106

observer and visual object cannot be represented.

6.4. Visual Interest Flows

6.4.1. Representation as flow data

The LVI can be changed to flow data if the person's response to visual stimuli is regarded as a spatial phenomenon consistent with an object moving from one grid to another. This data transformation enables us to extend the analysis of LVI. In this section, I determine the data characteristics of visual interest flows, and suggest fundamental geo-visualization methods applicable in this case.

6.4.2. O-D matrix

Generally, the number of flows between two points of the considered network is quantified by using one square matrix table referred to as the "Origin - Destination (O-D) matrix" (Figure 6-4). O-D matrix is composed of rows and columns which are the same length, indicating origin i and destination j. T_{ij} is a component of the matrix that is equivalent to the number of flows from origin i to destination j. The sum of rows O_i means the total number of generation flows exiting zone i, and sum of columns D_j indicates the total number of arrival flows entering zone j. In this study, zones are defined as grid polygons overlaid on the map and LVI distribution.

This O-D matrix is decomposed into intra-grid flows and extra-grid flows. The flow on the diagonal of matrix, for example, from grid 1 to grid 1, is intra-grid flow. All others, which are out the diagonal, are extra-grid flows.
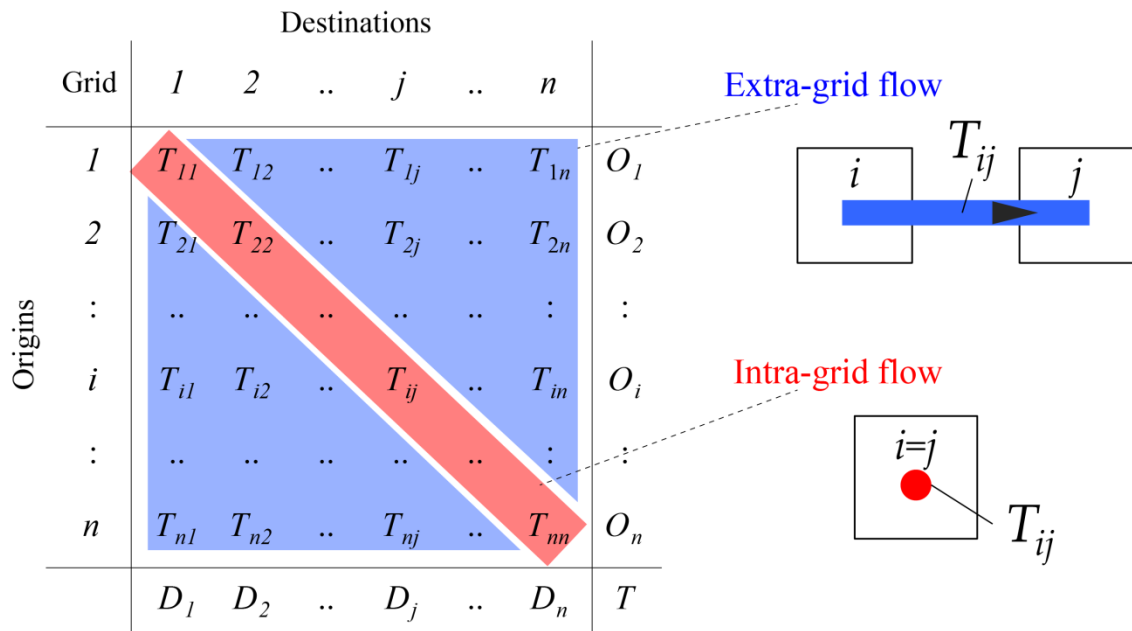
Figure 6-4. Origin / Destination matrix and flow representation

The process of making the O-D matrix of visual interest flows is as follows; first, the ID numbers of the grid polygons were added to the attribute table of the start and end points of LVI corresponding to the inside of each grid, using the ArcGIS 10 spatial join function. The start and end point of each LVI has the own ID that is the same in each, and the grid ID that may be either the same or different according to flow type, intra-grid or extra-grid. Based on these two types of IDs, I computed the O-D matrix using my original program.

6.4.3. Visualization of visual interest flows

To visualize the visual interest flows, I need to use different symbols for the intra-grid and extra-grid flows because of possible confusion if using the same symbol

108

for each. A circle symbol is used for intra-grid flow, and an arrow symbol is used for extra-grid flow. The symbol sizes are changed by the quantity of flow.

I made the shape files of flow data, separated into intra-grid and extra-grid flows using my original program. The point data, located on the grid center, is made for the intra-grid flows. The line data that links the two grid centers is made for the extra-grid flows.

Figure 6-5 show the observed visual interest flows with 20m×20m and 30m×30m grids. It may be the most easily understandable of all the maps shown in this chapter, capturing the occurrence patterns of visual interest. However, the grid size affected the results strongly. Comparing to the grid sizes, patterns of spatial distribution are remarkably different. This reason might be that the flow data were made depending on only the starting and end points of LVI, not considering the directional data of LVI.

(a)   (b)
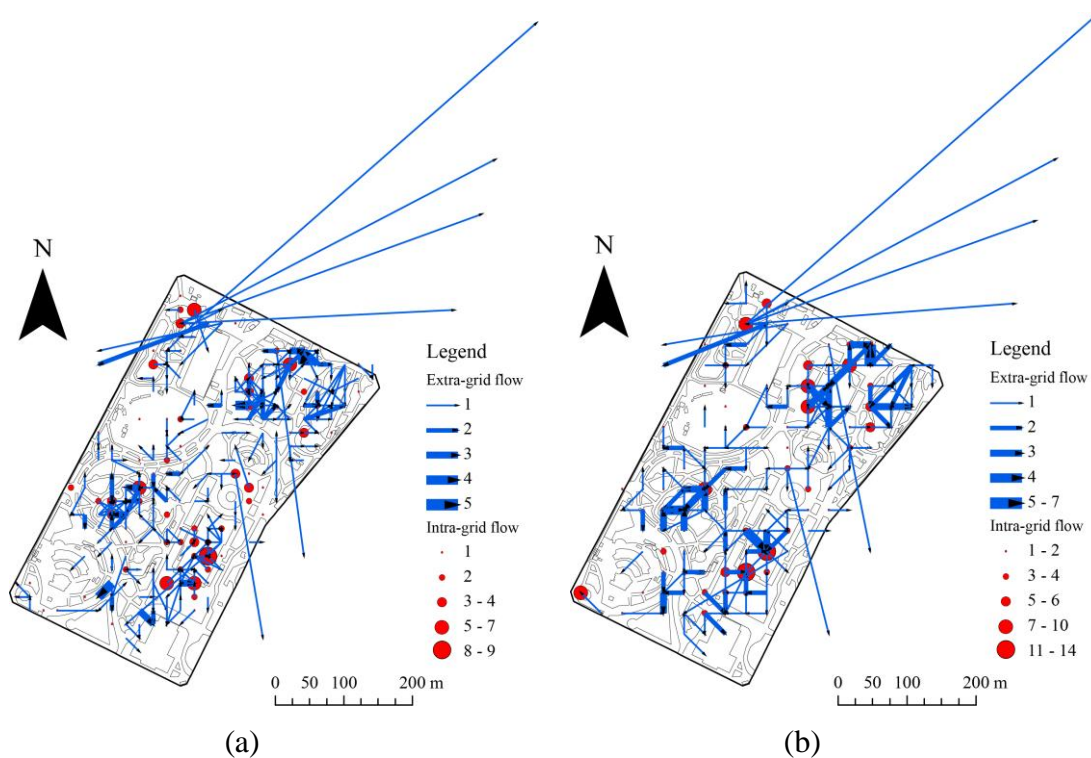
Figure 6-5. Visualization of visual interest flows based on (a) 20m×20m grids and (b) 30m×30m grids

Moreover, because these points are aggregated and the flows are summarized, the accuracy of flow locations is reduced. Although there is such a problem, the method displays some merit in data representation and analysis compared with former two approaches. The flow data can represent the spatial relationship between grids, and permit effective application of statistical techniques for traditional flow data, such as spatial interaction models.

6.5. Visualization on 3-D Landscape Models

While the vectors of some LVI move from the interior of Hibiya Park to the exterior, most LVI do not. All such irregular LVI show the participants' visual lines to the skyscrapers surrounding the park. Therefore, it is desirable that the landscapes of both the interior and exterior of the park are visualized considering the height and volume of objects such as buildings, with LVI or other representations of spatial intensity of visual lines. To achieve this, I recommend 3-D visualization using 3-D landscape models. This approach will be more effective than a 2-D map in terms of evaluation, as it considers the relationship between both perceptual and physical landscapes. Figure 6-6 shows the LVI and visual interest flows in the 3-D landscape models created by layering raster images and polygon vector data on ArcScene. In Figures 6-7 and 6-8, these are shown in more realistic 3-D models from Google Earth. The former is simple and composed of only four types of landscape elements, which might be suitable to more easily understand the overall trend of the relation between distributions of visual interest and landscape objects. However, developing this model takes time and money. The latter models are visualized as more realistic 3-D models. The outlines of 3-D
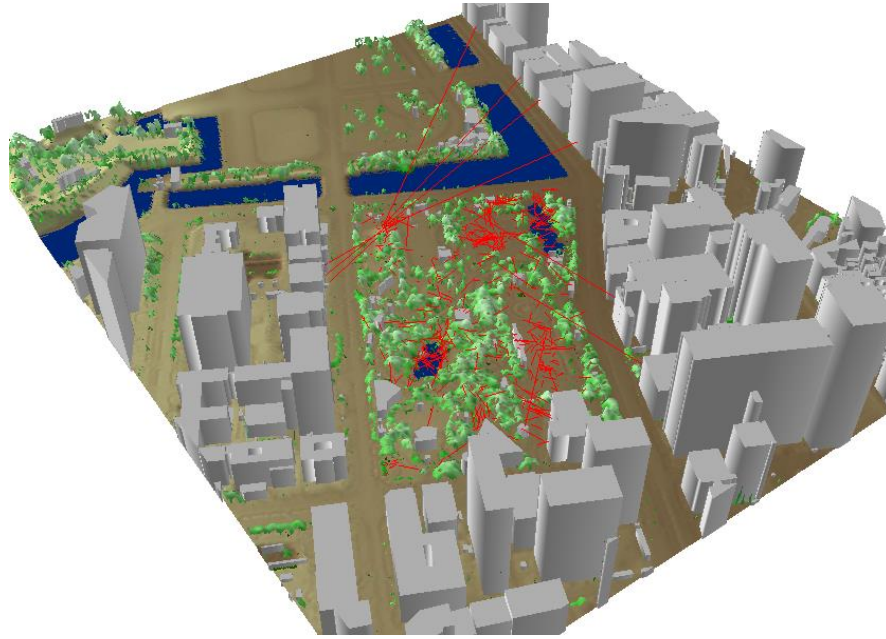
(a)
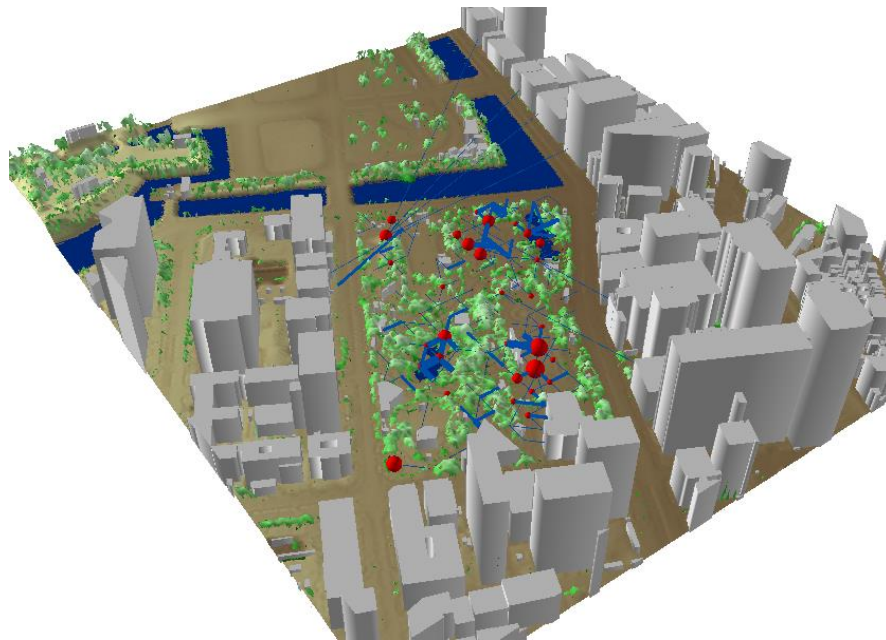
(b)

Figure 6-6. Visualization of visual interest in 3-D landscape model created using ArcScene: (a) LVI and (b) visual interest flows with 30m×30m grids
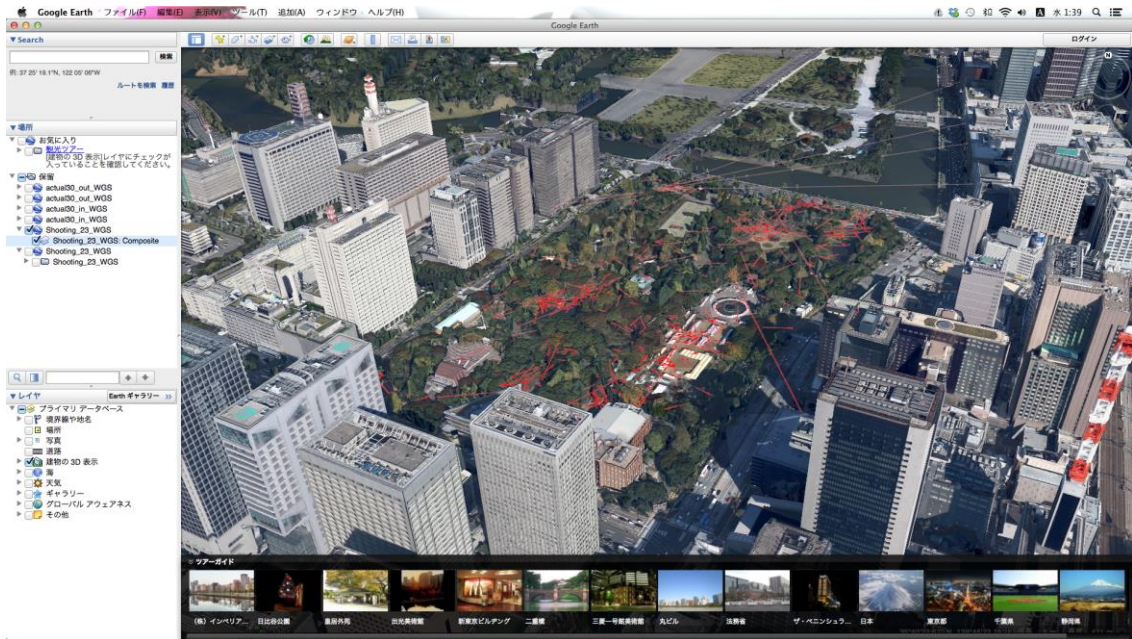
(a)
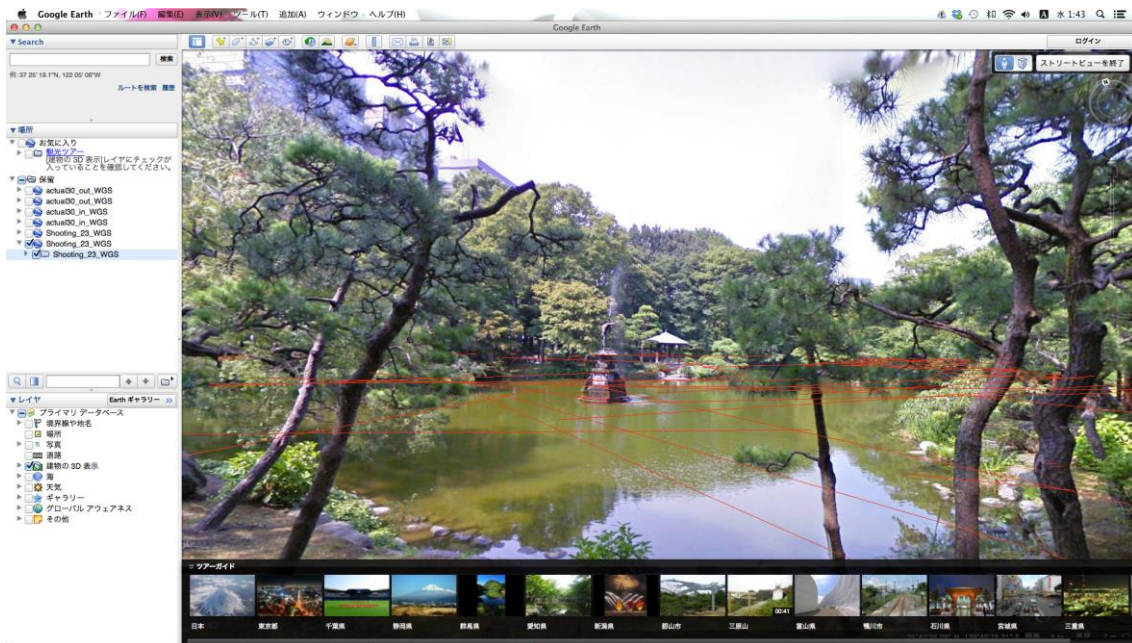
(b)

Figure 6-7. LVI visualized on Google Earth in: (a) a bird's eye view and (b) Street View
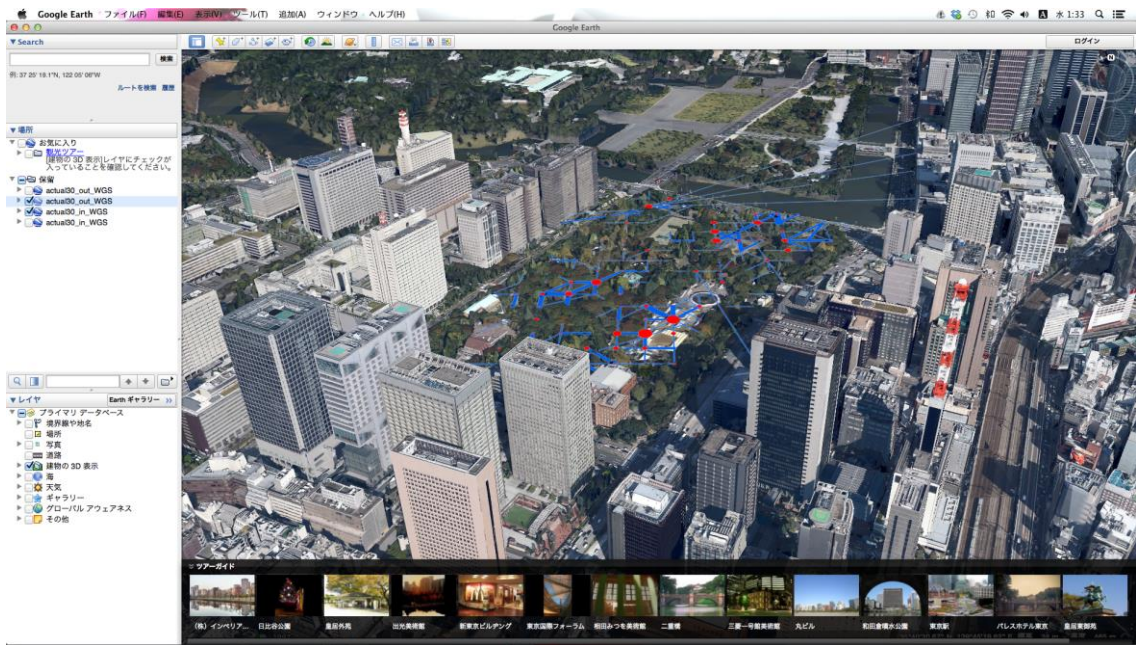
(a)
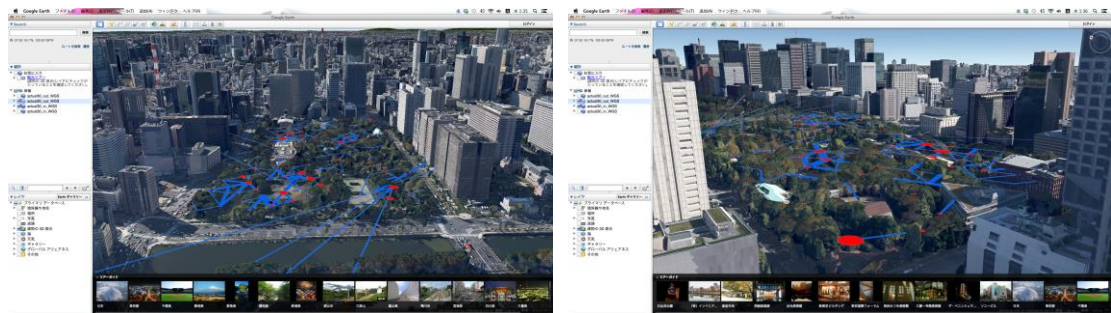
(b)   (c)

Figure 6-8. Visual interest flows with 30m×30m grids visualized on Google Earth in a
bird's-eye view from: (a) southeast, (b) north, and (c) southwest

objects such as trees and buildings are obtained from satellite and other types of
photographic images, and the shapes of buildings are more precise than those on
ArcScene depicted in Figure 6-6. Google Earth is free software and covers most places
in the world. Originally created spatial statistical data can be easily displayed by using
ones with kml format and operated interactively. In addition, it is possible to see
photographs in human-scale view at a particular local point on a street by using the

Street View function (Figure 6-7(b)). Line vector data such as LVI can be visualized on Street View, which is useful for determining the movement of visitors' visual interest—from where to what visual objects—based on their visual lines.

6.6. Summary

This chapter provided methods to acquire the spatial data related to the distance between an observer and visual object, and analyze and visualize it spatially using GIS and other relevant techniques. Firstly, the photo-shooting distances are estimated based on the fundamental equation of optics; thin lens formula and magnification of an object and image height. The required input variables were acquired by two on-site surveys; the photography survey by visitors, and the survey of object height measurements. Secondly, the spatial linear features of visual lines, called Lines of Visual Interest (LVI), were extracted, and the analysis and visualization techniques used with these features were suggested. For map representation of the spatial intensity of LVI accumulation, the kernel density estimation and the grid-based aggregation were conducted. In addition, the LVI were transformed to flow data between grids. Two types of flow, the extra-grid flow and the intra-grid flow, were identified and displayed as different representation symbols. Finally, the 3-D landscape models were used as base maps for more effective visualization that enables us to understand the relationship between participants' visual interest and physical landscape in the study area.

Chapter 7

Prediction of Visual Interest Flows

Previous research into GIS-based visual resource assessment and modeling has generated visualizations of visual quality or attractiveness of landscape based on the location specific environment, using biophysical and geomorphological spatial data. For example, Chhetri and Arrowsmith (2008) predict the attractiveness of certain nature-based landscapes by using a multiple regression model that contains indicators of landscape elements. Their model is created based on surveying visitors' landscape perceptions by using a simple questionnaire. In addition, combining objective and perception-based assessment is a recent, advanced technique. The study of modeling sightseeing potential presented in Chapter 5 may also correspond to this type.

As an alternative approach, this chapter presents a modeling technique for scenic resource attractiveness considering the positional relation of the interaction between visitor and visual object during on-site experience; this model predicts where or which object visitors' interest go toward from which place.

Scenic attractiveness modeling can contribute to the effective planning and management of tourist/recreational spaces by clarifying management priorities and the importance of certain locations. This study uses a multi-method approach in order to evaluate spots and scenes as well as their spatial relationships, thereby allowing us to evaluate the targeted area comprehensively. In addition, examining the spatial

interaction between spots and scenes contributes to recognizing the importance of understanding a person's environmental preferences in a geo-spatial context.

This chapter predicts the spatial pattern of visual interest flows using a prediction model constructed based on the spatial interaction model. Section 7.1 explains the fundamental structure of spatial interaction model. Section 7.2 describes the application of prediction models of visual interest flows. Finally, in the Section 7.3, the predicted results are visualized on maps, and compared with observed flows.

7.1. Applying Spatial Interaction Models

As it is an important methodology in the analysis of flow data, spatial interaction modeling is widely available. Spatial interactions cover a wide variety of movements, so many spatial scientists have applied this to analyze movements or evaluate a location's potential. The visual interest flows in this study are also targeted at this application.

The spatial interaction model includes several model types, including a gravity model, an entropy model, and a Huff model, among others. Considering the data characteristics, I chose the gravity model as being suitable for analysis of visual interest flows.

7.1.1. Classical gravity model

The general form of classical gravity model is expressed as

$$T_{ij} = k \frac{U_i^{\beta_1} V_j^{\beta_2}}{d_{ij}^{\beta_3}} \qquad (22)$$

where T_{ij} is the interaction intensity or the volume of flows between zone i and j, k is the proportionality constant, U_i is the mass of the zone of origin, D_j is the mass of the zone of destination, d_{ij} is the distance between two zones. β_1 is the potential parameter to generate flows, β_2 is the potential parameter to attract flows, and β_3 is a parameter reflecting the distance decay.

Taking logarithmic formation of both sides of the equation, the non-linear form can be converted into a linear form.

$$\ln T_{ij} = \ln k + \beta_1 \ln U_i + \beta_2 \ln V_j - \beta_3 \ln d_{ij} \qquad (23)$$

This log-normal model is better known as the empirical gravity model. However, several problems have been noted when using the log-normal model (Flowerdew & Aitkin, 1982). Firstly, the logarithm transformation affects the nature of the estimated values. The estimated flows produced by the regression are the logarithms of T_{ij}, not T_{ij} themselves. The total flows may therefore be underestimated when these estimates are converted into the antilogarithms. Secondly, the log-normal model assumes the random variables are log-normally distributed. However, there is little reason to suppose that these values are log-normal. Thirdly, the log-normal model assumes that the variances of random variables are identical, and that the expected difference between the estimates and observations is the same for all pairs of origins and destinations. This causes a problem when there are many cases where the estimate and observed flows are very low: the small absolute differences may result in a large difference between the two when compared in logarithmic form. Finally, when some of the flows are zero, the use of the logarithm transformation is difficult because the logarithms of zero cannot be computed. A small positive number is usually added to observations but the

choice of this number can have a considerable impact on the coefficients of the model and the output results.

7.1.2. Poisson / Negative Binomial gravity model

In order to overcome the problems of the log-normal gravity model, fitting the gravity model to the Poisson distribution is one of the suitable solutions (Flowerdew & Aitkin, 1982). The Poisson distribution is a discrete probability distribution that expresses the probability of a given number of events, also called count data, occurring in a fixed interval of time or space. This distribution is based on the premise that the dependent variable is a nonnegative integer, where the mean is small and a zero value is likely to occur. The data of visual interest flows in this study displays these characteristics. Therefore, we can consider that the probability of visual interest flows follow the Poisson distribution given by following formula

$$P_P(t_{ij}) = \frac{e^{-\lambda_{ij}} \lambda_{ij}^{t_{ij}}}{t_{ij}!} \qquad (24)$$

where λ_{ij} is the parameter that contributes to determining the shape of the distribution and is a positive real number, and λ_{ij} is equal to the expected value of t_{ij} and also to its variance. This characteristic is the constraint on the Poisson distribution. In real world, there are actually many datasets not satisfying this constraint: the conditional variance is often higher than the conditional mean (Burger et al., 2009). Therefore, I suggest also using the Negative Binomial distribution to fit the model given as below.

$$P_{NB}(t_{ij}) = \frac{\Gamma(t_{ij}+r^{-1})}{t_{ij}!\,\Gamma(r^{-1})} \left(\frac{r^{-1}}{r^{-1}+\lambda_{ij}}\right)^{r^{-1}} \left(\frac{\lambda_{ij}}{r^{-1}+\lambda_{ij}}\right)^{t_{ij}} \qquad (25)$$

where r is the dispersion parameter that defines the skewedness of the distribution. As r decreases towards 0, the Negative Binomial distribution is closer to the Poisson distribution. The Negative Binomial distribution is therefore similar to the Poisson distribution; however, this assumes that the variance of observed data is larger than the mean value. Researchers may generally employ the Negative Binomial model as the standard choice for a basic count data model (Greene, 2008).

By using these two probability distributions, the parameter λ_{ij} can be logarithmically linked to a linear combination of the logged independent variables.

$$\lambda_{ij} = \exp(\beta_0 + \beta_1 \ln U_i + \beta_2 \ln V_j + \beta_3 \ln d_{ij}) \qquad (26)$$

This procedure is known as the Poisson regression or Negative Binomial regression, carried out within the generalized linear modeling (Nelder & Wedderburn, 1972) framework in analysis. In these cases, no adjustment methods to handle zero flows are required. Moreover, the sums of observed and predicted flows are approximately equal and the sizes of the distributions of the observed and predicted flows are similar.

7.2. Construction of Prediction Model

7.2.1. Defined models for prediction

I define the prediction model of visual interest flows in this study by using the vec operator as follows:

$$\lambda = \exp(\alpha 1_n + \alpha_{intra} 1_{intra} + X_o \beta_o + X_d \beta_d + X_{intra} \beta_{intra} + \gamma d) \qquad (27)$$

where the dependent variable λ is the number of visual interest flows between two grids. The model is divided into extra-grid and intra-grid flows. Extra-grid flows are predicted by using the variables 1_n, X_o, X_d, and d as well as the parameters that function

to these, namely α, β_o, and β_d. Moreover, 1_n functions as the intercept term with α and this takes one value when the origin and destination grids are the same. Further, X_o is the matrix that contains more than one kind of origin-grid variable, X_d is the matrix for destination-grid variables, and d is the geographical distance between the centers of these two grids. By contrast, intra-grid flows are explained by using the variables of 1_{intra} and X_{intra} and their parameters α_{intra} and β_{intra}; in this case, 1_{intra} is composed of the intercept term together with α_{intra} and it takes one value when the two grids have different IDs, while X_{intra} is the set of explanatory variables for intra-grid flows. The explanatory variables in both extra-grid and intra-grid flows do not affect each other because one variable becomes zero when another takes a value.

The model separating approach is conducted in several studies targeting analysis of flow data, such as population flows (LeSage & Pace, 2008; Tamesue & Tsutsumi, 2012) and tourist flows (Marrocu & Paci, 2013). They have been successful in predicting the flows, with good accuracy. The intra-grid flow model and the extra-grid flow model can be integrated into a simpler form like the traditional gravity model. At this time, the determination of distance for the intra-grid flow is required. Some researchers have defined it by the original computational method, however, it is hard to find a clear rationale for this. Moreover, in the case of this study, the number of modified shooting distances are very large, totaling more than half the observations under 20 m (Figure 7-1). If the simpler model is used, the parameters of total generation and arrivals would be significantly influenced by the intra-grid flows. As a result, the extra-grid flows will be considerably underestimated. In making the
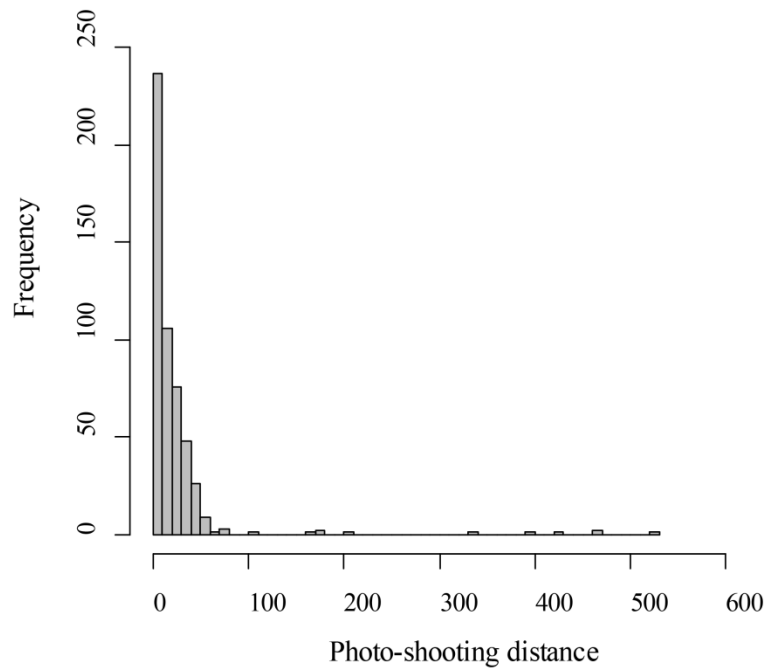
Figure 7-1. Histogram count of the modified shooting distances

prediction model, increasing the goodness-of-fit is a high priority. With the aim of achieving high estimation accuracy using the model, I do not assume a distance for intra-grid flow but use a separate model.

7.2.2. The first prediction model

I construct two types of prediction models by combining the explanatory variables. The first prediction model explains the intensity of visual interest flows based on their origin and destination potentials (Figure 7-2 (a)). Flow quantity can be assumed to increase as one or both potentials grow, but this change is limited by the distance decay effect. The concrete explanatory variables are shown in Table 7-1. To measure the origin-grid potential in the extra-grid flow model, the count of photo-taking locations, which equals the starting points of LVI, in the origin grid, is used. This measure can be

regarded as the total flow generation of the origin grid in the description of the spatial interaction. The destination-grid potential is represented by the count of the end points of LVI, indicating the total flow arrivals of the destination grid. The distance between the origin and destination pairs is the Euclidian distance between the centers of the two grids. The intra-grid flow model also takes the same types of variables as the extra-grid flow model but it does not contain the distance variable; rather, it is determined by using the grid potential in order to generate or attract flows. Here, a small positive number, log(0.01), is added to each grid point except for the distance variable (which has no count number), because to assume the origin and destination grids have no
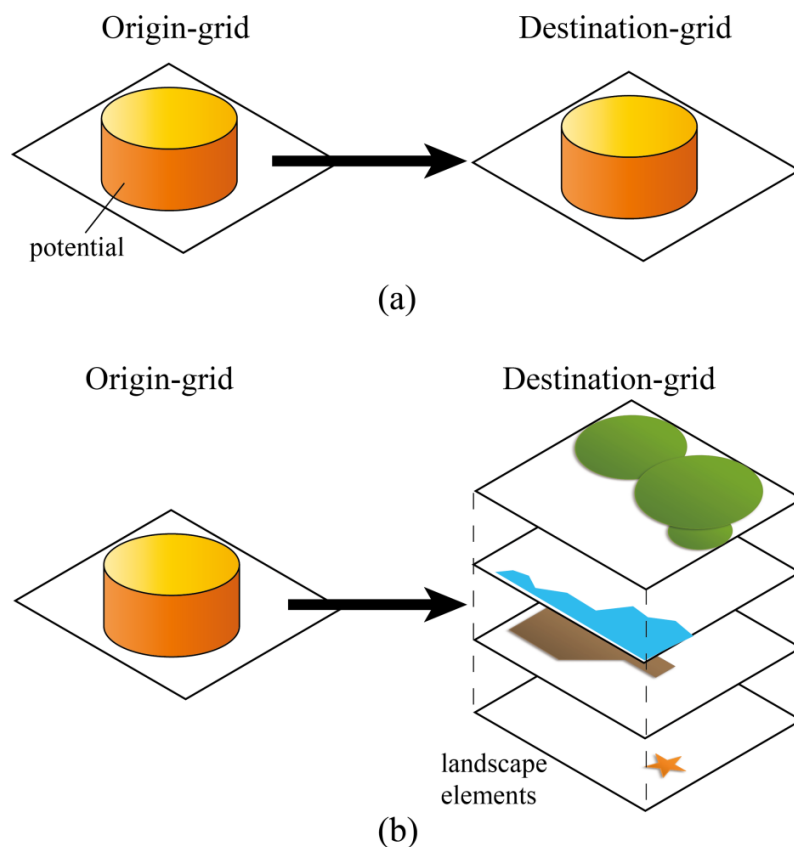
Figure 7-2. Conceptual diagrams of the prediction of visual interest flows based on the indicators of origin and destination grids: (a) using the degree of potential in each grid and (b) using the landscape element variables instead of the destination potential

122

Table 7-1. Explanatory variables related to the data on visual interest flows

Symbol	Variable	Data
$lnOriginP_{i, intra}$	Potential of the origin grid	Logarithm of the number of starting points of LVI
$lnDestinationP_{j, intra}$	Potential of the destination grid	Logarithm of the number of end points of LVI
$lnDistance$	Distance between the origin and destination grids	Logarithm of the Euclidian distance

potentials is unnatural. Such an assumption would indicate that the grid has no potential to generate flows. Therefore, I added the very small number that will not significantly influence the observed data of the explanatory variable. This processing does not affect the total amount of flows, even if the individual estimates will be somewhat influenced.

This first model will provide results that fit the predictors to the observers well because it uses explanatory variables that directly relate to the attractiveness of both the origin and the destination. However, acquiring the number of end points of LVI is time consuming because we need to measure the object height and estimate the photo-shooting distances. If these tasks could be reduced, the evaluation system in this study would become more practical for planning and management. Therefore, I suggest another prediction model that does not contain the number of end points of LVI.

7.2.3. The second prediction model

Previous research on the relationship between a person's scenic perception and landscape elements has clarified those factors that affect individual scenic preferences. For example, water is known to be one of the most important elements for attracting

visitors to nature landscapes (Zube et al., 1982). Wong and Domroes (2005) also showed that visitors tend to prefer a scene that contains water and greenery in an urban park setting. These findings indicate that a person's scenic preferences can be predicted based on the condition of the visual objects in this location. Indeed, some studies have tried to construct prediction models of scenic preferences from landscape factors (Bishop & Hulse, 1994; Bishop, 1996), with some authors having recently identified the potential of a specific location by using spatial data on landscape elements and visualizing the result in a GIS environment (Bishop, 1996; Chhetri & Arowsmith, 2008). In the same way, it is possible to predict a person's interest in a visual object by using spatial information on landscape elements as the explanatory variables. The combination and condition of these variables thus describe the spatial intensity of visual interest flows.

The second prediction model is composed of the variables for origin potential and the landscape elements of the targeted area as an alternative to destination potential (Figure 7-2 (b)). Table 7-2 shows the explanatory variables related to the landscape elements and their creation method by using the LiDAR and spatial vector data. These variables are developed based on the eight visual object categories of frequent photographs. Which variables are selected to appear in the intra-grid or extra-grid model and which ones affect the model positively or negatively can be confirmed by classifying the photo-shooting distances (Figure 7-3). For instance, because the photo-shooting distances of photographs of "structures", "streets", "water", and "open spaces" are comparatively long on average, the variables related to these categories tend to positively affect the extra-grid flow model.

In the extra-grid flow model, the variable that indicates the existence of a hill ($Hill_i$) is set as the origin variable because it strongly relates to the participant's own condition rather than to the visual object. In other words, a high place often provides a better opportunity of a panoramic view. The opening degree of a destination grid ($lnOpening_j$) measures the spatial and compositional effect of open space, which is assumed to positively affect the prediction because the majority of photographs of "open spaces" have a long photo-shooting distance. Moreover, architecture was noted as attractive by participants in the photography survey and thus the existence of houses or buildings ($House_j$) increases visual interest. Ponds also attracted participants' attention. Because participants tended to view the center of the pond, the pond area in each grid ($lnPond_j$) is better suited to the model explanation compared with a dummy variable that only indicates pond existence.

The number of trees ($lnTreeN_j$), average height of trees ($TreeH_j$), and existence of a festival ($Festival_j$) in the grids all negatively affect the extra-grid flow model because of the numerous short photo-shooting distances in the "people" and "vegetation" categories. The variable "$Landmark_j$" indicates the existence of noteworthy small landmarks such as monuments, sculptures, and large trees. Most of these landmarks are located at conspicuous places designed to induce a visitor's gaze such as the center of a pond or in an open space. Therefore, this variable may increase extra-grid flows.

In the intra-grid flow model, the hypotheses about the effects of the studied variables are opposite to the case of the extra-grid flow model. Thus, positive effects are induced by the number of trees ($lnTreeN_{intra}$), average height of trees ($TreeH_{intra}$), and existence of a festival ($Festival_{intra}$).

Table 7-2. Explanatory variables related to landscape elements

Symbol	Variable	Data
$\text{Hill}_{i,\ intra}$	Existence of a hill in an origin grid	Whether the > 6 m average height of elevation is in a grid or not (dummy)
$\text{lnOpening}_{j,\ intra}$	Opening degree of a destination grid	Logarithm of the number of DHM points of 0 ± 0.5m in a grid
$\text{House}_{j,\ intra}$	Existence of an architectural building in a destination grid	Whether the polygon of this building is in a grid or not (dummy)
$\text{lnPond}_{j,\ intra}$	Pond area in a destination grid	Logarithm of the pond area (km^2) in a grid
$\text{lnTreeN}_{j,\ intra}$	Number of trees in a destination grid	Logarithm of the number of DHM points in the range 5–40 m in a grid
$\text{TreeH}_{j,\ intra}$	Average height of trees in a destination grid	Average height of DHM points in the range 5–40 m in a grid
$\text{Landmark}_{j,\ intra}$	Existence of a landmark in a destination grid	Whether a small landmark such as a monument or large tree is in a grid or not (dummy)
$\text{Festival}_{j,\ intra}$	Existence of a festival in a destination grid	Whether the festival is held in a grid or not (dummy)
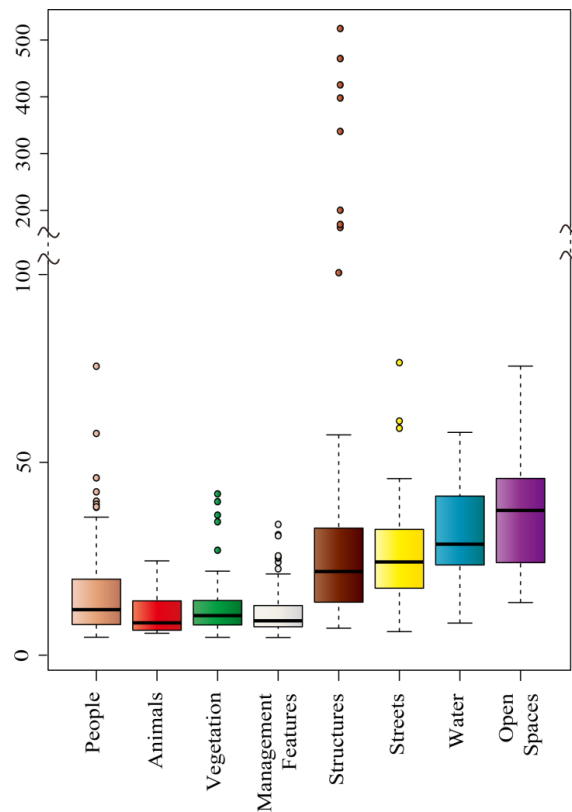
Figure 7-3. The boxplot of modified shooting distances in each category

126

7.2.4. Estimation of model parameters

The parameters of variables are estimated by maximum likelihood estimation (MLE). The MLE is a method used to seek the probability distribution that makes the observed data most likely, and the estimate is obtained by maximizing the likelihood function. The likelihood function is defined by reversing the roles of the data vector and the parameter vector in the probability density function that specifies the probability of observing data. The likelihood function represents the likelihood of the parameter given the observed data. In most actual cases, the logarithm of the likelihood function, called the log-likelihood function, is used for MLE. For the Poisson distribution in Equation (24), the log-likelihood function is given as

$$\ln L_P = \sum_{k=1}^{N} (T_k \ln \tilde{T}_k - \tilde{T}_k + \ln(T_k!)) \tag{28}$$

where N is the total number of flows, T_k is the observed flows and $\tilde{T}_k$ is the predicting flows. As the same, the log-likelihood function for the Negative Binomial distribution is as follows.

$$\ln L_{NB} = \sum_{k=1}^{n} \left\{ \sum_{l=1}^{T_k-1} (\ln 1 + r^{-1}) - \ln T_k! - (T_k - r^{-1}) \ln(1 + \tilde{T}_k) - T_k \ln r^{-1} + T_k \ln \tilde{T}_k \right\} \tag{29}$$

The optimization method for maximizing these log-likelihood functions is conducted based on the quasi-Newton method (also known as a variable metric algorithm).

7.2.5. Accuracy

To indicate goodness-of-fit, I use the root mean square error (RMSE). The RMSE is a frequently used measure of the differences between values predicted by a model and

values actually observed.

$$\text{RMSE} = \sqrt{\frac{1}{N} \sum_{k=1}^{N} (T_k - \tilde{T}_k)^2} \qquad (30)$$

Thus, the formula of RMSE is simple, and it can be flexibly divided into groups. I show the RMSE of three types; all flows, the extra-grid flows and the intra-grid flows. However, the comparison among groups has no meaning because the variance of each is different. We should normalize the RMSE by dividing by the standard deviation of the observed data σ_T. The normalized RMSE is defined as

$$\text{NRMSE} = \text{RMSE}/\sigma_T \qquad (31)$$

The NRMSE attains a value 1 if the method of prediction is no more accurate than forecasting the unconditional mean of the prediction set (Ted, 1997). This normalization is useful practice for interpreting and comparing the results. I also show the NRMSE of three types as the same with the results of RMSE.

7.3. Predicted Visual Interest Flows

7.3.1. Estimates of the first prediction model

The results of the estimated parameters, accuracy in RMSE and NRMSE values, and scatterplot of the observed and predicted flow values for the first model are shown in Table 7-3, Table 7-4, and Figure 7-4, respectively. Only the Poisson models are shown because the goodness-of-fit of the negative binomial models is worse than that of the Poisson models. All parameters of all models exhibit p-values less than 0.01, indicating they have the significance for the model. On the extra-grid flow models, the parameter values for lnOriginP$_j$ and lnDestinationP$_j$ are positive but the distance parameter is

negative. Therefore, the results show that the potentials of origin and destination grids provide the flow generation, but that the distance causes the predicting values to decay. This fact demonstrates that the spatial interaction model can be applied to explain the spatial occurrence patterns of visitors' visual interest in on-site environments. On the intra-grid flow models, the parameters for the origin- and destination-grid potentials are both positive but under 1. This is due to the large number of intra-grid flows and no decay effects.

The RMSE value of the extra-grid flows is largest in any models. According to the results, the NRMSE of extra-grid flows are larger than those of intra-grid flows. It means that the predictions of intra-grid flows are relatively accurate, but those of extra-grid flows cannot be estimated with enough precision. Comparing the cases of 20m×20m grids and 30m×30m grids, the values of NRMSE decrease as the grid

Table 7-3. Estimated parameters of the first prediction model

Coefficient	20m×20m grids				30m×30m grids			
	Estimate		Std. Error	Z value	Estimate		Std. Error	Z value
Intercept	6.229	***	0.389	16.000	8.822	***	0.591	14.938
Intercept_{intra}	-0.909	***	0.117	-7.751	-0.885	***	0.146	-6.063
$\ln\text{OriginP}_i$	0.790	***	0.064	12.422	0.732	***	0.072	10.160
$\ln\text{DestinationP}_j$	0.783	***	0.062	12.703	0.723	***	0.065	11.161
lnDistance	-2.983	***	0.107	-27.921	-3.452	***	0.152	-22.777
$\ln\text{OriginP}_{intra}$	0.628	***	0.081	7.717	0.628	***	0.095	6.598
$\ln\text{DestinationP}_{intra}$	0.553	***	0.079	6.972	0.546	***	0.091	5.980
Null Deviance	7108.2				6199.1			
Residual Deviance	1410.3				977.6			
Adj. Pesudo-R^2	0.715				0.758			
AIC	2262.9				1658.3			

Pseudo-significant level ***: p<0.001, **: p<0.01, *: p<0.05

Table 7-4. Accuracy of the first prediction model

	20m×20m grids		30m×30m grids	
	RMSE	NRMSE	RMSE	NRMSE
All	0.035	0.639	0.069	0.478
Extra-grid	0.031	0.853	0.060	0.817
Intra-grid	0.389	0.423	0.571	0.294

(a) (b)
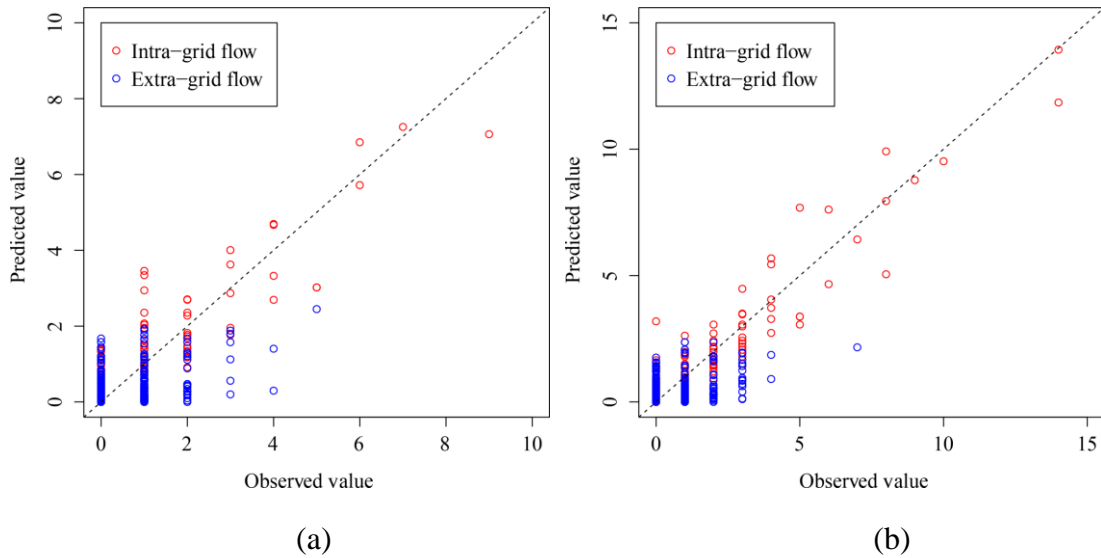
Figure 7-4. Relationship between the observed and predicted values of visual interest flows based on the first prediction model in (a) 20m×20m grids and (b) 30m×30m grids

polygon size increases from 20 m to 30 m. While the NRMSE of intra-grid flows largely decreases (the model become more precise), there is not the big change in the NRMSE of extra-grid flow models. This tendency can be seen on the scatterplots of the observed and predicted flow values for each grid size. If the accuracy of each model is good, a scatterplot of actual and predicted values on respective axes should indicate a data spread close to a 45-degree line from the origin (the line itself represents perfect positive correlation of the two variables). The plots of the intra-grid flows in the case

of 30m×30m grids are therefore found to be in better condition as a whole. On the other hand, there are many under-predicted values in the extra-grid flows in both cases.

7.3.2. Predicted spatial flows of the first prediction model

The predicted flows are shown on the maps (Figure 7-5 (c) and (d)) and compared with the observed flows (Figure 7-5 (a) and (b)). I do not show the predictions with less than 0.7 values because such low values deviate greatly from the range of observations. As a whole, the flows by the intra-grid flow model were predicted well. However, the extra-grid flows seem to have some problems.

While the observed flows are widely distributed around the park, the predicted flows are comparatively concentrated in specific spaces. This tendency is especially strong with the extra-grid flows. The reasons would be the effect of the distance-decay parameter, and concentration in the grids having the large number of total flow generations or arrivals at particular spaces. The extra-grid flow models depend on the potential of each grid and the closeness between grids. Because the absolute values of their parameters are very similar, even if one of their variables is low, the model would not predict the flow occurrence.

The characteristics of the extra-grid flow model also make it difficult to predict the occurrence of irregular flows that have a very long length. For example, though several observed flows that have long length generated from the specific location in the northern west of the park to the building out of the park, the models did not predict them. This spot is located on the top of hill, so the topographic condition of place influences the spatial pattern of visual interest flows. Adding new explanatory

variables, such as the elevation of locations, might be effective to improve the flexibility of the models for the prediction of the extra-grid flows.

I used the total number of flow generation and arrivals for the model variables. It is possible to use other indicators related to the attractiveness of space. For example,
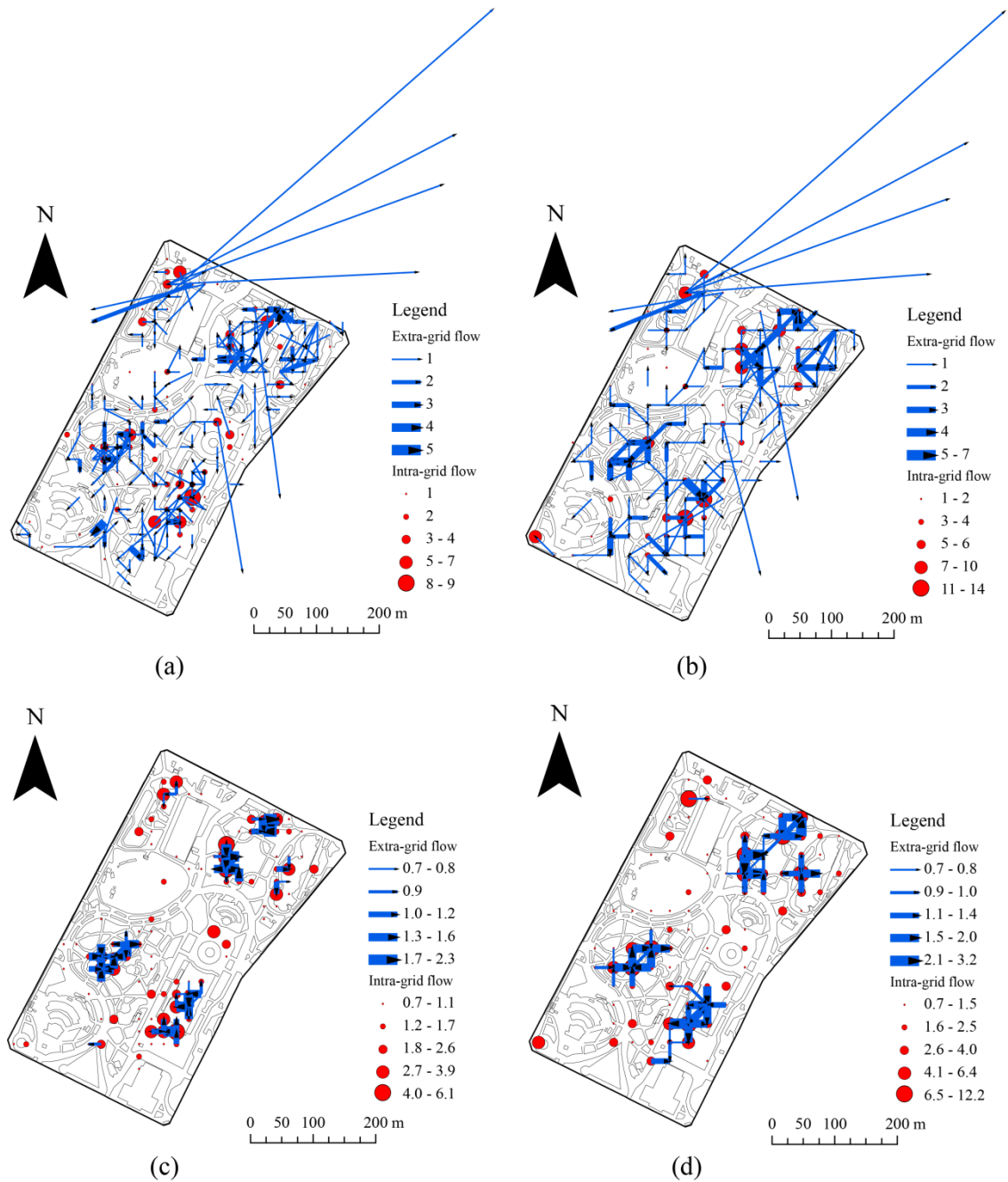
Figure 7-5. Observed and predicted visual interest flows of the first model based on (a) and (c) 20m×20m grids, and (b) and (d) 30m×30m grids

instead of the total number of flow arrivals, the score of attractiveness of each grid evaluated by some kind of method beforehand could be adopted for the explanatory variable. Such an approach might make prediction process easier and more precise. Similarly, the idea of using the landscape elements as destination variables is presented in the next session.

7.3.3. Estimates of the second prediction model

All 18 explanatory variables of both the intra-grid and the extra-grid flow models are set in the second model, while their optimum combination is examined and estimated in a step-wise manner (Table 7-5). The results for only the Poisson models are shown as with the first model. RMSE and NRMSE accuracy and the scatterplots of the observers and predictors are shown in Table 7-6 and Figure 7-6, respectively.

The selected coefficients show few differences in the 20m×20m and 30m×30m grid models. Notably, the model for the 30 m grid size takes fewer coefficients and its goodness-of-fit is better than that for the 20 m grid size. Further, the origin potential ($lnOriginP_{j,intra}$) and distance between grids ($lnDistance$) are determined as important variables, as they were in the first model.

In the extra-grid model, the existence of houses ($House_j$) and landmarks ($Landmark_j$) as well as having a pond area ($lnPond_j$) in the grids are shown to be those variables that have positive effects, whereas the opening degree of space ($lnOpening_j$), number of trees ($lnTreeN_j$), and existence of a festival ($Festival_{intra}$) are found to decrease the predicted values. Therefore, the hypotheses are supported for most variables except the opening degree of space, which by itself does not have sufficient power to attract

133

visitors in the study area. A specific condition, such as combination with the other visual objects (e.g., water, landmarks, and events), may be needed to entice people toward an attractive visual scene. Indeed, most photographs taken in a space with a high opening degree include other unique visual objects, meaning that these were not recognized as "open spaces" as such. The photographs taken in "open spaces" were rather limited to a particular area such as the First Flower Garden. In the intra-grid flow model, only one or two variables besides the intercept and origin potential were selected, and their significances were not high. These findings suggest that many of the intra-grid flow values can be predicted by the origin potential: the low values of NRMSE for the intra-grid flow models, shown in Table 7-6, confirm this fact.

According to the RMSE and NRMSE results (Table 7-6), although the accuracy of both the intra-grid and the extra-grid flow models in the second prediction is lower than that in the first, there is not a large difference between them. In addition, the distribution of the observed and predicted values in the scatterplots is also similar in the first and second models (see Figures 7-4 and 7-6). Therefore, the second prediction model is valid as well as the first, suggesting that landscape element data are a useful and effective resource for constructing a prediction model of visual interest flows as the explanatory variables.

7.3.4. Predicted spatial flows of the second prediction model

The predicted visual interest flows of the second model are spatially visualized in Figure 7-7 (c) and (d). The overall tendency is similar to that for the first prediction model, with these flows focused on specific places. However, the predicted flows for

Table 7-5. Estimated parameters of the second prediction model

Coefficient	20m×20m grids				30m×30m grids			
	Estimate		Std. Error	Z value	Estimate		Std. Error	Z value
Intercept	8.698	***	0.470	18.495	11.674	***	0.684	17.060
Intercept$_{intra}$	-0.744	***	0.212	-3.507	-0.345		0.304	-1.135
lnOriginP$_i$	1.007	***	0.065	15.475	0.878	***	0.070	12.514
lnOpening$_j$	-0.151	**	0.054	-2.821	-0.131	*	0.059	-2.235
House$_j$	0.432	**	0.138	3.138	0.359	*	0.140	2.561
lnPond$_j$	0.161	***	0.029	5.607	0.176	***	0.028	6.209
lnTreeN$_j$	-0.347	***	0.046	-7.627	-0.304	***	0.042	-7.149
Landmark$_j$	0.528	**	0.187	2.829	0.485	**	0.181	2.681
Festival$_j$	-0.367	*	0.158	-2.315				
lnDistance	-3.328	***	0.107	-31.012	-3.733	***	0.151	-24.773
lnOriginP$_{intra}$	0.995	***	0.079	12.605	1.069	***	0.078	13.631
lnTreeN$_{intra}$	-0.087		0.049	-1.770				
TreeH$_{intra}$					-0.216	*	0.104	-2.063
Festival$_{intra}$	0.256		0.159	1.609				
Null Deviance	7180.2				6199.1			
Residual Deviance	1706.4				1129.5			
Adj. Pesudo-R^2	0.676				0.735			
AIC	2571.0				1818.1			

Pseudo-significant level ***: p<0.001, **: p<0.01, *: p<0.05

Table 7-6. Accuracy of the second prediction model

	20m×20m grids		30m×30m grids	
	RMSE	NRMSE	RMSE	NRMSE
All	0.039	0.714	0.078	0.545
Extra-grid	0.033	0.904	0.065	0.880
Intra-grid	0.510	0.555	0.754	0.389
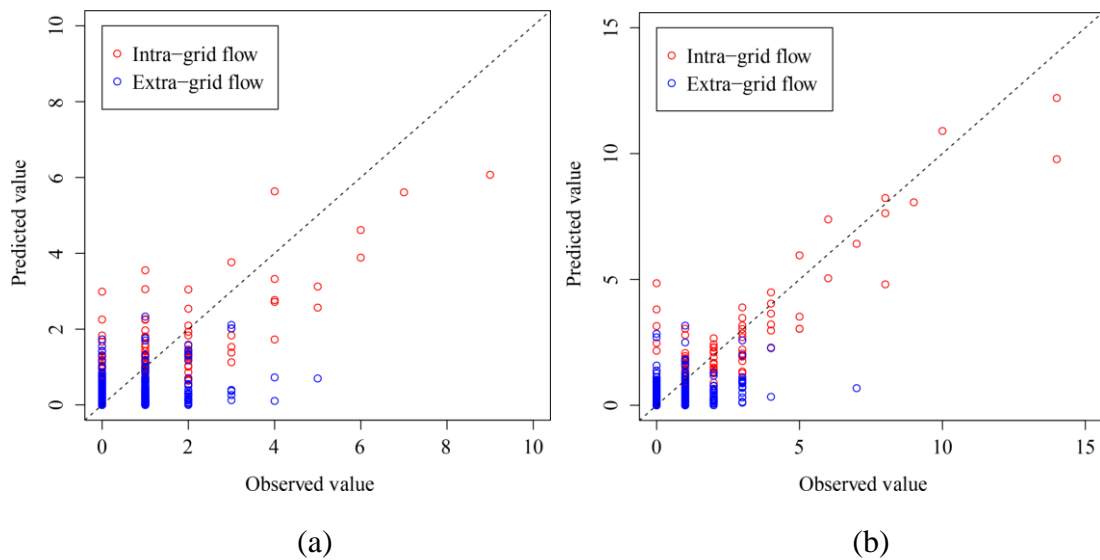
Figure 7-6. Relationship between the observed and predicted values of visual interest flows based on the second prediction model in (a) 20m×20m grids and (b) 30m×30m grids

the second model are stronger than those for the first in their tendency for the extra-grid flows to move toward specific spatial objects such as architectural buildings and water. For example, in the predictors with 30m×30m grids shown in Figure 7-7 (d), the extra-grid flows existing at the south of the park turn on to the architecture in their surrounding spots. Similarly, at the Shinji Pond that is located at the northeast of the park, many predicted extra-grid flows turn on to the pond from the grids that have banks. These trends are not seen in the first prediction model (Figure 7-5). This effect can be considered to be due to the use of landscape elements as explanatory variables in the second model.

The first models predict that the flows generated from an origin grid that has high potential only move toward destination grids that have high potential, whereas the second models show that the distribution of predicted flows is influenced by the combination of the landscape elements in the grids. Indeed, although the assumptions
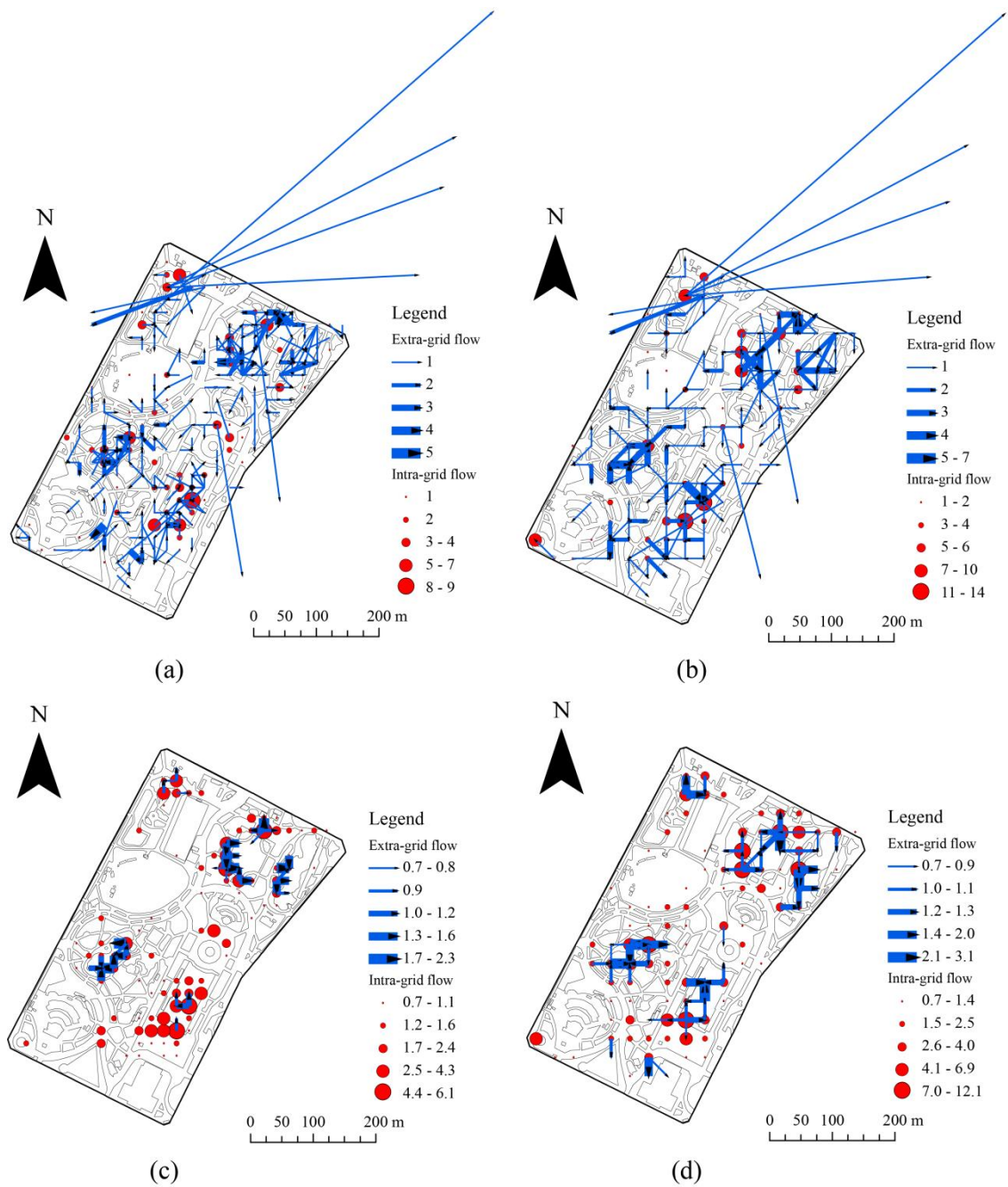
Figure 7-7. Observed and predicted visual interest flows of the second model based on (a) and (c) 20m×20m grids, and (b) and (d) 30m×30m grids

in each model do differ, the results of the predicted flows are similar. This finding is very important in visual resource assessment and modeling because it means that persons' on-site visual interest can be predicted from environmental data to a precise

level. However, one limitation remains. Irregular flows that take a very long distance cannot be predicted in either model. In order to overcome this problem, constructing a new model or variable for predicting only flows that have long distances and integrating this into the basic model might be effective.

7.4. Summary

The prediction models of visual interest flows were constructed based on the spatial Interaction model, and two types of prediction models were suggested. The first prediction model was explained by the origin and destination potentials and geographical distance between them, represented by the total number of flow generations (the number of starting points of LVI), total number of flow arrivals (the number of end points of LVI), and Euclidian distances between grids. The second model took account of the variables related to landscape elements as an alternative to destination potential, as explained by the optimum combination of explanatory variables. As a result of the estimation of the model parameters, the spatial patterns of visual interest flows were found to hold well in both models in the context of a spatial interaction model.

Thus, the spatial data of visual lines, such as LVI, has various possibilities for the analysis and modeling of persons' awareness and evaluations of spaces. In technical terms, we can apply other statistical methods to search for patterns of data, and also develop prediction models by examining further new explanatory variables or applying in other environments. For the experimental studies, these theoretical and applied research methods, focusing on the distance between the observer and visual object, will

certainly contribute to the research fields of scenic/landscape perception and sightseeing behavior.

Chapter 8

Conclusion

Landscapes or visual resources are among the most important kinds of locations in contemporary tourism (Jacobsen, 2007). Their visual quality is directly linked to the recreation quality for visitors (Schirpke et al., 2013), and have the great power to affect visitors' evaluations to the destinations. Therefore, as the fundamental studies for design, planning, and management of tourist/recreational spaces, previous studies have clarified humans' scenic/landscape perceptions in various settings and approaches. At the same time, various kinds of visual resource assessment methods have been developed. Geo-spatial information technologies such as GIS are effective tools for advancing such efforts. This thesis presented an innovative approach using visitor-oriented and computer-aided techniques for analyzing and assessing tourist/recreational spaces. This final chapter concludes the contents of thesis by summarizing the results and findings, and discussing possible future work.

8.1. Summary of This Thesis

This thesis developed methods for the analysis and modeling of visitors' visual interest during their on-site experiences in geographic space. Most of the previous studies on visitors' on-site perceptions to visual stimuli have engaged in analysis of scene specific evaluation of visual resources by visitors, using only photographic

image data. To overcome such limitations, a combination of digital cameras and geo-spatial information tools such as GIS were suggested. A series of data acquisitions, visualization, statistical analysis, and modeling potential provides as core components of this thesis.

In order to acquire the spatial data related to visitors' visual interest, two surveys were conducted at Hibiya Park in Tokyo, Japan as the case study area. In the first survey, 21 recruited participants were asked to photograph positive scenes during walking around the park freely, and thereafter they answered questionnaires for evaluation of preference level of each visual experience and categorization of each visual object. In the second survey, the heights of over two hundred objects projected in the photographs taken by participants were measured using the laser distance meter. Based on acquired data in these field surveys, spatial point and line data of visitors' visual interest were extracted.

Four types of studies for analysis and modeling of visitors' visual interest were presented. Two studies attempted to analyze based on the point data of locations that visitors' interest generated. The first application was the exploratory analysis of spot characteristics; several spatial clusters were extracted by spatial autocorrelation analysis, based on similarity of likeability scores. The characteristics of seven representative spots were statistically described in multiple indicators including the above clusters. The second application was modeling and visualizing the sightseeing potential of locations. Weighted scores accounting for the preference level and removing certain biases were attached into the algorithm of density computation. This

operation created more suitable maps of potential sightseeing preferences than the non-weighted density maps.

The subsequent two studies mainly focused on the spatial line data of visitors' visual lines on their interest. The third application was the visualization of the spatial intensity of visual lines, represented as spatial linear features. Three map representation techniques were demonstrated; density estimation for line data, grid-based aggregation and flow data representation. In addition, the advantages and disadvantages of each were described. The final application described was the construction of a prediction model for visual interest flows. Spatial interaction models were used for predicting the amount of total flows between locations by the variables of origin potential, destination potential or landscape elements, and distance between locations The model parameters were estimated to have high significance levels in all cases, and the predicted values exhibited good agreement with the observed data.

8.2. Results and Findings

8.2.1. Field survey and data acquisition

Hybrid methods combining on-site photographic methods and geo-spatial tools were used to conduct the study. The results of (1) the photography survey by visitors and (2) the survey of object height measurements, provided seven main data types in total; photo-taking locations, photo-taking directions, photo-shooting distances, photo-taking time, photographic images, visual object categories, and likeability scores. These data were transformed into the spatial point and line data of visitors' visual interest, named points of visual interest (PVI) and lines of visual interest (LVI); PVI are constructed

with the photo-taking locations (spatial object) and attribute values, and LVI is composed of line vector data of the visual line from observers' standing location to the position of the visual object.

8.2.2. Exploratory spot analysis

Exploratory analysis methods were used for searching emotional similarity of PVI in their neighborhood relations, determining spot ranges and describing spot characteristics. The results of the global and local Moran's *I* statistics and the spot profiles of seven representative ones derived four significant spatial clusters and the hierarchy of spot preferences. The spots including many high-high or low-low clusters, evaluated in consensus of preference levels; the former are regarded as the best spots, placed at the top of the hierarchy of spots, and the latter may be ordinary spots. The other spots were composed of the non-clustered PVI and a few low-high or high-low clusters, constituting the middle level of hierarchy. Finally, the spaces accumulating no interest did not receive any evaluations; these were ranked lowest in the overall hierarchy.

8.2.3. Modeling sightseeing potential

The density map of PVI was created for evaluation of the space potential, based on their visual preferences. To reduce certain modeling biases in the maps made using the kernel density estimation (KDE) method, two types of weighted scores were used in the density computation and five indicators were set as the components of the weighted scores. These were the scores of likeability, which indicates the emotional distance

with each photograph, the scores based on the object types of photos, the reciprocal number of photographs created by each participant, the distance between the photo-taking locations and the participants' starting points, and the reciprocal of the photo-taking time. The weighted scores enabled more accurate density maps of the photo-taking locations, better indicating the potential of locations when compared to the result with non-weighted scores.

8.2.4. Visualization of spatial intensity of visual lines

Visualization techniques applicable to the spatial intensity of LVI were suggested using three different approaches. The kernel density estimation (KDE) of LVI was the easiest tool to find the degree of LVI accumulation, but the directional information of LVI was entirely abstracted. Grid-based aggregation can represent the degree of accumulation and mean direction of LVI, but the spatial relationship between an observer and visual object cannot be described as well as KDE. Flow data representation overcame such problems, and permits interpretation of spatial intensity, spatial relationships, and directional information, regardless of summarization of the accurate LVI locations.

8.2.5. Prediction of visual interest flows

The prediction models of visual interest flows were constructed based on the Poisson/Negative Binomial Gravity model, with separate models for the intra-grid flows and the extra-grid flows. Two types of prediction models were constructed based on the difference in the explanatory variables for destinations; the total flow arrivals

(the number of end points of LVI) or the physical landscape elements. As a result of estimation of model parameters, the first model showed a high probability in terms of significance level, indicating a positive effect from the origin and destination potential whereas distance showed a negative effect. Moreover, the predicted flows were excellent in terms of the goodness-of-fit parameter. The second model also determined the origin potential and distance as important variables, and consisted of five to six types of landscape elements as variables for extra-grid flow model and one or two types for intra-grid flow model. The accuracy of the second model prediction was good as same as the first, indicating persons' on-site visual interest can be predicted from environmental data to a precise level.

8.3. Research Novelty and Contribution

In this work, a unique and innovative contribution has been made to the field of visual resource assessment and modeling research. The novelty and contribution of my studies are summarized in the following section.

Firstly, I succeeded in quantifying and analyzing the spatial patterns of a subject's visual interest, occurring in a recreational setting, by using geo-spatial information technologies. The spatial data constructed from the photography-related data recorded by visitors represented the location and spatial relationship of the observers and/or visual objects geographically; this information included not only location and orientation data, but also psychological aspects such as likeability and the type of visual object preferred. Moreover, such data was extremely effective when used in spatial analysis and modeling of visitors' visual interest in geographical terms. These

processes are linked to the idea of "spatial thinking" in geospatial sciences, defined as the extraction of meaning from the shape, size, orientation, location, direction or trajectory, of certain objects, processes or phenomena, or the relative positions in space of multiple objects, processes or phenomena (National Research Council, 2006). GIS techniques have assisted in various situations requiring such a way of thinking, such as spatial representation, analysis, and prediction of visual interest.

Secondly, the study details designs for assessment procedure, constructs and presents a methodological standard for visual resource assessment and modeling using a combination of visitor-oriented photography and geospatial tools. Each of the data acquisition, visualization, statistical analysis, and modeling potential techniques are important parts of research process that provide the ability to explore visitors' interest, and evaluate scenic and spot attractiveness in specific tourist/recreational sites. The micro-scale assessment I demonstrated requires understanding of the sensitivity of the digital tools to acquire reliable, high-quality data because the characteristics of the data have an influence on the quality of analysis and assessment results. In my study, I was able to manage the data acquisition seamlessly and obtain all the various data I required with good quality, through careful design of the studies; as the result, could show that the various analysis and modeling techniques were applicable to collected data.

Thirdly, the methods provided in this thesis enabled us to assess the entire area of the targeted site, not only scenes visitors perceived (Figure 8-1). The importance of this outcome should be emphasized mostly because I was able to overcome the notable limitations of typical photographic surveys, and clearly showed new and useful

146
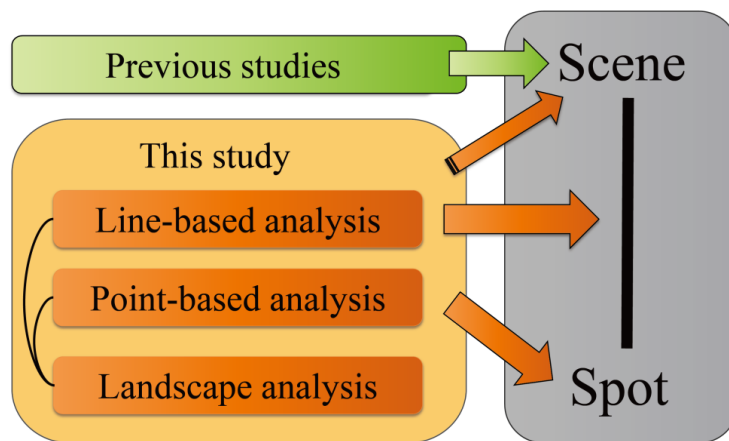
Figure 8-1. Novelty of this thesis compared with the previous studies

techniques for visual resource management of specific sites. The spatial intensity of PVI and LVI and the subsequent geo-visualization provided location specific potential and attractiveness of scores for scenes and spaces. The results will contribute to management of tourist/recreational spaces, or to policies relating to the conservation and maintenance of visual resources. For example, ranking such scenes and spaces could prove useful in prioritizing their management. Highly-preferred spaces can be conserved on a priority basis, whereas less preferred spaces could be improved so that they attract more visitors. It could also be used in tourism promotion, as a means of promoting a targeted site's most likeable scenes and spaces.

8.4. Future Works

This section refers to possible future works in this field of study using the approaches described, focusing on survey design and technical issues.

8.4.1. Survey design

The work presented in this thesis has some limitations, which are attributed mainly to the sample size. The small sample of 21 young participants may arguably reduce the general applicability of the results. The methods showed in this thesis are suitable for further investigations employing additional and various types of participants, clarifying visitors' preferences for scenery and spots within each group. The findings of such a study would be more useful for the planning and management of recreational spaces, accounting for the recreational preferences of different visitor classes.

The participants evaluated the scenes based on preference level only, as specified by a five-point likeability index. A greater variety of appraisal indices could be used to determine the quality of a visitor's experience of scenes or landscapes, and to assess the spot quality in more detail. Traditional perception-based landscape assessments have classified the aesthetic quality of visual resources in multiple dimensions by using such indices; such existing studies provide a valuable resource for future work.

It is also necessary to consider the validity of the scale of my studies. This thesis aimed to assess small tourism/recreational areas, which are often composed of complex natural and cultural elements; the results demonstrated the effectiveness of methods, and the techniques may be applied in other settings. Linear environments may be one of the most relevant examples, because photographic surveys by actual visitors were originally developed to assess visual resources existing along touring routes such as hiking trails (Cherem & Driver, 1983). If we conduct the surveys in larger scale areas, which do not correspond to linear settings, more data is required, and thus more participants should be recruited. On-site evaluation generally entails a high cost, and it

is difficult to obtain many respondents. Recruiting a sufficient number of participants is a problem that needs to be considered in the future.

8.4.2. Technical issues

Point data of photo-taking location, and line data of photo-shooting distance from an observer's standing location to a visual object's location, were extracted as spatial logs of participants' visual interest: the former represents the observer's standing location where his or her visual interest generates and the latter indicates the observer's sight line to the visual object. These techniques are certainly innovative in scenic preference assessment studies and spatial information studies. However, it is still insufficient to represent perceptual scenes as spatial features, because visitors often recognize a spatial extension of landscape during their personal evaluation. The collection and visualization of visitor's fields of vision is a further challenge: a polygon feature may be suitable to represent visual field as spatial data. If possible, the comparison and evaluation of three basic spatial representations of visual interestuch as PVI, LVI and polygon data of visual fields would be a significant step towards clarifying the advantages and disadvantages of each in technique of spatial analysis and visualization. 3D geo-visualization of these data would also be a valuable area for advancing these techniques. Some photo-shooting distances oriented toward an oblique direction were necessarily transformed into the horizontal direction. Visualizing and analyzing the LVI and visual field polygons as 3D spatial objects in a 3D environment would enable more detail evaluation considering actual visitor behavior.

Finally, this thesis did not cover some fundamental aspects of scenic/landscape perception of visitors, in order to remain focused on the development of GIS-based analysis and modeling of visitors' on-site visual experiences. The quantification of visual distance in perceived scenes is an unprecedented area of study, and clarifying the relationship between visual distance and other indicators, such as aesthetic quality of the landscape, will contribute to a deeper understanding of visitors' on-site experiences. Image analysis of photographs may be also effective in quantifying the visual components of the photographed scenes, and analyzing the relationship between various perceived and physical aspects of the landscape.

Thus, despite presenting various new methods for perception-based visual resource assessment and modeling, and proving the effectiveness of these methods, some problems have been left unresolved. Future work is required to improve aspects of the research, and to advance and extend the research approach by applying it to various settings and different purposes. It is believed that these efforts will accomplish widespread knowledge and acceptance of these techniques, and permit more sensible recreation planning and management that reflects visitors' preference for visual resources.

Bibliography

Akbar, K. F., Hale, W. H. G., & Headley, A. D. (2003). Assessment of scenic beauty of the roadside vegetation in northern England. *Landscape and Urban Planning, 63*, 139–144.

Amsden, B., Stedman, R. C., & Luloff, a. E. (2011). Exploring contexts of place: The role of setting and activity in a high-amenity tourism community. *Tourism Geographies, 13*, 531–548.

Andrienko, G., Andrienko, N., Demsar, U., Dransch, D., Dykes, J., Fabrikant, S. I., Jern, M., Kraak, M.-J., Schumann, H., & Tominski, C. (2010). Space, time and visual analytics. *International Journal of Geographical Information Science, 24*, 1577–1600.

Anselin, L. (1995). Local indicators of spatial association—LISA. *Geographical analysis, 27*, 93-115.

Anselin, L. (1996). The Moran scatterplot as an ESDA tool to assess local instability in spatial association. In M. Fischer, H. Scholten, & D. Unwin (Eds.), *Spatial Analytical Perspectives on GIS in Environmental and Socio- Economic Sciences* (pp. 111–125). London: Taylor and Francis.

Anselin, L., Syabri, I., & Kho, Y. (2006). GeoDa: An introduction to spatial data analysis. *Geographical Analysis, 38*, 5–22.

Arai, H. (2011). Circular statistics for the analysis of directional geological data. *The Journal of the Geological Society of Japan, 117*, 547–564. [in Japanese with English abstract]

ArcGIS Resource Center. (n.d.a). *ArcGIS help 10.1: What is lidar data?* Retrieved February 21, 2014, from http://resources.arcgis.com/en/help/main/10.1/index.html#/What_is_lidar/015w00 000041000000/

ArcGIS Resource Center. (n.d.b). *ArcGIS help 10.1: Using viewshed and observer points for visibility analysis.* Retrieved February 21, 2014, from http://resources.arcgis.com/en/help/main/10.1/index.html#/Using_Viewshed_and _Observer_Points_for_visibility_analysis/00q90000008n000000/

ArcGIS Resource Center. (n.d.c). *ArcGIS help 10.1: How kernel density works.* Retrieved February 21, 2014, from http://resources.arcgis.com/en/help/main/10.1/index.html#//009z00000011000000

Arrowsmith, C., & Inbakaran, R. (2002). Estimating environmental resiliency for the Grampians National Park, Victoria, Australia: A quantitative approach. *Tourism Management, 23*, 295–309.

Bailey, T. C., & Gatrell, A. C. (1995). *Interactive spatial data analysis*. Essex: Longman.

Bíl, M., Bílová, M., & Kubeček, J. (2012). Unified GIS database on cycle tourism infrastructure. *Tourism Management, 33*, 1554–1561.

Bishop, I. D. (1996). Comparing regression and neural net based approaches to modelling of scenic beauty. *Landscape and Urban Planning, 34*, 125–134.

Bishop, I. D., & Hulse, D. W. (1994). Prediction of scenic beauty using mapped data and geographic information systems. *Landscape and Urban Planning, 30*, 59–70.

Bolbol, A., Cheng, T., Tsapakis, I., & Haworth, J. (2012). Inferring hybrid transportation modes from sparse GPS data using a moving window SVM classification. *Computers, Environment and Urban Systems, 36*, 526–537.

152

Born, M., & Wolf, E. (2013). *Principles of optics: Electromagnetic theory of propagation, interference and diffraction of light*. Cambridge University Press.

Brabyn, L., & Sutton, S. (2013). A population based assessment of the geographical accessibility of outdoor recreation opportunities in New Zealand. *Applied Geography, 41*, 124–131.

Brandl, M. (2002). *Thin spherical lenses*. Retrieved February 21, 2014, from http://www.physnet.org/modules/pdf_modules/m223.pdf

Brickell, K. (2012). Visual critiques of tourist development: Host-employed photography in Vietnam. *Tourism Geographies, 14*, 98–116.

Brunsdon, C., & Corcoran, J. (2006). Using circular statistics to analyse time patterns in crime incidence. *Computers, Environment and Urban Systems, 30*, 300–319.

Burger, M., van Oort, F., & Linders, G.-J. (2009). On the specification of the gravity model of trade: Zeros, excess zeros and zero-inflated estimation. *Spatial Economic Analysis, 4*, 167–190.

Cadwallader, M. (1977). Frame dependency in cognitive maps: An analysis using directional statistics. *Geographical Analysis, 9*, 284–292.

Chamberlain, B. C., & Meitner, M. J. (2013). A route-based visibility analysis for landscape management. *Landscape and Urban Planning, 111*, 13–24.

Chen, B., Adimo, O. a., & Bao, Z. (2009). Assessment of aesthetic quality and multiple functions of urban green space from the users' perspective: The case of Hangzhou Flower Garden, China. *Landscape and Urban Planning, 93*, 76–82.

Chenoweth, R. (1984). Visitor employed photography: A potential tool for landscape architecture. *Landscape Journal, 3*, 136–143.

Cherem, G. J., & Driver, B. L. (1983). Visitor employed photography: A technique to measure common perceptions of natural environments. *Journal of Leisure Research, 15*, 65–83.

Chhetri, P. (2006). Modelling the attractiveness potential of scenic views: A case study of the Grampians National Park, Australia. *Tourism Recreation Research, 31*, 101–107.

Chhetri, P., & Arrowsmith, C. (2008). GIS-based modelling of recreational potential of nature-based tourist destinations. *Tourism Geographies, 10*, 233–257.

Chhetri, P., Arrowsmith, C., & Jackson, M. (2004). Determining hiking experiences in nature-based tourist destinations. *Tourism Management, 25*, 31–43.

Chhetri, P., Corcoran, J., & Arrowsmith, C. (2010). Investigating the temporal dynamics of tourist movement: an application of circular statistics. *Tourism Analysis, 15*, 71–88.

Chiesura, A. (2004). The role of urban parks for the sustainable city. *Landscape and Urban Planning, 68*, 129–138.

Chiou, W.-B., Wan, C.-S., & Lee, H.-Y. (2008). Virtual experience vs. brochures in the advertisement of scenic spots: How cognitive preferences and order effects influence advertising effects on consumers. *Tourism Management, 29*, 146–150.

Corcoran, J., Chhetri, P., & Stimson, R. (2009). Using circular statistics to explore the geography of the journey to work. *Papers in Regional Science, 88*, 119–132.

Daniel, T. C. (2001). Whither scenic beauty? Visual landscape quality assessment in the 21st century. *Landscape and Urban Planning*, *54*, 267–281.

Daniel, T.C., & Boster, R.S., (1976). *Measuring landscape aesthetics: The scenic beauty estimation method*. USDA Forest Service Research Paper RM-167. Rocky Mountain Forest and Range Experiment Station, Fort Collins, CO.

Dorwart, C. E., Moore, R. L., & Leung, Y.-F. (2009). Visitors' perceptions of a trail environment and effects on experiences: A model for nature-based recreation experiences. *Leisure Sciences, 32*, 33–54.

Fairweather, J. R., & Swaffield, S. R. (2001). Visitor experiences of Kaikoura, New Zealand: An interpretative study using photographs of landscapes and Q method. *Tourism Management, 22*, 219–228.

Fairweather, J. R., & Swaffield, S. R. (2002). Visitors' and locals' experiences of Rotorua, New Zealand: An interpretative study using photographs of landscapes and Q method. *International Journal of Tourism Research, 4*, 283–297.

Fisher, N. I. (1995). *Statistical analysis of circular data*. Cambridge University Press.

Flowerdew, R., & Aitkin, M. (1982). A method of fitting the gravity model based on the Poisson distribution*. *Journal of Regional Science, 22*, 191–202.

Fotheringham, A., & Brunsdon, C. (1999). Local forms of spatial analysis. *Geographical Analysis, 31*, 340-358.

Fridgen, J. D. (1984). Environmental psychology and tourism. *Annals of Tourism Research, 11*, 19–39.

Fyhri, A., Jacobsen, J. K. S., & Tømmervik, H. (2009). Tourists' landscape perceptions and preferences in a Scandinavian coastal region. *Landscape and Urban Planning, 91*, 202–211.

Garrod, B. (2008). Exploring place perception a photo-based analysis. *Annals of Tourism Research, 35*, 381–401.

GeoDa Center. (n.d.). *Glossary of key terms*. Retrieved February 21, 2014 from https://geodacenter.asu.edu/node/390

Gimblett, H. R., Richards, M. T., & Itami, R. M. (2001). RBSim: Geographic simulation of wilderness recreation behavior. *Journal of Forestry, 99*, 36–42.

Gong, H., Chen, C., Bialostozky, E., & Lawson, C. T. (2012). A GPS/GIS method for travel mode detection in New York City. *Computers, Environment and Urban Systems, 36*, 131–139.

Greene, W. (2008). Functional forms for the negative binomial model for count data. *Economics Letters, 99*, 585–590.

Hallo, J. C., Beeco, J. a., Goetcheus, C., McGee, J., McGehee, N. G., & Norman, W. C. (2012). GPS as a method for assessing spatial and temporal use distributions of nature-based tourists. *Journal of Travel Research, 51*, 591–606.

Haywood, K. M. (1990). Visitor-employed photography: An urban visit assessment. *Journal of Travel Research, 29*, 25–29.

Heyman, E. (2012). Analysing recreational values and management effects in an urban forest with the visitor-employed photography method. *Urban Forestry & Urban Greening, 11*, 267–277.

Hollenstein, L., & Purves, R. (2010). Exploring place through user-generated content: Using Flickr tags to describe city cores. *Journal of Spatial Information Science, 1*, 21-48.

Hull, R. B., & Stewart, W. (1992). Validity of photo-based scenic beauty judgments. *Journal of Environmental Psychology, 12*, 101–114.

Hull, R., Stewart, W., & Yi, Y. (1992). Experience patterns: Capturing the dynamic nature of a recreation experience. *Journal of Leisure Research, 24*, 242-250.

Hunter, W. C. (2008). A typology of photographic representations for tourism: Depictions of groomed spaces. *Tourism Management, 29*, 354–365.

Jacobsen, J. K. S. (2007). Use of landscape perception methods in tourism studies: A review of photo-based research approaches. *Tourism Geographies, 9*, 234–253.

Japan Travel Bureau Foundation. (n.d.). *A guide to the Japan Travel Bureau Foundation*. Retrieved February 21, 2014, from http://www.jtb.or.jp/en

Jenkins, O. (2003). Photography and travel brochures: The circle of representation. *Tourism Geographies, 5*, 305–328.

Kienast, F., Degenhardt, B., Weilenmann, B., Wäger, Y., & Buchecker, M. (2012). GIS-assisted mapping of landscape suitability for nearby recreation. *Landscape and Urban Planning, 105*, 385–399.

Kliskey, A. D. (2000). Recreation terrain suitability mapping: A spatially explicit methodology for determining recreation potential for resource use assessment. *Landscape and Urban Planning, 52*, 33–43.

Kurata, Y. (2012). Potential-of-interest maps for mobile tourist information services. *Proceedings of the International Conference in Helsingborg, Sweden, January 25–27, 2012*, 239–248.

Lee, S.-H., Choi, J.-Y., Yoo, S.-H., & Oh, Y.-G. (2013). Evaluating spatial centrality for integrated tourism management in rural areas using GIS and network analysis. *Tourism Management, 34*, 14–24.

LeSage, J. P., & Pace, R. K. (2008). Spatial econometric modeling of origin-destination flows*. *Journal of Regional Science, 48*, 941–967.

Li, Y. (2000). Geographical consciousness and tourism experience. *Annals of Tourism Research, 27*, 863–883.

Lo, I. S., McKercher, B., Lo, A., Cheung, C., & Law, R. (2011). Tourism and online photography. *Tourism Management, 32*, 725–731.

Loeffler, T. A. (2004). A photo elicitation study of the meanings of outdoor adventure experiences. *Journal of Leisure Research, 36*, 536–556.

Longman English Dictionary Online. (n.d.) *Potential*. Retrieved February 21, 2014, from http://www.ldoceonline.com/dictionary/potential_2

Lwin, K. K., & Murayama, Y. (2011). Modelling of urban green space walkability: Eco-friendly walk score calculator. *Computers, Environment and Urban Systems, 35*, 408–420.

MacKay, K. J., & Couldwell, C. M. (2004). Using visitor-employed photography to investigate destination image. *Journal of Travel Research*, 42, 390–396.

Mardia, K. V., & Jupp, P. E. (1999). *Directional statistics*. John Wiley & Sons.

Markwell, K. W. (1997). Dimensions of photography in a nature-based tour. *Annals of Tourism Research, 24*, 131–155.

Marrocu, E., & Paci, R. (2013). Different tourists to different destinations: Evidence from spatial interaction models. *Tourism Management, 39*, 71–83.

Matteucci, X. (2013). Photo elicitation: Exploring tourist experiences with researcher-found images. *Tourism Management, 35*, 190–197.

McKercher, B., Shoval, N., Ng, E., & Birenboim, A. (2012). First and repeat visitor Behaviour: GPS tracking and GIS analysis in Hong Kong. *Tourism Geographies, 14*, 147–161.

Meijles, E. W., de Bakker, M., Groote, P. D., & Barske, R. (2013). Analysing hiker movement patterns using GPS data: Implications for park management. *Computers, Environment and Urban Systems,* http://dx.doi.org/10.1016/j.compenvurbsys.2013.07.005. (in press)

Mizoo, Y., Ichihara, Y., Watanabe, T., & Kezuka, H. (1975). Evaluation of tourist resources: An application of multidimensional analysis. *Geographical Review of Japan, 48*, 694–711. [in Japanese with English abstract]

Mizoo, Y., & Osumi, N. (1983). Geographical study of landscape evaluation: A case study of lakes in Japan. *Japanese Journal of Human Geography, 35*, 40–56. [in Japanese with English abstract]

Moulin, B., Chaker, W., & Gancet, J. (2004). PADI-Simul: An agent-based geosimulation software supporting the design of geographic spaces. *Computers, Environment and Urban Systems, 28*, 387–420.

Múgica, M., & Lucio, J. V. De. (1996). The role of on-site experience on landscape preferences: A case study at Donana National Park (Spain). *Journal of Environmental Management, 47*, 229–239.

Nahuelhual, L., Carmona, A., Lozada, P., Jaramillo, A., & Aguayo, M. (2013). Mapping recreation and ecotourism as a cultural ecosystem service: An application at the local level in Southern Chile. *Applied Geography, 40*, 71–82.

Naoi, T., Airey, D., Iijima, S., & Niininen, O. (2006). Visitors' evaluation of an historical district: Repertory grid analysis and laddering analysis with photographs. *Tourism Management, 27*, 420–436.

Naoi, T., Yamada, T., Iijima, S., & Kumazawa, T. (2011). Applying the caption evaluation method to studies of visitors' evaluation of historical districts. *Tourism Management, 32*, 1061–1074.

National Land Information Division, National Spatial Planning and Regional Policy Bureau, MILT of Japan (n.d.). *National Land Numerical Information download service*. Retrieved February 21, 2014, from http://nlftp.mlit.go.jp/ksj-e/index.html

National Research Council. (2006). *Learning to think spatially: GIS as a support system in the K-12 curriculum*. Washington, DC: The National Academies Press.

Navarro Jurado, E., Tejada Tejada, M., Almeida García, F., Cabello González, J., Cortés Macías, R., Delgado Peña, J., Fernández Gutiérrez, F., Gutiérrez Fernández, G., Luque Gallego, M., Málvarez García, G., Marcenaro Gutiérrez, O., Navas Concha, F., Ruiz de la Rúa, F., Ruiz Sinoga, J., & Solís Becerra, F. (2012). Carrying capacity assessment for tourist destinations: Methodology for the creation of synthetic indicators applied in a coastal area. *Tourism Management*, 33, 1337–1346.

Nelder, J. A., & Wedderburn, R. W. M. (1972). Generalized linear models. *Journal of the Royal Statistical Society. Series A (General), 135*, 370–384.

Nielsen, A. B., Heyman, E., & Richnau, G. (2012). Liked, disliked and unseen forest attributes: Relation to modes of viewing and cognitive constructs. *Journal of Environmental Management, 113*, 456–66.

Oku, H., & Fukamachi, K. (2003). Occurrence pattern of landscape experience during forest recreation. *Journal of the Japanese Forestry Society, 85*, 63‑69 [in Japanese with English abstract].

Oku, H., & Fukamachi, K. (2006). The differences in scenic perception of forest visitors through their attributes and recreational activity. *Landscape and Urban Planning, 75*, 34–42.

Orellana, D., Bregt, A. K., Ligtenberg, A., & Wachowicz, M. (2012). Exploring visitor movement patterns in natural recreational areas. *Tourism Management, 33*, 672–682.

Ostermann, F. O. (2010). Digital representation of park use and visual analysis of visitor activities. *Computers, Environment and Urban Systems, 34*, 452–464.

Qiu, L., Lindberg, S., & Nielsen, A. B. (2013). Is biodiversity attractive?—On-site perception of recreational and biodiversity values in urban green space. *Landscape and Urban Planning, 119*, 136–146.

Rangel-Buitrago, N., Correa, I. D., Anfuso, G., Ergin, a., & Williams, a. T. (2013). Assessing and managing scenery of the Caribbean Coast of Colombia. *Tourism Management, 35*, 41–58.

Ray, S. F. (2002). *Applied photographic optics: Lenses and optical systems for photography, film, video, electronic and digital imaging*. Taylor & Francis.

Rigaux, P., Scholl, M., & Voisard, A. (2001). *Spatial databases: With application to GIS*. San Francisco: Morgan Kaufmann Publishers.

Schirpke, U., Tasser, E., & Tappeiner, U. (2013). Predicting scenic beauty of mountain regions. *Landscape and Urban Planning, 111*, 1–12.

Shoval, N. (2008). Tracking technologies and urban analysis. *Cities, 25*, 21–28.

Shoval, N., & Isaacson, M. (2007a). Sequence alignment as a method for human activity analysis in space and time. *Annals of the Association of American Geographers, 97*, 282–297.

Shoval, N., & Isaacson, M. (2007b). Tracking tourists in the digital age. *Annals of Tourism Research, 34*, 141–159.

Shoval, N., McKercher, B., Ng, E., & Birenboim, A. (2011). Hotel location and tourist activity in cities. *Annals of Tourism Research, 38*, 1594–1612.

Silverman, B. W. (1986). *Density estimation for statistics and data analysis*. New York: Chapman and Hall.

Stedman, R., Beckley,T., Wallace, S., & Ambard, M. (2004). A picture *and* 1000 words: Using resident-employed photography to understand attachment to high amenity places. *Journal of Leisure Research, 36*, 580-606.

Stepchenkova, S., & Zhan, F. (2013). Visual destination images of Peru: Comparative content analysis of DMO and user-generated photography. *Tourism Management, 36*, 590–601.

Sugimoto, K. (2011a). Examination of photography investigation using digital camera: About social trend, consideration when investigating and individual variation of the number of sheets of taking a picture. *The International Journal of Tourism Science, 4*, 89-98. [in Japanese]

Sugimoto, K. (2011b). Analysis of scenic perception and its spatial tendency: Using digital cameras, GPS loggers, and GIS. *Procedia - Social and Behavioral Sciences, 21*, 43-52.

Sugimoto, K. (2012). Evaluation of park trails based on visitors' visual experiences: An analytical technique using digital cameras, GPS, and GIS. *GIS-Theory and Application, 20*, 39-49. [in Japanese with English abstract]

Sugimoto, K. (2013). Quantitative measurement of visitors' reactions to the settings in urban parks: Spatial and temporal analysis of photographs. *Landscape and Urban Planning, 110*, 59-63.

Tamesue, K., & Tsutsumi, M. (2012). Modeling spatial dependence in origin-destination flows based on a Negative Binomial Gravity Model. *Proceedings of the Institute of Statistical Mathematics, 60*, 121–130. [in Japanese with English abstract]

Taylor, J. G., Czarnowski, K. J., Sexton, N. R. & Flick, S. (1995). The importance of water to Rocky Mountain National Park visitors: An adaptation of visitor-employed photography to natural resources management. *Journal of Applied Recreation Research, 20*, 61-85.

Ted, J. (1997). The Prediction Test for Nonlinear Determinism. In Kiel D. L., & Elliott E. W. (Eds.), *Chaos Theory in the Social Sciences: Foundations and Applications* (pp. 67–88). University of Michigan Press.

Tomczyk, A. M., & Ewertowski, M. (2013). Planning of recreational trails in protected areas: application of regression tree analysis and geographic information systems. *Applied Geography, 40*, 129–139.

Van Riper, C. J., Kyle, G. T., Sutton, S. G., Barnes, M., & Sherrouse, B. C. (2012). Mapping outdoor recreationists' perceived social values for ecosystem services at Hinchinbrook Island National Park, Australia. *Applied Geography, 35*, 164–173.

Wong, K., & Domroes, M. (2005). The visual quality of urban park scenes of Kowloon Park, Hong Kong: Likeability, affective appraisal, and cross-cultural perspectives. *Environment and Planning B: Planning and Design, 32*, 617 – 632.

Xie, Z., & Yan, J. (2008). Kernel Density Estimation of traffic accidents in a network space. *Computers, Environment and Urban Systems, 32*, 396–406.

Yamashita, S. (2002). Perception and evaluation of water in landscape: Use of Photo-Projective Method to compare child and adult residents' perceptions of a Japanese river environment. *Landscape and Urban Planning, 62*, 3–17.

Yang, B., Madden, M., Kim, J., & Jordan, T. R. (2012). Geospatial analysis of barrier island beach availability to tourists. *Tourism Management, 33*, 840–854.

Zube, E. H., Sell, J. L., & Taylor, J. G. (1982). Landscape perception: Research, application and theory. *Landscape Planning, 9*, 1–33.